VYSOKÉ UČENÍ TECHNICKÉ V BRNĚ
BRNO UNIVERSITY OF TECHNOLOGY

FAKULTA STROJNÍHO INŽENÝRSTVÍ
ÚSTAV AUTOMOBILNÍHO A DOPRAVNÍHO INŽENÝRSTVÍ

FACULTY OF MECHANICAL ENGINEERING
INSTITUTE OF AUTOMOTIVE ENGINEERING

SINGLE CYLINDER SI ENGINE FOR FORMULA STUDENT

ZVÝŠENÍ PRUŽNOSTII ZÁŽEHOVÉHO JEDNOVÁLCOVÉHO MOTORU FORMULE STUDENT

DIPLOMOVÁ PRÁCE
MASTER'S THESIS

AUTOR PRÁCE
AUTHOR
BC. LADISLAV ADÁMEK

VEDOUCÍ PRÁCE
SUPERVISOR
ING. DAVID SVÍDA

BRNO 2011

ABSTRAKT

Diplomová práce je zaměřena na konstrukční návrh sacího potrubí pro vůz Formula Student. Pro pohon vozu je použit jednoválcový atmosférický benzinový motor Husaberg FE 570. Sací potrubí je navrhováno tak, aby bylo v souladu s pravidly Formula Student. Pro zvýšení plnící účinnosti sací potrubí využívá resonančního efektu. Délky sacího potrubí byly spočítány v software Lotus Engine simulation

KLÍČOVÁ SLOVA

sací potrubí, rezonanční potrubí, sací ventil, škrticí klapka, airbox, restriktor, proudění, CFD

ABSTRACT

The aim of this diploma thesis is the design and tuning of the intake manifold for the Formula Student car. The single cylinder SI engine Husaberg FE 570 is used as a powertrain unit. The intake manifold is designed according to the Formula Student rules. The intake manifold uses the ram wave effect to improve the engine charging efficiency. Lengths of the runners are calculated in the Lotus Engine simulation software.

KEYWORDS

intake manifold, resonance manifold, intake valve, throttle body, airbox, restrictor, flow, CFD

BIBLIOGRAFICKÁ CITACE

ADÁMEK, L.*Single cylinder SI engine for Formula Student*. Brno: Vysoké učení technické v Brně, Fakulta strojního inženýrství, 2011. 102 s. Vedoucí diplomové práce Ing. David Svída.

ČESTNÉ PROHLÁŠENÍ

Prohlašuji, že tato práce je mým původním dílem, zpracoval jsem ji samostatně pod vedením Ing. David Svídy a spoužitím literatury uvedené v seznamu.

V Brně dne 25. května 2011 ……..……..……..

Ladislav Adámek

PODĚKOVÁNÍ

Tímto bych chtěl poděkovat Ing. Davidu Svídovi, za jeho pomoc, užitečné rady a čas strávený konzultacemi. Dále pak Ing. Martinu Beranovi za velmi přínosné rady a pomoc při měření. V neposlední řadě bych chtěl poděkovat Vlastě Hofbauerové za korekturu anglického textu, vstřícnou komunikaci a užitečné rady a připomínky a zvláště pak celé mé rodině za velikou podporu v období mého studia.

CONTENTS

INTRODUCTION

Motorsport is a world leader in the use and implementation of new concepts and technologies in the automotive engineering. It is an area where components are tested to their limits with no space for mistakes. The racing car as a whole has to be a perfectly working unit; engineers are making an effort to tune every car component to its maximum. The engine represents one of the most important car design groups..

There are many differences between common and racing engines. Generally, naturally aspirated racing engines have a higher combustion pressure and a better charging efficiency but – due to the tuning of the resonance manifold – it only applies to short spectrum of engine speeds. One of the many differences in supercharged engines lies in a higher charging pressure, this being a result of the charging efficiency of the used turbocharger or the compressor. Due to the rules, the engines for most of the motorsport classes are not built from scratch and that is why serial engines that need to be tuned are used here.

Basic conditions leading to the successful engine tuning include optimizing the intake and exhaust manifolds, tuning the resonance manifold, optimizing the flow through intake ports and valve seats etc. Therefore engineers work with the simulation software that can analyze the impact of the engine component changes on the final engine performance. Using the simulation software leads to a shortening of the engine optimizing and tuning time but the results and data obtained this way need to be verified experimentally.

The aim of this diploma thesis is the design and tuning of the intake manifold for a Formula Student car according to the Formula Student rules. For this purpose our “Engine team” has chosen a single cylinder engine from a motocross motorbike. This engine will be overcharged by the intake manifold using the ram wave effect.

As has been mentioned before, this diploma thesis is closely related to the Formula Student project, therefore some data in this work is shared with other “Engine Team” members. Namely: Bc. Jindřich Dolák, Bc. Martin Fajkus.

1 FORMULA STUDENT POWERTRAIN SPECIFICATION

This chapter contains a summary of the formula SAE rules concerned with the powertrain. The rules are available at sources [1]

1.1 ENGINE LIMITATION

"The engine(s) used to power the car must be a piston engine(s) using a four-stroke primary heat cycle with a displacement not exceeding 610 cc per cycle. Hybrid powertrains, such as those using electric motors running off stored energy, are prohibited". [1]

1.2 AIR INTAKE SYSTEM

LOCATION OF AIR INTAKE SYSTEM

„All parts of the engine air and fuel control systems (including the throttle or carburetor, and the complete air intake system, including the air cleaner and any air boxes) must lie within the surface defined by the top of the roll bar and the outside edge of the four tires". (Fig. 1) [1]

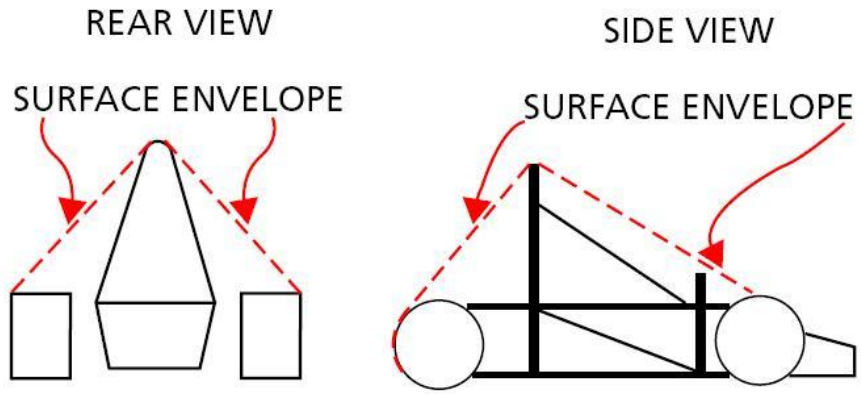

Fig. 1 car surface envelopes [1]

INTAKE MANIFOLD

"The intake manifold must be securely attached to the engine block or cylinder head with brackets and mechanical fasteners. This precludes the use of hose clamps, plastic ties, or safety wires. The use of rubber bushings or hose is acceptable for creating and sealing air passages, but is not considered a structural attachment". [1]

1.3 THROTTLE BODY AND THROTTLE ACTUATION

THROTTLE BODY

"The car must be equipped with a carburetor or throttle body. The carburetor or throttle body may be of any size or design". [1]

THROTTLE ACTUATION

"The throttle must be actuated mechanically, i.e. via a cable or a rod system. The use of electronic throttle control (ETC) or "drive-by-wire" is prohibited. The throttle cable or rod must have smooth operation, and must not have the possibility of binding or sticking. The throttle actuation system must use at least two (2) return springs located at the throttle body, so that the failure of any component of the throttle system will not prevent the throttle returning to the closed position. A positive pedal stop must be incorporated on the throttle pedal to prevent over stressing the throttle cable or actuation system." [1]

1.4 FUEL

"The basic fuel available at competitions in the Formula SAE Series is unleaded gasoline with an octane rating of 93 (R+M)/2 (approximately 98 RON) and E85. Nothing may be added to the provided fuels. This prohibition includes nitrous oxide or any other oxidizing agent." [1]. Fuel additives are prohibited as well.

1.5 INTAKE SYSTEM RESTRICTOR

"In order to limit the power capability from the engine, a single circular restrictor must be placed in the intake system between the throttle and the engine and all engine airflow must pass through the restrictor. Any device that has the ability to throttle the engine downstream of the restrictor is prohibited. The restrictor must be located to facilitate measurement during the inspection process. The circular restricting cross section may NOT be movable or flexible in any way, e.g. the restrictor may not be part of the movable portion of a barrel throttle body." [1]

THE MAXIMUM RESTRICTOR DIAMETERS

- Gasoline fuelled cars – 20 mm (0.7874 inch)
- E85 fueled cars – 19 mm (0.7480 inch)

Fig. 2 Formula SAE car (TU Brno racing)

2 ENGINE DATA

For the purpose of the Formula Student competition our team has chosen an engine from a HUSABERG FE 570 motocross motorbike (Fig.2). Our team´s intention is to build a small and a very light Formula car and this compact powertrain unit perfectly fits to our car conception. It is a four stroke water cooled single cylinder SI engine with a displacement 565.5ccm and it weighs less than 33 kilograms. The valve mechanism is controlled via two valve rockers and is powered by a single camshaft via a cam tooth chain. IDI (indirect fuel injection) is used here because of better air/fuel mixing at higher engine speeds; the fuel is injected by a single injector which is a part of the throttle body..

Fig.3 section through Husaberg FE 570 engine.[2]

Engine data that I am going to work with in this chapter, I have partly gained from the source [3] and also by the engine measurement.

2.1 HUSABERG FE 570 BASIC ENGINE DATA

Tab.1Basic engine data

DESIGN	1-cylinder, 4- stroke engine, water cooled
DISPLACEMENT	565.6 cm^3
BORE	100mm
STROKE	72mm
COMPRESSION RATIO	12.2:1
CONTROL	OHC
ENGINE POWER	46 kW
ENGINE TORQUE	58 Nm

The engine construction is not similar to engines of the same category. "A sleeping engine" (Fig.4) construction means that the cylinder of this engine is inclined at 70 degrees angle to mass centralization, which is a big advantage in the motocross when a rider jumps with the motorbike; but for our formula car this could be a little disadvantage due to COG (center of gravity) requirements. Therefore we have put the engine to a frame inclined at 85 degrees, which means that the cylinder lies almost parallel with the track. Naturally we had to

Fig.4"sleeping engine" 70 degrees inclined [4]

check the water and oil pumps supply before that.

2.2 CRANKSHAFT CHARACTERISTICS

Tab. 2 crankshaft characteristics

CON ROD LENGTH	120.8mm
MAIN CRANKSHAFT BEARINGS	2
PISTON RINGS	2
CRANKSHAFT MATERIAL	Forged steel

In (Fig.1) we can see FE 570 crankshaft.

2.3 VALVE TIMING

Tab. 3Inlet and exhaust valve timing

INLET VALVE TIMING	
INLET VALVE OPENING	20° before TDC
INLET VALVE CLOSING	72° after BDC
INLET VALVE TOTAL OPENING ANGLE	272°
EXHAUST VALVE TIMING	
EXHAUST VALVE OPENING	65° before BDC
EXHAUST VALVE CLOSING	28° after TDC
EXHAUST VALVE TOTAL OPENING ANGLE	273°

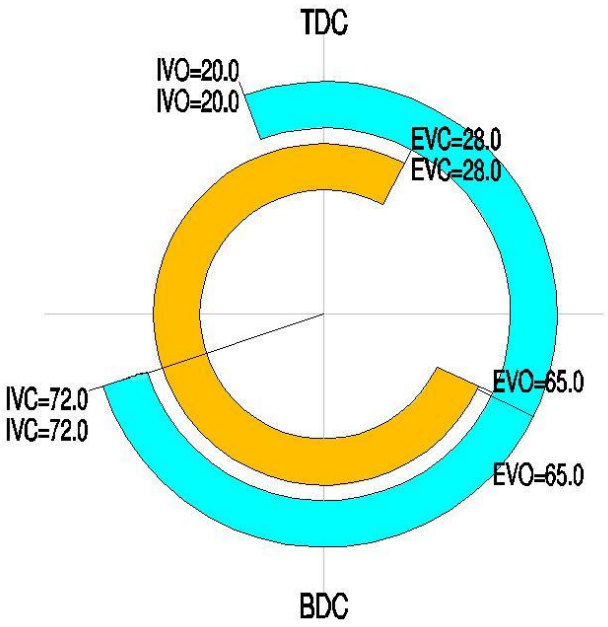

The valve train is realized by 2 rocker arms with rollers to minimize friction losses and it is powered by a single camshaft (Fig.5) via a tooth chain. The camshaft is also equipped with a decompressor beause of a better engine starting, when the engine is turned off.

Fig. 5 FE 570 camshaft [5]

2.4 VALVE CHARACTERISTICS

Husaberg uses titanium forged valves and valve seats for the FE 570 engine because of a high compression ratio and combustion pressures; therefore the engine can be frequently run under big loads without any serious problems.

Tab. 4 Valve characteristics

VALVES COUNT	4
INTAKE VALVE DIAMETER	38 mm
EXHAUST VALVE DIAMETER	32 mm
INTAKE VALVE LIFT	10 mm
EXHAUST VALVE LIFT	8.6 mm
INLET VALVE STEM DIAMETER	6 mm
EXHAUST VALVE STEM DIAMETER	5 mm

There are titanium valves and a cylinder head of F570 engine in (Fig.6)

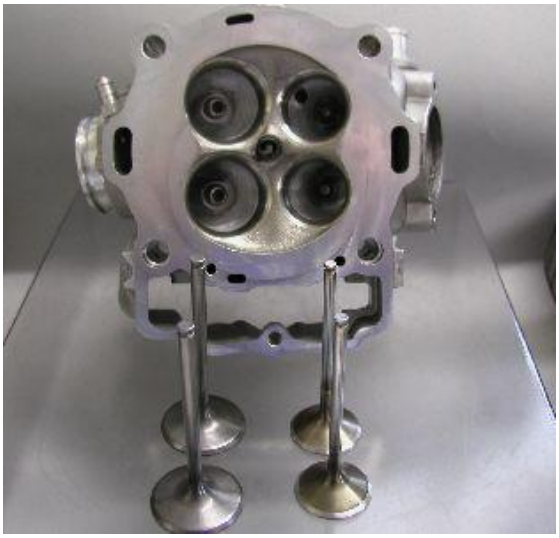

Fig. 6 FE 570 Cylinder head and valves [5]

2.5 EXHAUST SYSTEM

The factory exhaust system (Fig.5) is made of stainless steel and the exhaust silencer of high quality aluminium, therefore the silencer is light-weight and it meets all noise requirements.

Fig. 7 Factory exhaust system

All the basic parameters of the factory exhaust system are shown in Tab.5.

Tab. 5 Factory exhaust parameters

PART	DIAMETER		LENGTH
	INLET	OUTPUT	
EXHAUST MANIFOLD	41 mm	45 mm	925 mm
EXHAUST SILENCER	45 mm	28 mm	600 mm

2.6 INTAKE SYSTEM

At the beginning of the intake system there is an airbox (Fig.7) that includes an air filter, airbox flow into the throttle body of 42 mm in diameter and the length of 100 mm, and it is mounted over the rubber adaptor to the engine. There is no separate intake runner like in 4 cylinder engines with a similar displacement, but the throttle body provides a function of the intake runner here. In the cylinder head there is an elliptical intake port of dimensions 42 mm and 40 mm and the length of 50 mm, after that it is divided into 2 separate intake ports. The injection of fuel is provided by a single injector that is a part of the throttle body

Fig. 8 FE 570 airbox with air filter

Total intake system length from the valve seat to the airbox is 190 mm. The capacity of the airbox is approximately about 2 liters and the length of a resonance part of the intake system is 190 mm. In (Fig.9) we can see the intake system without the cylinder head.

Tab.6 Intake system parameters

RESONANCE LENGTH	190 mm
AIRBOX VOLUME	2 - 3 l
RESONANCE DIAMETER	42 mm
VALVE THROAT DIAMETER	34 mm

Fig. 9 Husaberg FE 570 intake system

3 PARTS OF THE RACING INTAKE SYSTEM

There are several requirements, which a good racing intake system should meet, and some of them differ depending on type of charging (naturally aspirated engines or supercharged and turbocharged engines).

Every good racing intake system should provide a good filtration with minimum pressure losses at the air filter, which can be reached by using a high-pass air filter. It also has to provide a perfect fuel-air mixing and a flow to each cylinder as direct as possible to minimize friction losses and air heating in the intake. Also the volumetric efficiency has to be as high as possible for the required engine speeds range through prefect tuning of lengths and diameters of the runners; or in case of a turbocharger it is important to choose an appropriate type of the turbocharger and set the adequate charging pressure. Another important feature of a good racing intake system is an optimized airbox which provides the flow stabilization and which contributes to the engine overcharging.

The whole intake system has to be installed to the engine compartment in an optimum way. Most racing cars use the ram intake system. To be able to overcharge this system with an air blast, intake cutouts must be placed on the bodywork to the surfaces with a maximum aerodynamic pressure. These surfaces are mostly found on the front bumper and the hood, which is a great advantage for cars with the front placed engine. Racing intake system also has to be very light-weight to minimize the total car weight, therefore materials like carbon fiber sandwiches and fiberglass are used. These have good strength characteristics as well. This is necessary due to high levels of velocity and depression in the whole intake system and that might be much higher here than in a serial intake system.

The intake system facture depends on the type of an engine. For naturally aspirated SI racing engines the components order in the air flow direction is usually as follows: an air filter (sometimes could be a part of the airbox), an airbox, a resonance runner with a throttle body, inlet ports, a valve throat, an inlet valve. For turbocharged engines the components order is quite similar to naturally aspirated engines, only a compressor part of the turbocharger, an intercooler and a blow off valve are added here. Obviously there are many sensors and measuring units in the whole intake system in order to provide important information for ECU, e.g. the volume, pressure and temperature of the induced air, pressure before the

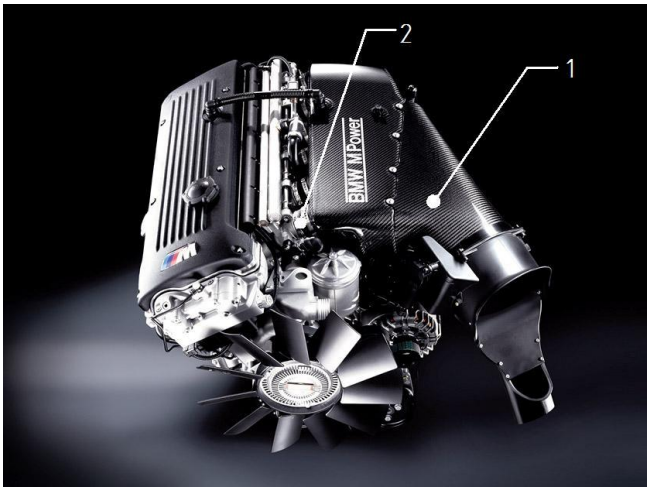

Fig. 10 Main part so intake system: 1,airbox with air filter 2, resonance runner with throttle body [6]

compressor housing etc.

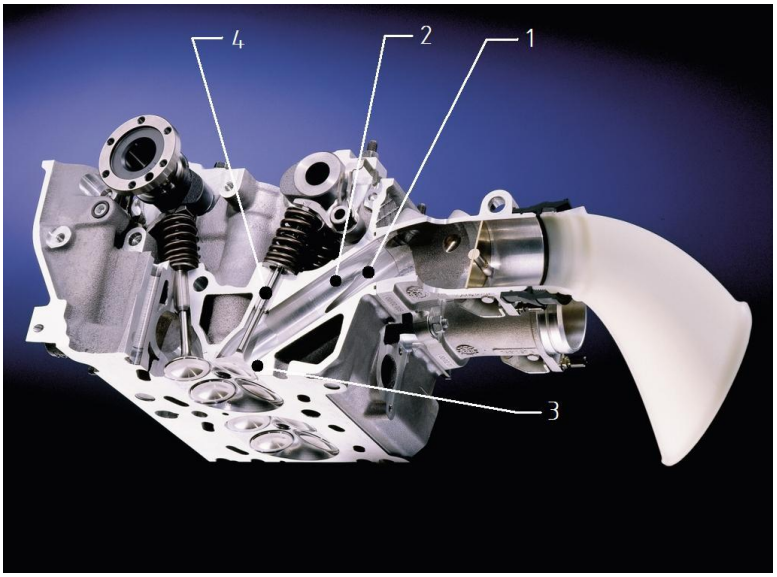

Fig.11 Main parts of the intake system in cylinder head: 1, intake port 2,intake port, 3valve throat, inlet valve [6]

3.1 AIR FILTER

main task of the air filter is to separate dust particles from the induced air and to protect the engine. Dust particles that get into the engine decrease the engine efficiency and may cause a great damage, especially at high engine speeds. Air filters also have positive effect on the noise reduction when the engine is running.

Most frequently racing cars use cotton or foam air filters with silicon oil. These air filters have much smaller pressure losses than ordinary paper filters that are frequently used in common cars. But on the other hand there are some groups of racing cars which do not use air filters at all. Circuit cars are a good example of these types. Because of very low dustiness on the racing circuits these cars do not use air filters, as all filters have some pressure and hydraulic losses and these losses have bad influence on the engine efficiency and performance. It is absolutely necessary to use an air filter in case of a turbocharged engine, due to very precise dimensions of the turbocharger compressor wheel

Today the world leading air filter producers are K&Nfilters,ITG and Mann Hummel.

Fig.12 ITG racing filters and otherintake components [7]

3.2 AIRBOX

The airbox in a common car is usually a box with an air filter which flows through a single throttle body to the resonant plenum.

In a racing car the function of the airbox is slightly different. The racing car airbox usually acts as a resonant plenum which is connected to the resonant runners. It is situated in the front part of the engine compartment to enable a better access of cold air which is delivered to the airbox through massive intake cutouts. The main function of the racing airbox is the engine overcharging when the throttle body is fully open and the car is on the corner exit. This happens when the car is entering the corner. It has to decrease its speed (throttle body closure) due to the physical point of view. At this moment the throttle bodies are closed but the air is still ramming to the airbox which leads to airbox blast overcharging. Then, on the corner exit when the throttle bodies are opened again, the excess of pressure from the airbox overcharges the cylinders. But this only works well when the throttle bodies are located between the engine and the airbox. When the engine has a single throttle body located in front of the airbox downstream of air flow, the airbox works as an ordinary resonator. Which means that it reflects pressure waves evoked by the transient flow while the engine is in the induction stroke. Racing airbox also equally distributes air to the individual cylinders.

Fig.13 Formula 3airbox(volkswagen) [8]

3.3 THROTTLE BODY

Nowadays most common and racing cars use a butterfly throttle body (Fig. 14). Design of this type is very simple and it is also easy to manufacture. The main disadvantage of the butterfly throttle body is that when it goes fully open, the cross section of the intake runner will never be complete. This leads to hydraulic losses when the induced air flows through the butterfly valve.

Another type of the throttle body is a roller barrel throttle body (Fig. 15), which is purely used for racing purposes. These throttle bodies are used in F1 engines because it is very important to have no barrier in the intake runners to avoid the aforementioned hydraulic and friction losses. But it is rather difficult to tune these throttle bodies to work perfectly together and to deliver the right mass of air to each cylinder in the right time.

Fig.14 Butterfly throttle bodies (BMW M3) [6]

There are two main types of throttle body controlling. "Drive by Wire" is a very popular controlling system nowadays. It is a throttle body that is controlled by an electromotor inside the throttle body. Butterfly valve turning angle is controlled by a potentiometer which is placed on the accelerator and by ECU as well. The second type of controlling, frequently used in motorsport, is "throttle cable controlling system". It is an ordinary system where the throttle body and the accelerator are connected with a cable and controlled mechanically by the driver´s foot.

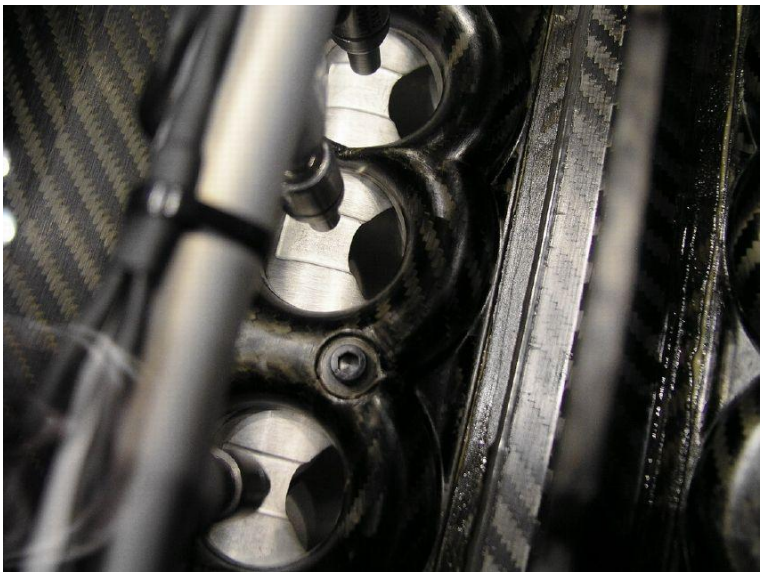

Fig.15 Roller barrel throttle body (F1 cosworth engine) [10]

3.4 INTAKE RUNNERS

They are usually placed between the cylinder head and the airbox, ended by a bellmouth. For common cars they are often made of aluminium alloys or plastic materials because of very low production costs. Racing engines usually used intake runners made of aluminum alloys in the past but nowadays most racing engines use carbon fiber sandwiches because of their low density, high strength and low weight.

The intake runners are often of a circular cross section due to better a circumference to area ratio, which brings the lowest hydraulic losses. Through the medium of diameters and lengths it is possible to tune the ram wave overcharging for required engine speeds.

Fig.16 Carbon fibre intake runners [11]

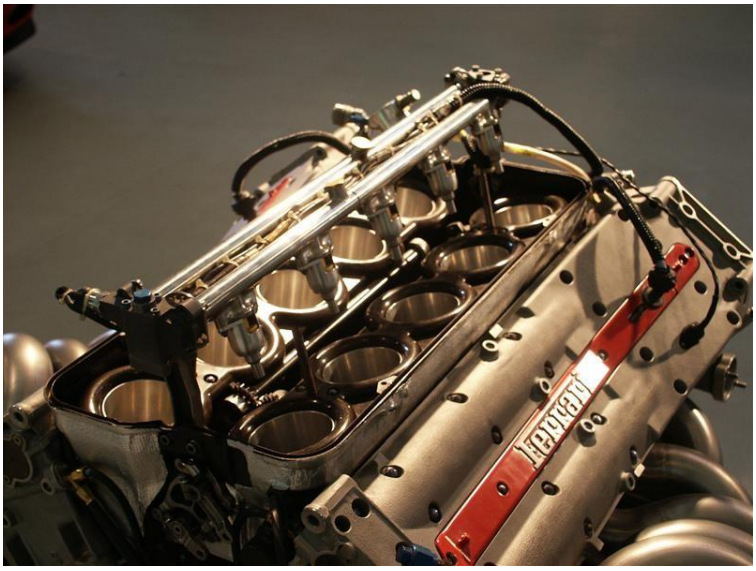

Fig.17 Intake runners (F1 Ferrari engine) [11]

3.5 INLET PORT DESIGN

The racing engine inlet ports should be as narrow as possible (Fig. 18 c) and they should make a sharp angle with the valve axis. If the inlet port is shaped like on (Fig. 18a), the flow direction is changed; this leads to flow inflation on the outer side of the port and this causes a reduction in the flow area. But it is not easy to realize a sharp angle condition. In order to keep a sharp angle, the valve spring has to be of quite a large diameter. This leads to the valve stem extension and thereby to the increase in both its weight and also the cylinder head height. Heavier valves are very inconvenient therefore 2 smaller and lighter valves are usually used instead of one.

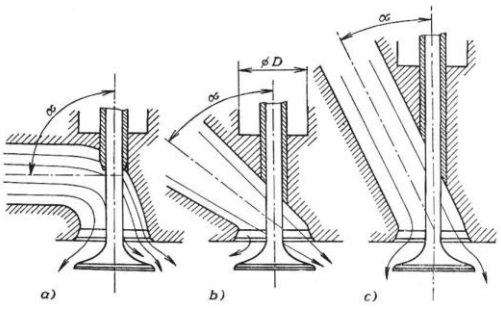

Fig.18 Inlet port design [12]

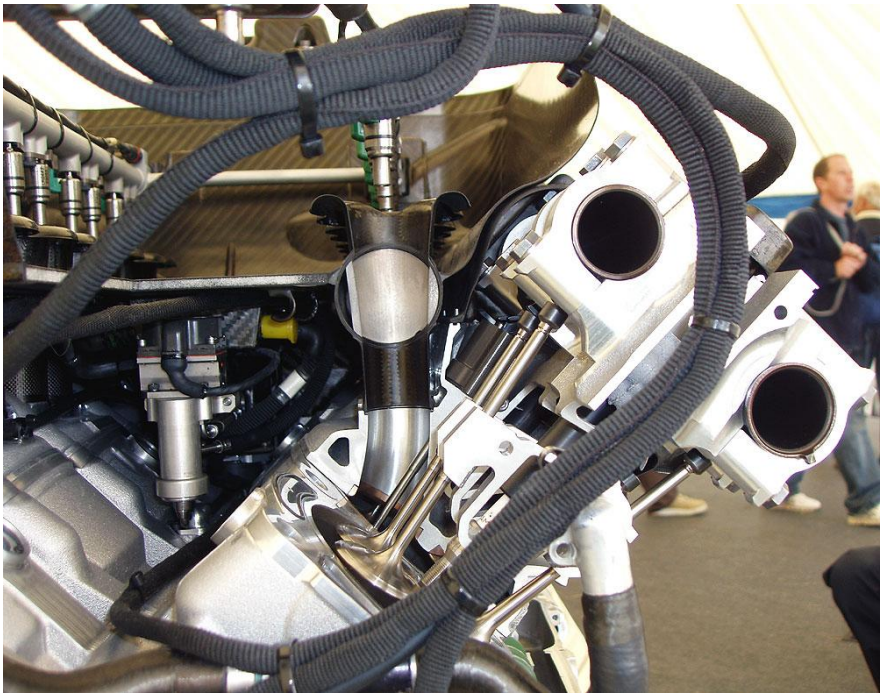

Fig.19 F1 intake system with narrow inlet port [11]

In (Fig. 19) we can see a precise narrow inlet port from a F1 engine.

3.6 INLET VALVE AND VALVE SEAT

The inlet valve separates the combustion chamber from the rest of the intake system. It is the most important throttling component (when the throttle body is fully opened) on the intake side. The whole air flow to the engine has to go through the inlet ports and therefore it is logical that parameters like the valve lift, the valve stem length, the valve stem thickness, the valve seat and the valve shaping critically influence the air flow coefficient. The valve throat area and the intake manifold aperture area belong to other very important parameters. These two areas define the manifold to port area ratio (Fig. 20) which is critical for the performance of the engine. This ratio controls the amplitude of any pressure wave created within the ducting by the cylinder state conditions.

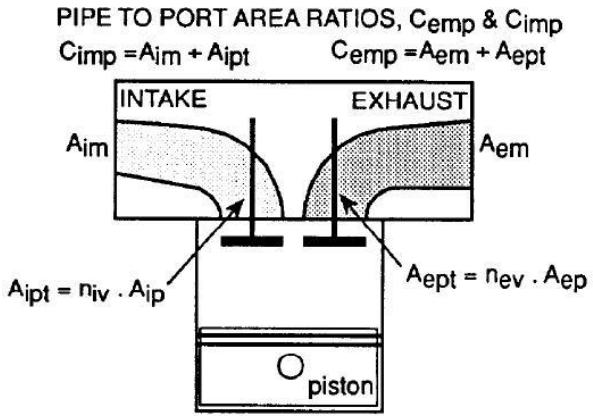

Fig.20 Pipe to port ratio [13]

There are eight engines in the chart in (Fig. 21). Each one is competitively famous for its purpose. The description of each engine simply means: swept volume, layout and number of cylinders, number of valves and application. F1 stands for Formula1, F2 for Formula 2, SRM stands for Supersports Motorcycle, SRC for Sport Racing Cars, ITC for Touring Cars and OPB stands for Offshore Powerboats.

	Measured manifold-port area ratio	
ENGINE	exhaust C_{emp}	intake C_{imp}
2.0L I4 4v F2	1.26	0.84
3.5L V12 4v F1	1.60	0.90
0.6L I4 4v SRM	1.40	1.00
3.0L V10 4v F1	1.40	0.90
3.5L V8 4v F1	1.60	0.90
4.5L V8 4v SRC	1.40	1.10
2.0L I4 4v ITC	1.20	1.00
8.2L V8 2v OPB	1.55	1.05

Fig.21 Measured manifold - port area ratio[13]

As is shown in (Fig. 21), the intake manifold to port area ratios of these top engines are keeping around 0.90 and 1.00which makes these values a good starting point in setting criteria for the intake port design.

The intake valve cross section area is another very important dimension. It should be around 0.6 D where D is the aforementioned cylinder bore. The valve should also be short to keep the weight at low levels but the above mentioned sharp angle of the intake port has to be adhereds. The valve seat angle should be around 45° which provides a good cylinder sealing. Racing engines also have radius shaping valve seats to secure better air flow. Sharp edges can cause a flow separation which decreases mass air flow through the valve seat.

Fig. 22 Racing valve cross section (F1) [14]

In (Fig. 22) there is a racing valve. As you can see the valve is hollow due to natrium cooling of the valve.

4 STRUCTURAL DESIGNS OF FORMULA STUDENT INTAKE SYSTEM

In contrast to common cars, where the intake system space layout matters, in racing prototypes like our Formula car several structural designs of intake system, providing the best charging, can be used.

There is not any best and clear solution of the intake system design. There are many factors that influence the intake system tuning. These factors will be mentioned in chapter 8 .

Generally there are three main variants of the intake system structural design: a system with the central airbox input under the main hoop, a system with the side airbox input, and a system with the central airbox input at the back of the car.

4.1 SYSTEM WITH CENTRAL AIRBOX INLET UNDER THE MAIN HOOP

This structural design (Fig. 23) is quite popular, especially for 4 cylinder engines. It can be slightly disadvantageous in terms of the COG (center of gravity) location but on the other hand the system is located against the driving direction, which enables the engine to be blast overcharged. The air stream-lines do not have to make any sharp bends which means that there are smaller velocity changes and thus the flow coefficient is better.

Fig. 23 System, with central airbox input under the main hoop [15]

4.2 SYSTEM WITH SIDE AIRBOX INLET

This structural design (Fig. 24) and (Fig. 25) can be very convenient due to a lower COG location and thus better assembling dimensions. This system is usually very compact and it perfectly fits to the free space above the engine. But there could be a problem with the equal air stream-lines directions to the intake runners - the last intake runner could be charged less than the first one.

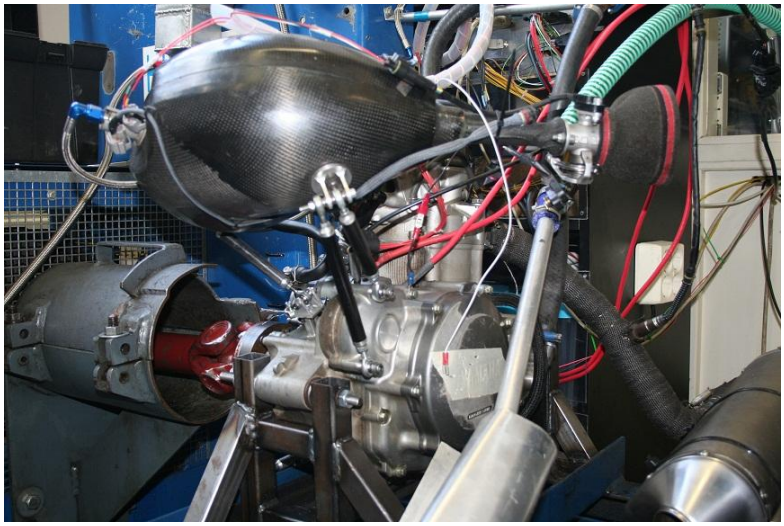

Fig. 24 System with side airbox input for 1-cylinder engine [16]

In (Fig. 24) you can see a TU Delft intake system; this big airbox can provide a better flow stabilization and engine charging, but because of the big airbox volume we can expect a worse engine response on the throttle.

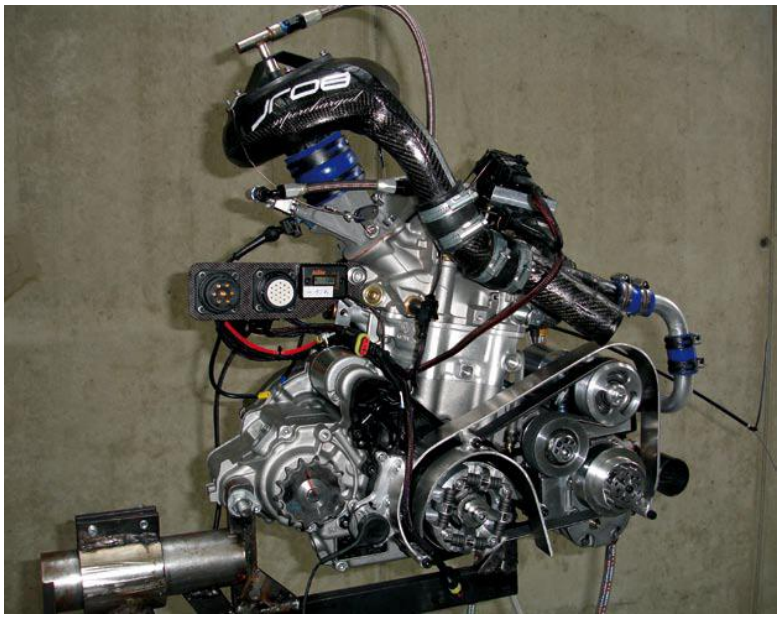

Fig. 25 System with side airbox input for supercharged engine [17]

4.3 SYSTEM WITH CENTRAL AIRBOX INLET AT THE BACK OF THE CAR

Owing to the low COG location, this structural design (Fig. 26) can have many advantages as well as the above mentioned system with the side airbox input. Air stream-lines go right to the airbox thanks to central airbox input and they do not have to make any bends.

This can be very positive regarding minimum hydraulic losses. On the other hand the intake system is located downstream the driving direction which means that the engine cannot be blast overcharged. The induction of hot air flowing from the hot engine could be another drawback. Hot air has a lower density which means that the engine will be able to induce less air; thereby the engine charging efficiency will fall and the engine performance will fall as well.

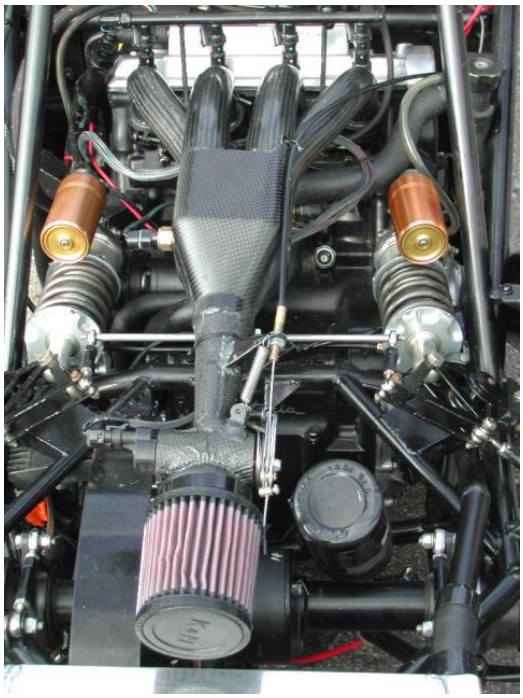

Fig.26 System with central airbox input at the back of the car [15]

The airbox in (Fig. 26) is quite small for a 4-cylinder engine; it could bring about worse charging, especially at higher engine speeds when the engine needs more air and has very little time for the induction.

5 RESONANCE OVERCHARGING

All naturally breathing racing engines use the resonance overcharging and our Formula Student engine is not an exception. It is very important to calculate perfectly both lengths and diameters of the intake runners to maximize the resonance effect on the engine overcharging. There is a rapid charging pressure increase at demanded engine speeds and when the resonance intake system is properly tuned, the charging efficiency rises as well. In some cases the charging efficiency can reach values around 120%.

There are three main principles how to overcharge the engine by resonance effects: Induction inertial ram cylinder overcharging, Induction wave ram cylinder overcharging and Helmholtz resonator cylinder overcharging. These effects work on a similar basis and they can occur together.

5.1 INDUCTION INERTIAL RAM CYLINDER OVERCHARGING

Most engines utilize the momentum acquired by the cylinder during its induction period (Fig. 27).

the beginning of the induction stroke, along with the end of the overlap period, the piston commences a move away from the TDC. The piston accelerates down the BDC and thereby the space between the cylinder head and the piston crown quickly expands. Depression, generated by this rapidly enlarging space, will be transmitted to the inlet port via the valve seat. Because of this pressure drop the column of charge, trapped in the induction manifold, moves towards the open inlet valve. Charge in the intake tract entering the cylinder acquires a high flow velocity due to a big difference in cross sectional areas of the piston and the intake tract. The momentum, built up by the fast-moving column of charge in the intake tract, comes to a halt when the inlet valve closes against the charge flow. Thus the kinetic energy generated by the fast-moving charge is converted to the pressure energy in the blanked out inlet port and consequently, the density of the charge rises. This pressure increase on the inlet port enables continuation in the cylinder charging after BDC. It also enables an earlier inlet valve opening due to pressurized charge that is stored behind the inlet valve head when it opens.[18]

"The greater momentum produce the greater pressure rise and if energy loses are very low in accelerating the flow, the inertial ram effect will be beneficial in cramming that extra mixture into the cylinder." [18]

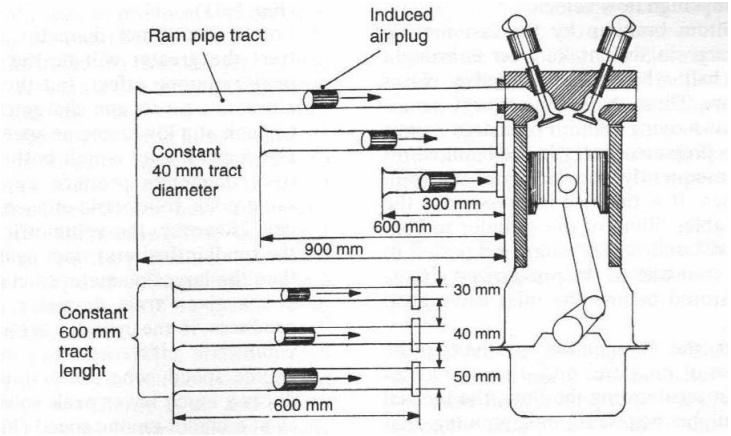

Fig.27 Method of evaluating inertial ram cylinder charging [18]

In (Fig 28) you can see the relationship between changing intake lengths from (Fig. 27) and the volumetric efficiency with a constant diameter.

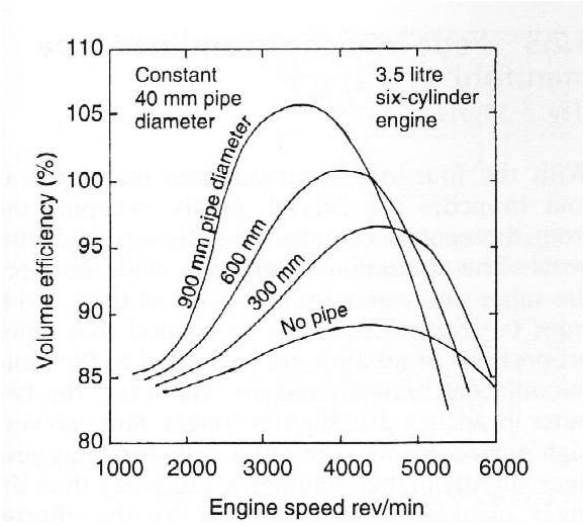

Fig.28 Relationship between inlet tract lengths and volumetric efficiency with constant diameter [18]

It is obvious that for a given tract diameter, the longer is the tract the greater is the charge column peak ramming effect; but the increased flow resistance causes the charge column pressure to peak at lower engine speeds. This could be a disadvantage for our Formula Student because we need both the maximum performance and the volumetric efficiency at high engine speeds.

In (Fig 29) you can see the relationship between changing intake diameters from (Fig. 27) and the volumetric efficiency with a constant length

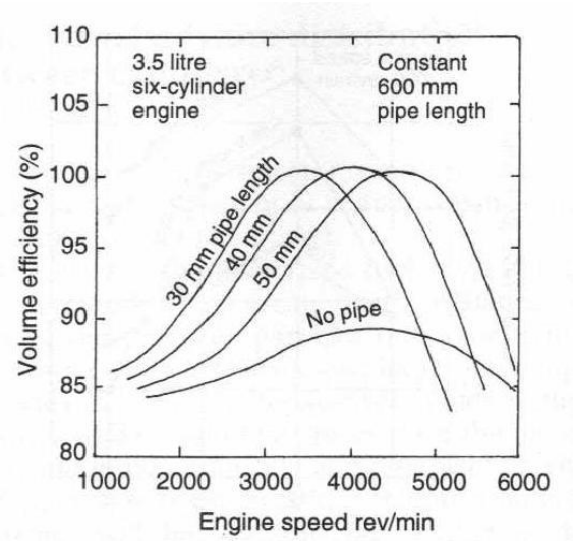

Fig.29 Relationship between inlet tract diameters and volumetric efficiency with constant length [18]

For a given tract length both small and large tract diameters produce approximately the same peak volumetric efficiency in the cylinder. However, the volumetric efficiency with the smaller diameter tract peaks much earlier than the larger one. [18]

5.2 INDUCTION WAVE RAM CYLINDER OVERCHARGING

When the engine is running, every time the inlet valve opens, the reduction in the cylinder produces a negative pressure-wave (primary wave), which travels at the speed of sound through the column of air (Formula (1) was used for the speed of sound calculation) from the back of the inlet valve to the open atmospheric end of the intake manifold. When this pressure-wave pulse reaches the atmosphere, there is a pressure change and as a result, a reflected positive pressure-wave is produced due to the inertia of the air; and this causes the pressure pulse to travel back to the inlet valve port. This wave, if timed correctly, is responsible for ramming the air into the cylinder when the piston is behind the BDC and is rising. When the pressure-wave reaches the inlet valve again, it reverses its direction and it is reflected outwards. These negative and positive pressure waves are continuously reflected backwards and forwards until the inlet valve is closed. When these waves move in a column of air, it is similar to a coil spring movement as you can see in (Fig. 30). [18]

To make use of the pressure wave pulse, it must be timed so that its first positive pressure wave arrives at BDC towards the end of the induction stroke at its peak amplitude.

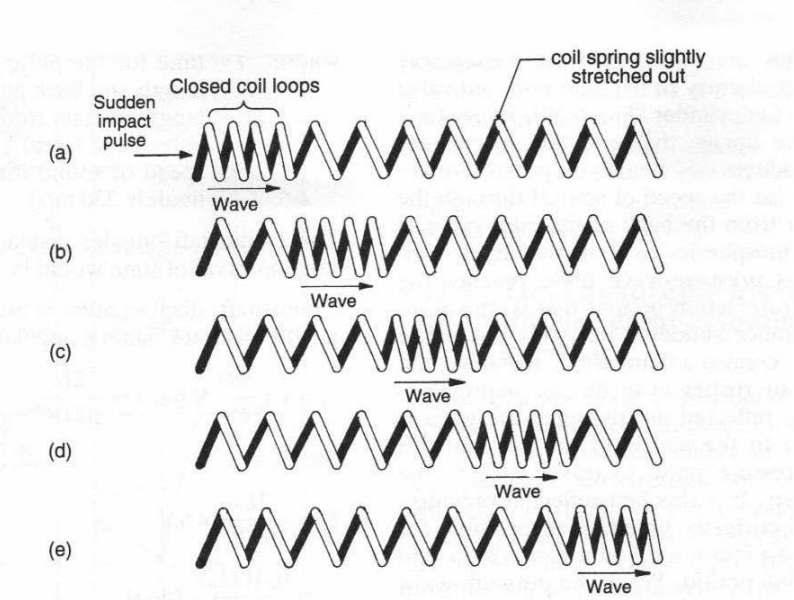

Fig.30 Illustration of wave moving [18]

"If the induction length is chosen so that θ_t= 90°(Fig. 31), that the cylinder pressure has risen to about atmospheric pressure at BDC and then moves to a positive pressure before the effective inlet valve closing point (EIC) that is effective inlet valve closing is reached. It can also be seen that the pressure-wave has peaked at BDC, which provides time for the charge in the inlet port to be transferred to the cylinder before the cylinder is cut off from its supply. This phasing of the resultant pressure-wave is therefore at its optimum for cramming the greatest amount of charge into the cylinder."[18]

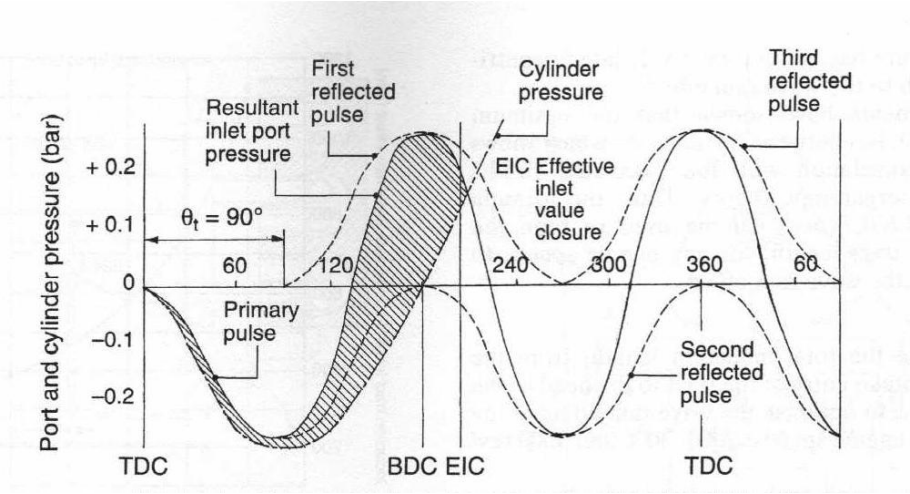

Fig. 31 Pressure wave movement [18]

SPEED OF SOUND CALCULATION

$$a = \sqrt{\kappa\, r\, T}, \tag{1}$$

κ – is Poisson constant,

r – gas constant for air,

T – air temperature.

There are two constants in the formula (1) and it is obvious that the temperature will have a major influence on the speed of sound magnitude which also can be seen in (Graph. 1).

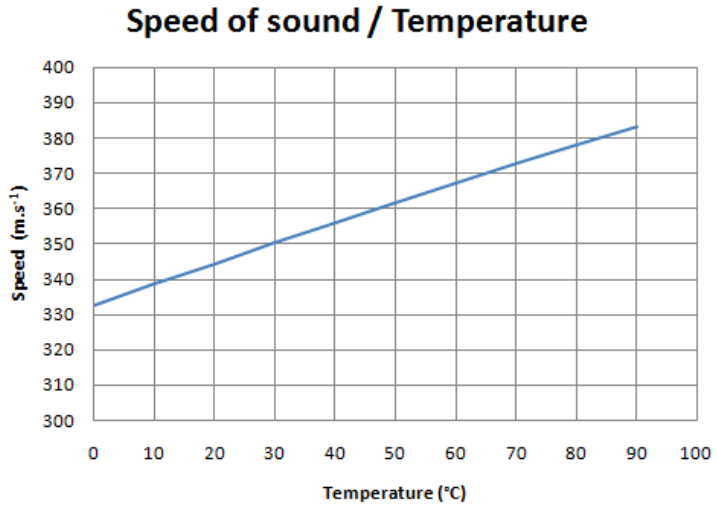

Graph. 1 Speed of sound on temperature relationship

That is why there are replaceable intake runners in racing cars which use the induction ram wave overcharging and which can be replaced when the weather changes before the race.

5.3 HELMHOLTZ RESONATOR CYLINDER CHARGING

The operating principle of the Helmholtz resonator is as follows: when the chamber of a given size is shaken, the air in the chamber will start oscillating at its own unique frequency, known as a natural frequency of vibration. Provided that this chamber is almost directly connected with the inlet port and the open ended pipe becomes the air intake tract, then every time the inlet valve is opened, a negative pressure wave pulse will disturb the air in the resonator chamber and the pipe. When the engine speed is increased so that the pressure wave pulse frequency corresponds to the natural frequency of the resonator, then the column of the air in the intake manifold will be excited to the resonance state and the amplitude of this pressure wave moving through the manifold will produce a series of jolts. If these waves are timed properly, they will bombard the cylinder with surges of the compressed air towards the end of the induction cycle when the piston goes against the incoming air-fuel mixture. As a result of this pressure wave bombarding, more charge will be crammed into the cylinder before the inlet valve closes.

The main principle is to choose the right volume of the manifold as well as the resonator resonating at an engine speed at where the boost of the torque is desired; it is also necessary to experiment with the tuned pipe length to reach the optimum results. But there can also arise problems caused by the interferences between the pressure wave pulses and the normal inertial ram effects; the cylinder filling may be impeded as a result. Therefore the experimental work has to be very careful to obtain the best possible compromise between the inertial and wave ram effects.

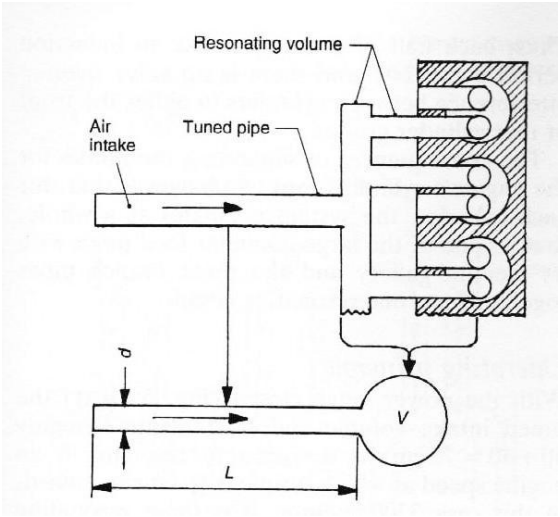

Fig. 32 Helmholtz resonator[18]

5.4 VARIABLE LENGTH INTAKE SYSTEM

All these ram induction charging systems produce an improvement in volumetric efficiency at certain engine speeds by means of individual cylinder induction pipes. This can be seen in (Fig 32).

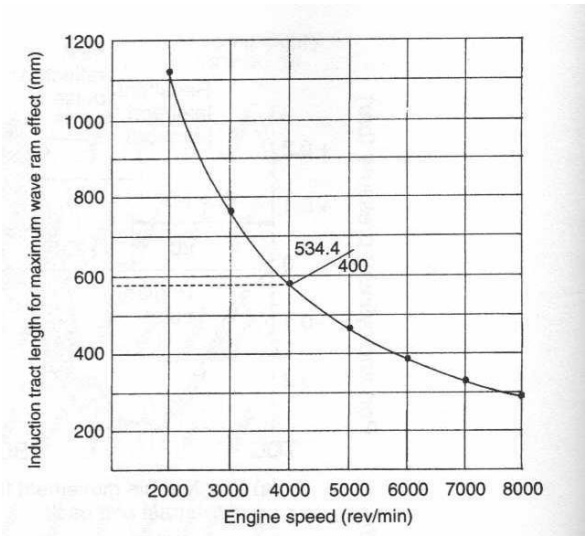

Fig.33 Relationship between intake tract length for maximum ram wave effect and engine speeds [18]

The variable length intake system has to be applied if we want to use the ram induction charging in a larger spectrum of engine speeds.

Two systems are the most common variable intake systems. These intake systems are composed of a mechanism that is able to switch between two various lengths of the intake runners. Longer intake runners provide better torque at low engine speeds and the shorter ones provide the maximum torque at high engine speeds. The switching part may be designed in many ways and almost every motor car company have their own system.

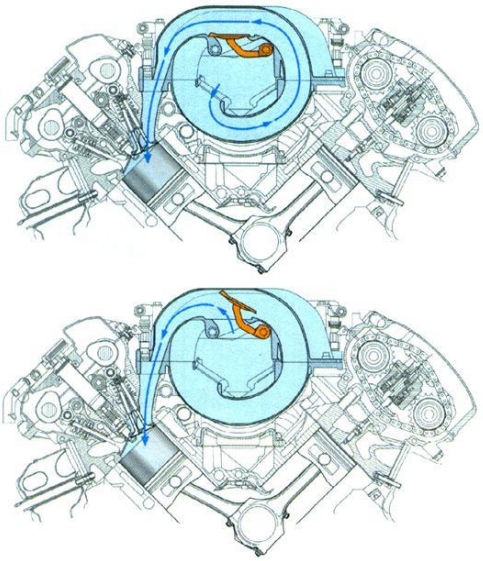

Fig. 35 Variable length intake system (AUDI) [18]

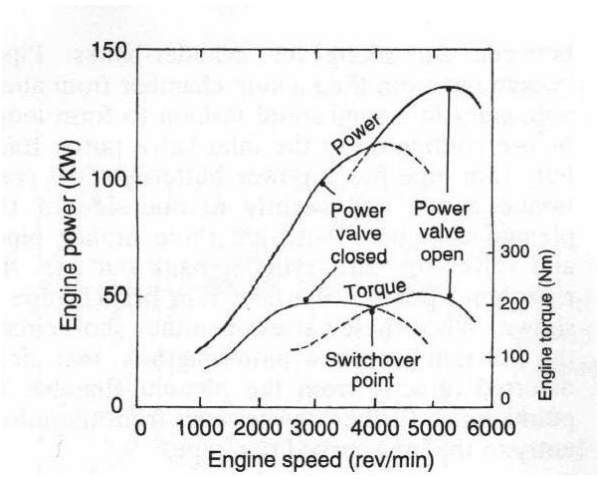

Fig. 34 Engine power and torque with variable length intake system (AUDI) [18]

In (Fig. 34) you can see the effect of a two stage variable intake. The mechanism switches the intake runner lengths at switching point (approximately 4,000 min^{-1})

Racing cars and motorcycles use simpler and yet very effective variable intake systems. In (Fig 36, Fig 37) there is a system used in Yamaha YZF-R1

Fig. 37 Variable intake system (Yamaha YZF-R1) [19]

Fig. 36 Variable intake system (Yamaha YZF-R1) [19]

The ideal intake system for today's naturally aspirated engines is a fully variable intake system, where there is an equivalent intake runner length for each engine speed. In (Fig. 38,Fig 39) there is a BMW full variable intake system. The rotating labyrinth is placed inside the resonator and it spins so that the maximum volumetric efficiency will be reached for every engine speed.

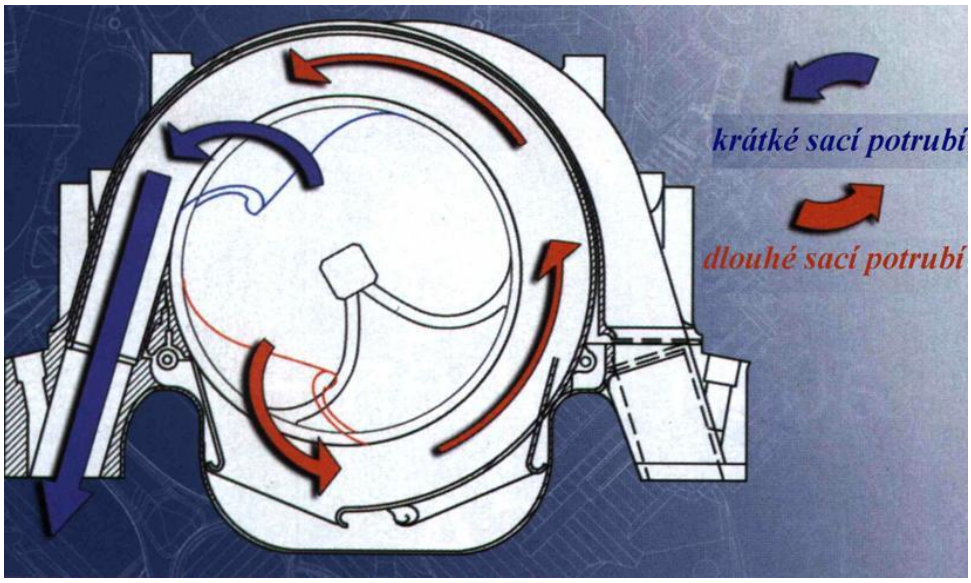

Fig. 38 Full variable intake system (BMW) [20]

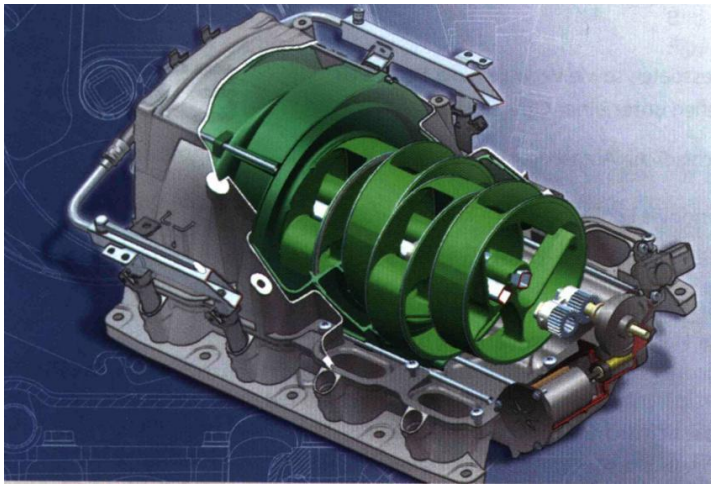

Fig. 39 Full variable intake system (BMW)[20]

5.5 DESIGN CALCULATION OF THE LENGTH OF RAM WAVE INTAKE RUNNER

For the design calculation I will use relation (1). As has already been noted, the temperature of the induced air has a main effect on the speed of sound in a given environment, and magnitude of this speed influences the length of the ram wave intake runner.

I have decided to choose a mean temperature in the intake system around 296K that means around 23°C.

MEAN SPEED OF SOUND CALCULATION

$a_s = \sqrt{1.4\ \ 289\ 296.15}$,

$a_s = 346.15\ m.s^{-1}$,

where: $\kappa = 1.4$,

$r = 289$ J.kg^{-1}.K$^{-1,}$

$T_S = 296.15$ K.

LENGTH OF THE RAM WAVE INTAKE RUNNER CALCULATION

$$l_{rez} = \frac{a_S}{8n}, \quad (2)$$

where: a_s – mean speed of sound,

n – engine speed [s^{-1}].

Computed values depending on the engine speeds

Engine speed [min^{-1}]	1,000	2,000	3,000	4,000	5,000	6,000	7,000	8,000	9,000
Runner length [m]	2.596	1.298	0.865	0.649	0.519	0.432	0.370	0.324	0.288

As has been explained before, the length of the ram wave intake runner is shortened with increasing engine speeds and as the (Graph. 2) shows, the dependence of the length on the engine speed is exponential.

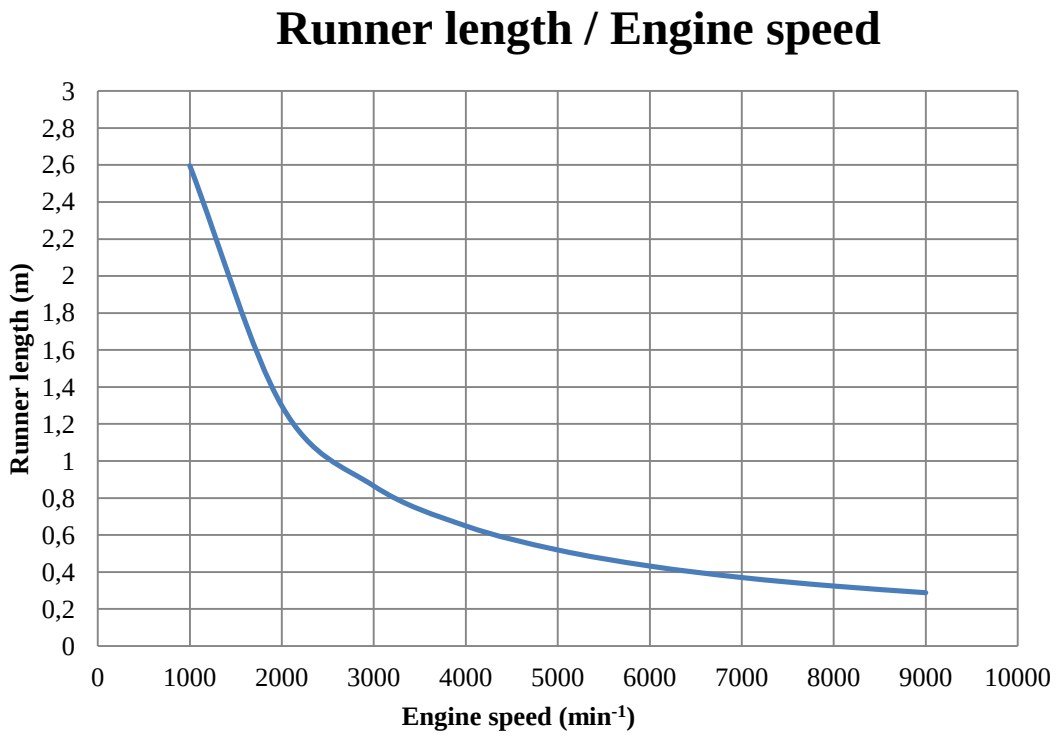

Graph. 2 Intake runner length to engine speed relationship

There are two possibilities of the runner length tuning, maximum torque and maximum performance tuning.

5.5.1 MAXIMUM TORQUE TUNING

If we want the best course of the torque through the spectrum of engine speeds, we need the runners as long as possible. But these long runners are not applied in practice because of too large intake manifold dimensions. We can use the Helmholtz resonator where volumes are used for the manifold tuning instead of the length. Therefore the Helmholtz resonator is a better choice for low engine speeds.

5.5.2 MAXIMUM PERFORMANCE TUNING

On the other hand we can also tune the intake manifold to the "maximum performance" through choice of very short intake runners that only provide the maximum ram wave effect at high engine speeds. The drawback of this tuning is that the engine only works in a narrow spectrum of engine speeds and the course of the torque is not as good as with longer intake runners. But this tuning is frequently used in the circuit racing where the course of the torque is not so important compared to the performance course. We can let the car held in this thin spectrum of maximum power.

Formula Student is a circuit competition as well. Because we use a one cylinder engine with a big displacement, our engine provides a lot of torque in a very large spectrum of engine speeds. As a result we can afford to tune the intake manifold to the maximum performance.

6 LOTUS ENGINE SIMULATION SOFTWARE

There is an engine cycle simulation tool, developed for the Lotus own engine research and development department. The tool has been developed thanks to Lotus extensive experience with application of the performance simulation in the engine design projects. The tool can be used to simulate the performance of two and four stroke, gasoline and diesel, naturally aspirated or supercharged and turbocharged engines. The Lotus Engine Simulation models the gas dynamics in the engine manifolds and enables the complex operating modes used in modern engines to be simulated, it combines a dimensionless model of the cylinder, combustion models, heat transfer models and 2D flow through each part.

6.1 MANIFOLD PROPERTIES

Every part of the manifold in the Lotus engine simulation can be described by the inlet diameter, the outlet diameter, the length, the wall thickness, the material and friction and heat transfer coefficients (Fig 40). The software also enables to use a model of manifolds which are defined by an exact diameter for individual lengths (Fig. 41).

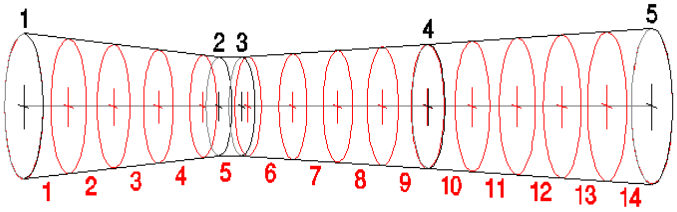

Fig.41 Model with different diameters for each length

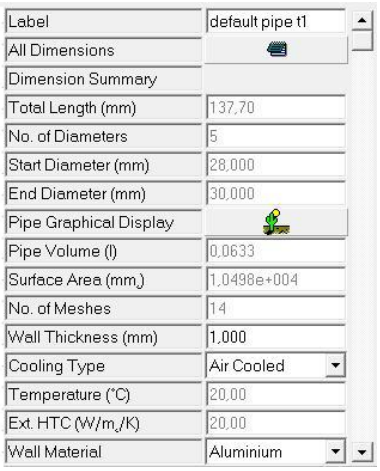

Fig.40 pipe input parameters

6.1.1 MANIFOLD ELEMENTS

As you can see in (Fig. 41), the manifold is divided into several elements. This provides a possibility to calculate instantaneous parameters of the flow through each element. When you set the basic manifold parameters, the software creates its own number of elements and it may be very accurate, which results in the slow-down of the calculation. Therefore, your own parts setting will be a better option. For the intake manifold the Lotus Engine Simulation recommends the length of the parts between 15 and 20mm and for the exhaust manifold between 25 and 30mm. These settings may enable a better calculation running but they can also induce some inaccuracies in the calculation because of very fast changes, e.g. changes of the temperature in the exhaust manifold with rising engine speeds.

As I have mentioned before, the Lotus Engine Simulation can only simulate a 1D flow, therefore the step changes in the manifold or in a manifold with big sequential changes in the flow area are not suitable for the calculation running and the results are very often non convergent.

6.1.2 MANIFOLD HEAT TRANSFER PROPERTIES

For the heat transfer calculation through the pipe the Lotus Engine Simulation uses an ordinary equation for simple convective heat transfer in the radial direction from the gas to the manifold. Formula (3) is the heat transfer per unit mass

$$q = \frac{4h}{\rho D}\left(T_w - T_g\right), \tag{3}$$

where: q – heat transfer,

h – convective heat transfer coefficient,

T_w – temperature of the pipe inner wall,

T_g – temperature of gas,

D – manifold diameter,

P – gas density.

6.1.3 MANIFOLD MATERIALS

The Lotus Engine Simulation uses the heat transfer through the pipe wall equation for its calculation. Therefore we can also choose which kind of material to use for the pipes and we also have to set the wall thickness. This provides a better model of the engine to us and the final calculation can be more accurate. The Lotus Engine Simulation includes some basic pre-set materials which can be seen in (Tab.7).

Tab 7 Pipe (manifold) material properties

MATERIAL	DENSITY [kg/m^3]	THERMAL CONDUCTIVITY [W/m/K]	SPECIFIC HEAT CAPACITY [kJ/kg]
STEEL	7,900	48	490
ALUMINIUM	2,700	204	940
PLASTIC (POLYAMIDE 6,6)	1,400	0.25	1,256
MAGNESIUM ALLOY (AS21)	1,760	86	1,005

For both the simulations that next chapter will concern, I have chosen types of materials according to the real situation on the engine so that the model is as accurate as possible. For the intake runner I have chosen plastic and for the inlet and exhaust port I have

selected aluminium because these two ports are inside the cylinder head that is made of aluminium alloy.

For the exhaust manifold steel has been chosen.

6.1.4 COOLING MEDIUM

The Lotus Engine Simulation also contains several cooling media (Tab. 8) because the temperature of the surroundings also influences the heat transfer calculation. Lotus offers two types of cooling media (water, air). Again I have selected a cooling medium according to the real situation on the engine. For the intake runners it is air and for the inlet and exhaust ports it is water in accordance with the water cooled cylinder head.

Tab 8 Pipe (manifold) data

COOLING MEDIUM	COOLANT TEMPERATURE [°C]	CONVECTIVE HEAT TRANSFER [W/m^2/K]
AIR	AMBIENT AIR TEMP.	20
WATER	100	5,000

6.1.5 LOSS JUNCTIONS

The intake and exhaust manifolds also include junctions like inlet ports, exhaust ports and exhaust branch pipes. If we want to build a simulation model of the engine as close to reality as possible, we have to involve the loss junctions as well (Fig. 42).

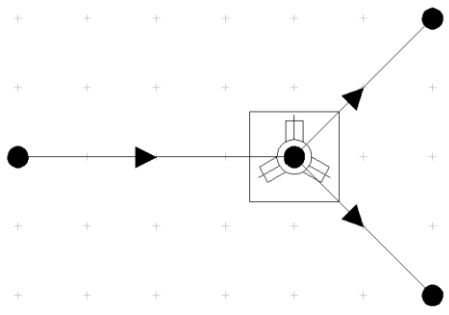

Fig. 42 Loss junction

These loss junctions should simulate hydrodynamic losses which come up with the friction between the pipe wall and gas or air fuel mixture when they flow through a real junction like the above mentioned intake or exhaust ports etc. As we know, the flow velocity has a radical influence on hydrodynamic losses. These losses are increased with a higher flow velocity and the flow velocity is logically increased by higher engine speeds. In (Fig. 43) a loss junction model from the Lotus Engine Simulation is shown. The red pipe is a reference and angles of all the other pipes are related to this reference. If the pipes are not in one plane, than another reference pipe is required (blue pipe).

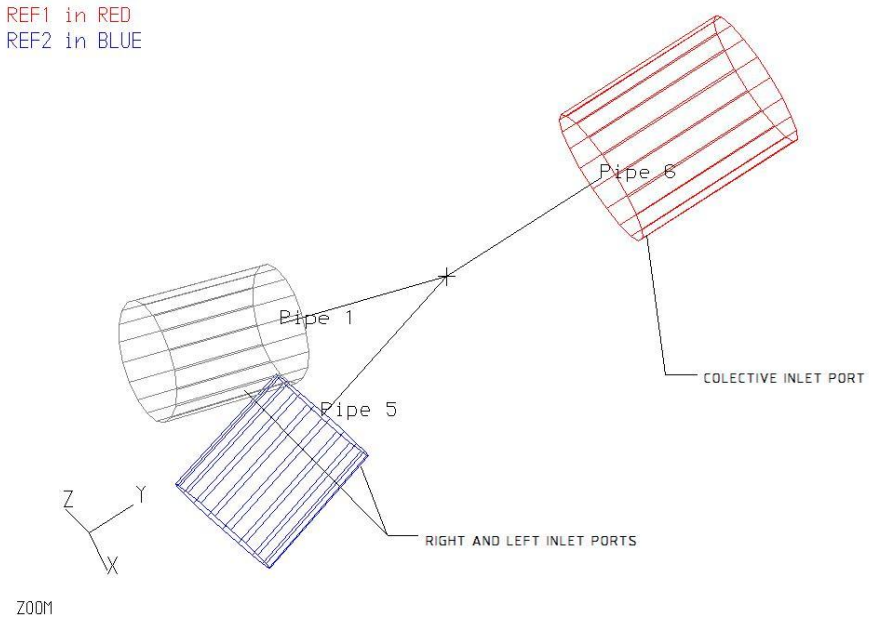

Fig.43 Loss junction model for intake port

6.2 ENGINE COMBUSTION MODELS

To be able to simulate the flow through the intake or exhaust manifolds precisely, we need to know how much heat was generated during the combustion and what was the combustion course. Mathematic combustion models are a fundamental basis of the engine thermodynamic simulations. There exist basic theoretical models but these models are not applicable because of the fact that they are working with ideal thermodynamic processes. The Lotus Engine Simulation uses combustion models which enable to describe state values changes in the cylinder.

Heat that is released during the combustion of the air-fuel mixture is a basis of the energy transformation in the cylinder. But the amount of the released heat is not the only factor that influences values like the engine heat efficiency, the indicated engine performance etc., Another factor is a course of the combustion which has a radical effect on the values as well. The amount of released heat is expressed by calorific value of fuel and the amount of burned fuel we can see expressed by Formula (4)

$$dQ_B = H_u . dm_b \, , \tag{4}$$

where: dQ_B – heat released from fuel,

H_u–calorific value of fuel,

dm_b – amount of burned fuel [kg].

6.2.1 VIBE COMBUSTION MODEL

A German engineer Vibe derived a dimensionless formula which is called the Vibe combustion model. It was derived in a semi-empirical way and the formula (5) indicates the relative amount of heat in dependence on the relative combustion time.

$$x = 1 - e^{-ay^{m+1}}, \tag{5}$$

where: a – unburned fuel in cylinder ratio,

m – combustion parameter.

x and y which are both dimensionless parameters are defined in formula (6),(7).

$$x = \frac{m_B(\varphi)}{m_B}, \tag{6}$$

$$y = \frac{t(\varphi)}{t_H}, \tag{7}$$

where: $m_B(\varphi)$ – mass of fuel burned in elapsed time $t(\varphi)$,

m_B – mass of fuel burned in total combustion time t_H,

$t(\varphi)$ – elapsed combustion time,

t_H – total combustion time.

Course of the Vibe formula for a changing parameter m is shown in (Graph. 3).

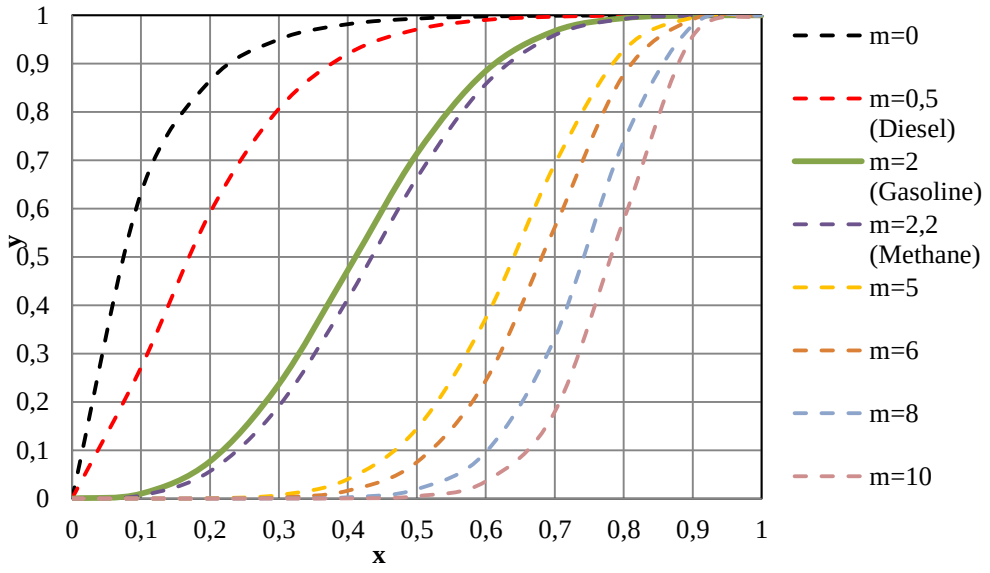

Graph. 3 Vibe fuel burning in cylinder

(Graph. 3) shows burned rate of fuel in dependence on the time rate of total combustion time. At the start of the combustion $y = 0$ and $x = 0$ and at the end of the combustion $y=1$ and x is shown at formula (8).

$$x = 1 - e^{-a}, \tag{8}$$

With the parameter *m* changes we are able to influence the course of combustion in the cylinder. When we differentiate the Vibe formula (formula (9)), we get the course of the combustion intensity in a given time. At (Graph. 4) we can see the course of combustion for a changing parameter *m*

$$\frac{dx}{dy} = a\,(m+1)\,y^{m}\,e^{-ay^{m+1}}, \tag{9}$$

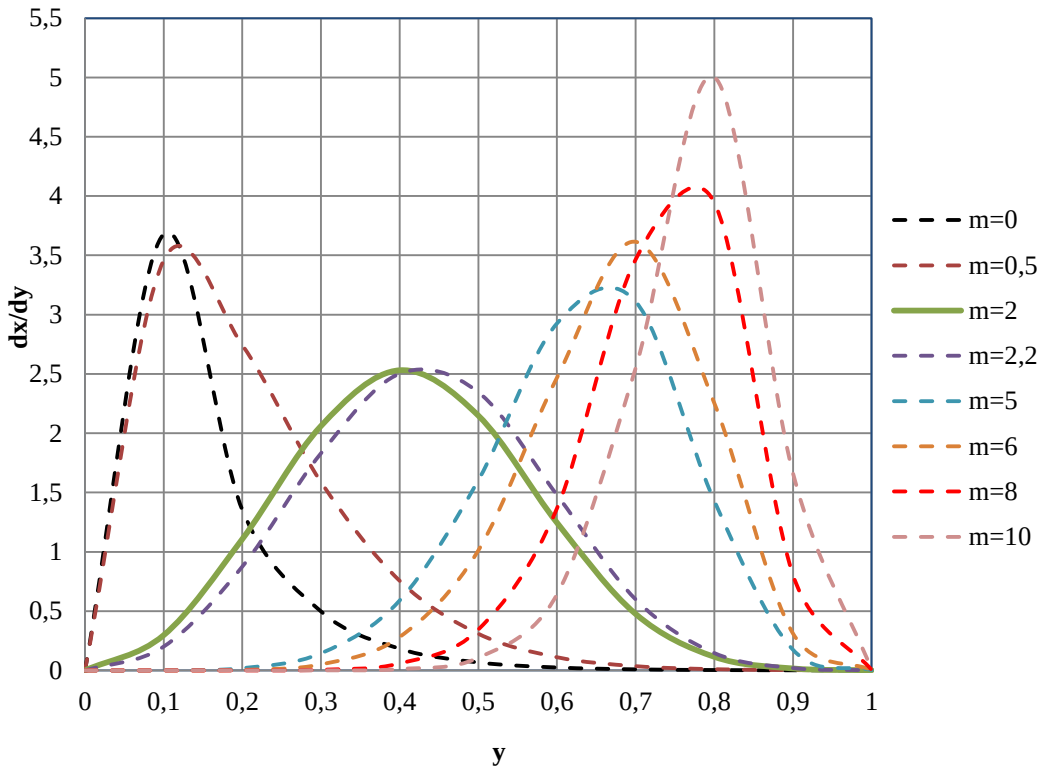

Graph.4 Courses of fuel combustion for changing parameter m

Many parameters (like pressures and temperatures in the cylinder) that radically influence the final engine performance depend on the course of combustion. The Vibe combustion model works with the aforementioned parameters *m* and *a*. These parameters cannot be chosen randomly because they depend on many other parameters like the shape of the combustion chamber, the fuel charge, the time of injection, the engine speed etc.

In the Lotus Engine Simulation I have simulated many variants of combustion models with different parameters *m* and *a*, I have observed behavior of the performance course with the same engine simulation model and from my point of view the parameters *m=2* and *a=10* seem to represent the most convenient choice.

6.2.2 CYLINDER HEAT TRANSFER

During the combustion process the heat transfer occurs between gas and the cylinder wall and also the losses caused by the heat passage occur through the cylinder wall. We can divide the whole cylinder heat transfer into three stages.

- convection heat transfer between gas inside the cylinder and the inside cylinder wall
- heat conduction through the cylinder wall
- heat transfer between the outside cylinder and the coolant (in our case, water)

The Lotus Engine Simulation uses a formula (10) for the calculation of the cylinder wall temperature.

$$q_w = \frac{T_w - T_c}{\frac{1}{\propto_c} + \frac{\delta_w}{\lambda_w}}, \tag{10}$$

where: T_w – wall temperature,

T_c – coolant temperature,

α_c – heat-transfer coefficient of coolant,

δ_w – heat conductivity of cylinder wall,

λ_w – cylinder wall thickness.

This formula is analogous to the Ohm's law as you can see in (Fig. 44). Heat transfers are serially lined up like resistors. But it does not describe a heat transfer between gas inside the cylinder and the inside cylinder wall. This convection heat transfer is computed by another formula.

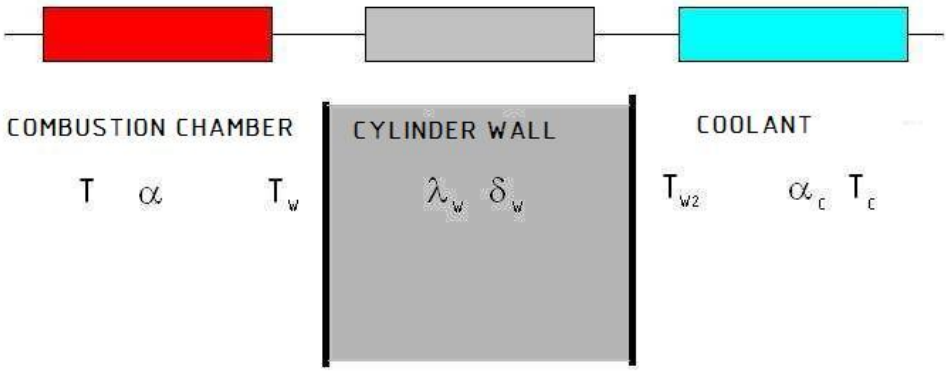

Fig.44 Heat transfer scheme [21]

Formula (10) is composed of two parts. First (formula (11)) is a part which represents heat convection through the cylinder wall.

$$q_{w2} = \lambda_w \frac{T_w - T_{w2}}{\delta_w}, \tag{11}$$

Second part (formula (12)) represents convection heat transfer between the outside cylinder wall and the coolant.

$$q_c = \alpha_c (T_{w2} - T_c), \tag{12}$$

Therefore we can deduce temperature of the cylinder wall T_w from formula (10). Formula of this temperature is formula (13).

$$T_w = q_w \left(\frac{1}{\alpha_c} + \frac{\delta_w}{\lambda_w} \right) + T_c , \tag{13}$$

Values from the formula (13) can be selected by a user or can be preset like default values in the Lotus Engine Simulation. Coolant temperature and heat transfer coefficient for the coolant are one of these preset values. We can also set the material of the cylinder head and the engine block with preset values of the heat conductivity (Tab. 9) or – in case we have sufficient measured data – we can define our own material with measured or computed values of the heat conductivity. For our purpose I have chosen aluminium alloy for both parts.

Tab.9 Heat conductivity of default Lotus materials

MATERIAL	**HEAT CONDUCTIVITY** (W/m/K)
ALUMINIUM	45
CAST IRON	150
STEEL	48
ZIRCONIUM	4.1

Calculation of the convection heat transfer between gas inside the cylinder and the inside cylinder wall is the last step of the total heat transfer calculation. Heat transfer inside the cylinder can be described with the basic analytic formula (formula (14)).

$$\dot{Q} = \alpha A (T_w - T), \tag{14}$$

where: α – heat-transfer coefficient,

A – instantaneous value of combustion chamber area depend on actual piston, location

T – gas temperature,

T_w – cylinder wall temperature.

The Lotus Engine Simulation also works with Annand, Woschni or Eichelberg heat transfer models. All these models are used for setting values of the cylinder heat-transfer coefficient.

6.3 CAM PROFILE

Because the cam curve of our engine was not available, we had to measure the cam curve ourselves.

6.3.1 CAM PROFILE MEASUREMENT

The measurement was carried out in the laboratory of the Automotive Engineering Institute Brno University of Technology.

Cam curve was measured with the cam shaft inside the cylinder head. Removing the ignition cover was the first step. Then I put a circle for the angle measuring (Fig. 45) to the ignition rotor and I also fixed a piece of wire to the engine block to be able to measure the actual crankshaft angle to a fixed point.

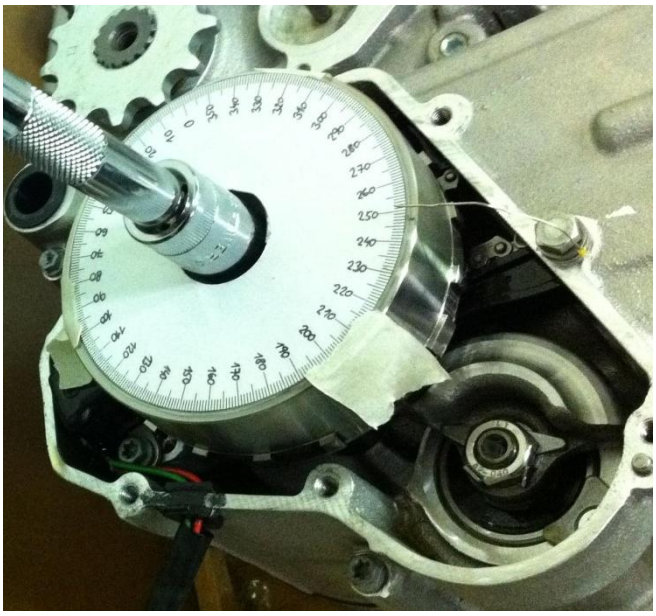

Fig. 45Cam profile measurement

Then I had to find a compression TDC which was not difficult because there is a TDC mark on the camshaft drive chain sprocket. After that I set the circle for the angle measuring to zero, which was followed by the dial indicator installation. I put it on the valve shim, so that the gauge was located in the axis of the valve (Fig. 47). This was important for the measurement accuracy. If the indicator was positioned anywhere else, the valve lift measurement would be very inaccurate. After that I started to rotate the crankshaft and every 5 degrees we measured and wrote down values of the valve lift on the valve shim. I did the measurement for each intake and exhaust valve.

Fig. 46 Dial indicator instalation

Fig. 47 Cam profile measurement

6.3.2 CAM MEASUREMENT COMPARISON

I put the data resulting from our measurement to Microsoft Excel and as a result the inlet and exhaust valve lift characteristics were obtained. I also wanted to verify our measurement which is the reason why I compared our measurement with the Lotus Engine Simulation.

Lotus has its own cam profile generator, (Fig. 48) and when the valve lift and the opening and closing angle are entered, Lotus is able to generate, using the preset polynominals. This method can only be used in case the engine uses a symmetric cam and the Husaberg FE 570 uses such a cam.

I first generated the cam profile in Lotus and exported the generated data to Microsoft Excel,

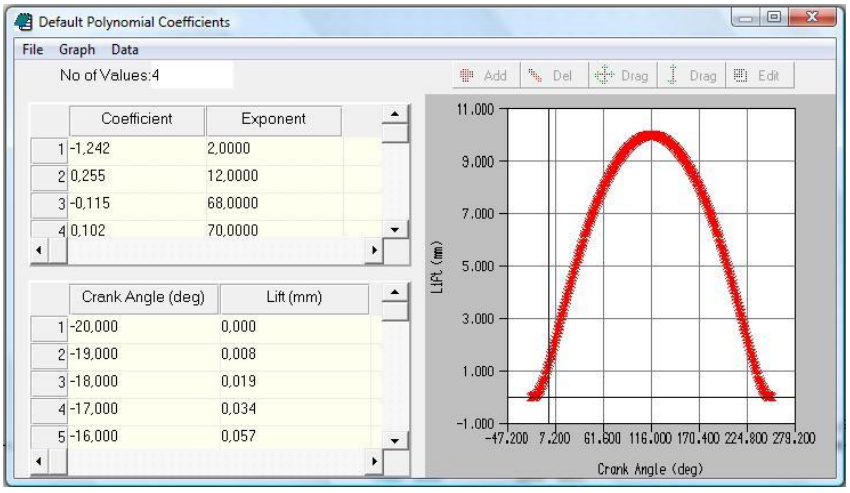

Fig. 48 Lotus cam profile generator

then I made a comparison of our measurement data and the Lotus data. Results for each valve can be seen at (Graph. 5, Graph. 6)

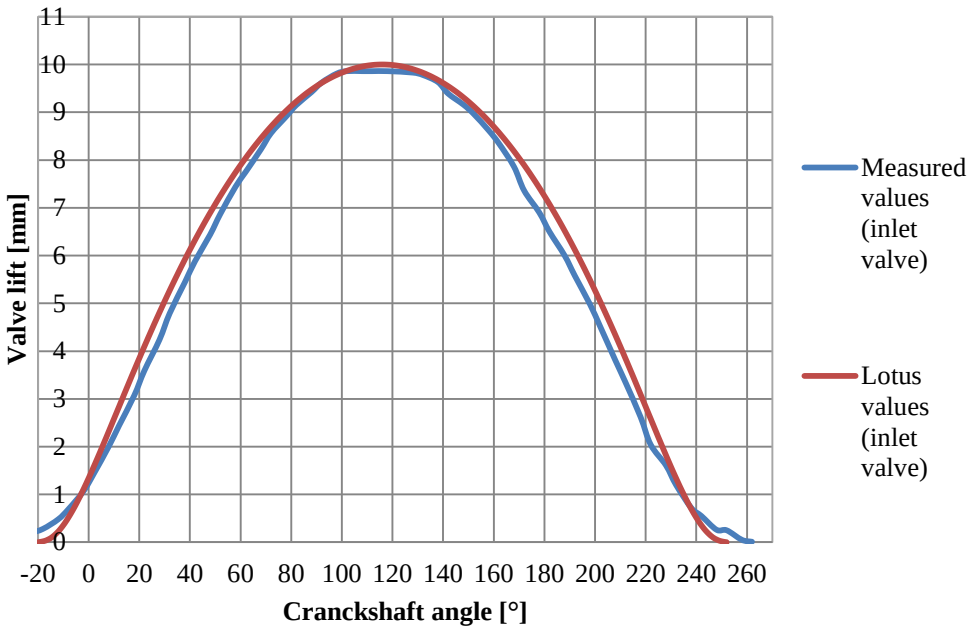

Graph.5 Comparison of measured and lotus values of inlet valve lift

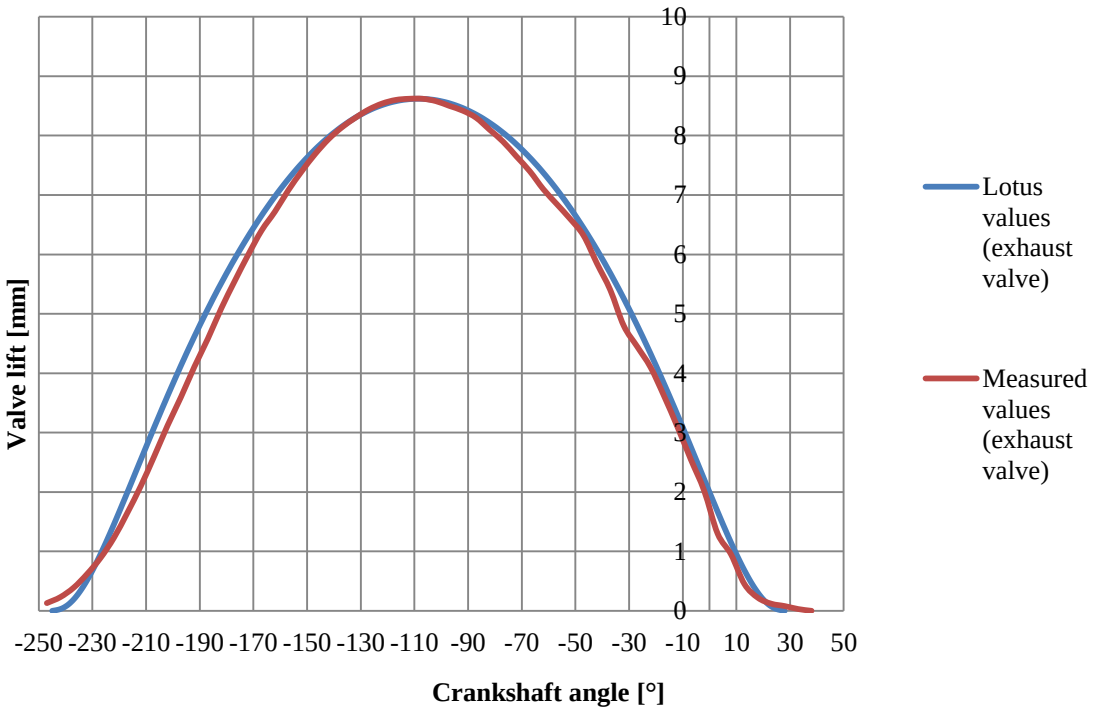

Graph.6 Comparison of measured and lotus values of inlet valve lift

For both the inlet and exhaust valves, measured values are very similar to the Lotus values. It can be seen in (Graph. 6). After the maximum exhaust valve lift, the exhaust valve is pushed down by a valve spring and here it was very hard to keep the crankshaft rotation by 5°. Therefore there are small offsets here. There is no doubt that these offsets are rather insignificant because the course of our cam profile is very similar to the Lotus course. I repeated this measurement 3 times for a better measurement accuracy.

This measurement was of high importance because the measured values are to help to improve the engine model for the simulation so that the results approach the reality.

6.4 PORT FLOW COEFFICIENTS

Good inlet and exhaust ports are the basis of high performance engines and global shape of these ports radically influences flow through the cylinder head and also the engine performance. Lotus simulates the shape of the port using C_f (port flow coefficient). This coefficient (formula. 15) depends on the valve lift/port throat diameter ratio. Lotus offers two possibilities of the data entry. There are few default ports with preset C_f values. This option can be used when you do not have any measured data on the C_f values. The second option provides a possibility to define our own inlet or exhaust port by the measured data.

$$C_f = \frac{\dot{m}_{real}}{\dot{m}_{theor}}, \tag{15}$$

where: C_f – port flow coefficient,

$\dot{m}_{real}$ – real mass flow through the port,

$\dot{m}_{theor}$ – theoretical flow through the port.

$$\dot{m}_{theor} = v\big(f(p_o, p_c, T)\big).S_{ref}.\rho\,, \tag{16}$$

where: - $v(f(p_o,p_c,T))$ – theoretical flow speed,

S_{ref} – valve throat area,

ρ – density of medium.

I decided to choose the second option, namely to use the measured data.

6.4.1 PORT FLOW DATA MEASUREMENT

The measurement was carried out in the laboratory of the Automotive Engineering Institute Brno University of Technology on the flow bench Super Flow SF-260.

First of all I mounted the cylinder head of the Husaberg FE 570 engine with the intake valves on the flow bench, then I had to mount the inlet pipe with the bellmouth on the inlet port (Fig. 49). When everything was mounted and prepared for the measurement, I set the pressure drop to 5,000 Pa (Fig. 50) and the valve lift to 1 mm. I measured the mass flow through the inlet port with a constant pressure drop. It was possible to measure the mass flow with a constant velocity but this solution did not meet our requirements.

Fig.49 Cylinder head on the flow bench

Then the measurement followed. I was opening the inlet valve by 1 mm at a time until I reached 10 mm which is the maximum measured valve lift. After every *mm* of the valve lift I recorded down the value of the mass flow which was measured in $l.s^{-1}$. Midway through the measurement I found out that the pressure drop is too big and the flow bench is not able to suck in sufficient amount of air due to the Husaberg enormous inlet ports, therefore I had to lower the pressure drop to 4,000Pa. After I had gained all the measured values for each valve

Fig. 50 Flow bench display

lift, I had to calculate port flow coefficients (C_f) for each valve lift. I used formulas (15,17,18) for the C_f calculation.

$$v_t = \sqrt{\frac{2(p_1 - p_2)}{\rho}} = \sqrt{\frac{2p_d}{\rho}}, \tag{17}$$

where: v – theoretical speed,

p_d – pressure drop,

ρ – density of medium.

Formula (15) represents a calculation of the theoretical velocity of flow at a given pressure drop.

$$\dot{m} = S.v = \pi \frac{D^2}{4} v_t, \tag{18}$$

where: S – area of valve throat ,

D – valve throat diameter.

(Tab. 10) shows the measured data and final port flow coefficient for each valve lift.

Tab.10 Measured values for each valve lift

VALVE LIFT(mm)	QV($l.s^{-1}$)- MEASURED	QV(m^3s^{-1}) - MEASURED	PRESSURE DROP (Pa)	CF
1	16.2	0.0162	5,000	0.099
2	31.2	0.0312	5,000	0.19
3	47.2	0.0472	5,000	0.29
4	60.9	0.0609	5,000	0.37
5	74.7	0.0747	5,000	0.46
6	77.8	0.0778	4,000	0.53
7	83.2	0.0832	4,000	0.57
8	86.9	0.0869	4,000	0.59
9	85.9	0.0859	4,000	0.59
10	86.5	0.0865	4,000	0.59

The Lotus Engine Simulation uses the port flow coefficient in dependence on the L/D ratio (valve lift /valve throat diameter) for the mathematical modelling of the port, therefore I put these values to (Graph. 7).

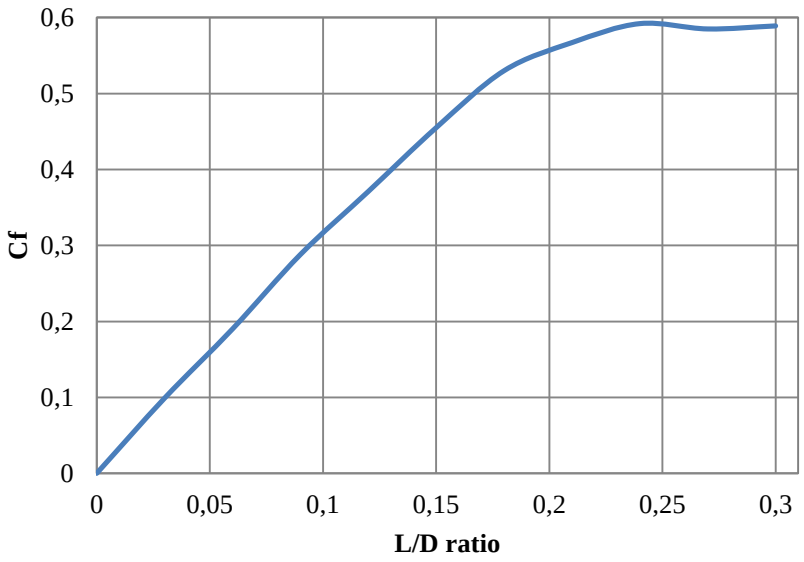

Tab 11 L/D ratio to portflow coeficient ratio

With help of this measurement and the obtained results, I was able to improve my engine model; these improvements led to specifications of the simulation and also its results. As you will see in the next chapter, there is a considerable difference between a default Lotus port model and a real model that is composed of the measured data. I repeated this measurement 3 times and I applied the mean average of all measured values. Flow Com measurement accuracy was +- 0,5% of reading.

7 CREATION OF STOCK ENGINE SIMULATION MODEL

Because no Performance/ Torque course could be found and the manufacturer did not provide these characteristics either, I had to make a simulation model of the stock engine so that our team could have at least some information about the aforementioned characteristics. When I entered the data to Lotus, I made an effort for every parameter to be as close to reality as possible. Naturally I could not set every parameter exactly as if on the engine, because Lotus only allows entering the circular geometry for the pipe elements. Therefore I had to substitute elliptical areas like the inlet port input, which is located in the cylinder head, or connection area of the inlet ports. In (Fig. 51) you can see a simulation model of the stock engine.

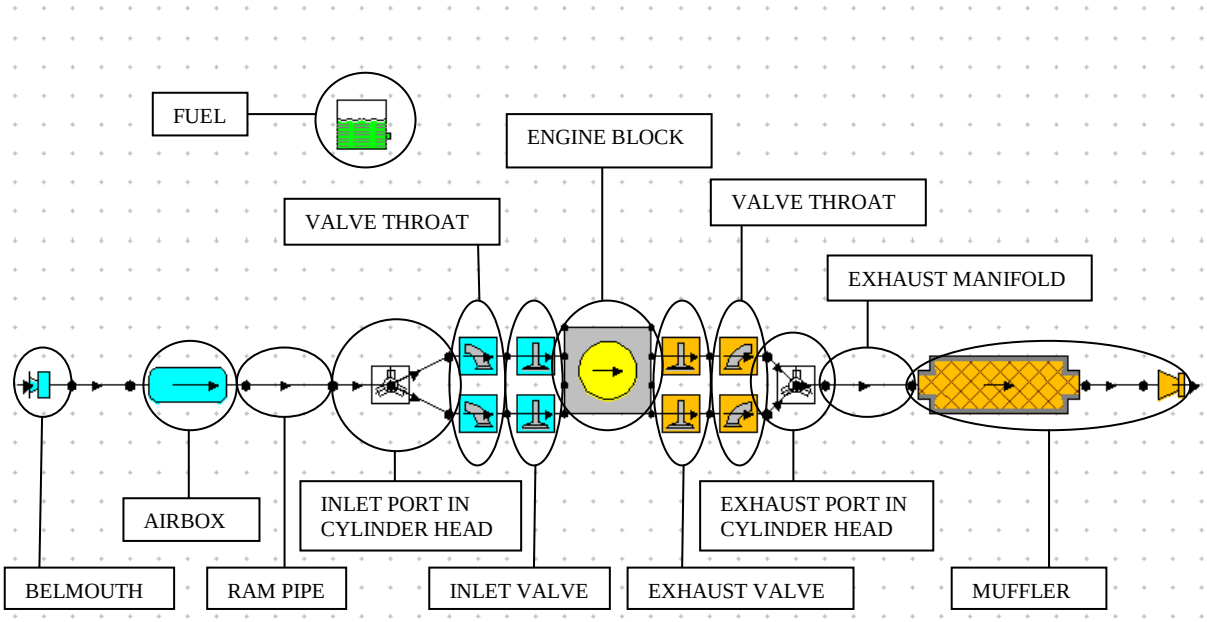

Fig.51 Simulation model of stock engine in Lotus engine simulation

The last step remaining to bring the model as close to reality as possible, was measuring the inlet port geometry.

7.1 INLET PORT GEOMETRY MEASUREMENT

This measurement included 2 steps. The first step was casting of the inlet ports to get a solid model of the inlet ports. The second step consisted of scanning and modelling of the inlet port casting to get CAD data of the inlet port geometry and cross section areas of the inlet ports. These areas were exported to Lotus

7.1.1 INLET PORT CASTING

Considering previous experience I decided to cast the inlet port from double-barrelled silicon caoutchouc Lukopren N 1522. However, as it turned out, it was not the right decision because Lukopren was not elastic enough and when I was trying to pull the casting out, it ripped up. For another test I chose Lukopren N 5221 which is convenient for more exacting castings, has better elasticity and tearing resistance as well.

The whole casting process was carried out in the laboratory of the Automotive Engineering Institute Brno.

The first step was sealing off the valve throat with valves, than I had to prepare the casting Lukopren mixture. When all preparations had been carried out, I poured the mixture to the inlet port and after that I let the mixture solidify. As the next step came pulling the casting out. In (Fig. 52) you can see the final inlet port casting.

Fig. 52 Inlet port casting

7.1.2 SCANNING AND MODELLING OF INLET PORT CASTING.

The whole scanning process was carried out in the laboratory of the Automotive Engineering Institute Brno on the ATOS 3D optical scanner

First I had to mark the inlet port casting with special scanning points, then I calibrated the scanner to meet the measurement accuracy requirements. After that I set parameters of the scanning, like a fineness of scanning element, which has a major influence on the model accuracy, and also the amount of the model data. When everything had been properly set and calibrated, I started to scan the casting. After a scanning there are several steps that need to be done. To begin with, I had to convert a scanned model format to STL format, than I inset the model with primitive elements (cylinder, sphere, cube, etc.) due to better work with the model in CAD software. Last step was covering blind spots which were a result of the scanning points placement. A final model of the inlet port can be seen in (Fig. 53). After all these operations had been carried out, I exported the model to CAD system, made several cross sections through both parts of the inlet port model and finally I measured areas of these cross sections. Through application of the measured values I was able to find equivalent diameters that correspond with the areas of the cross sections and that can be used in the simulation.

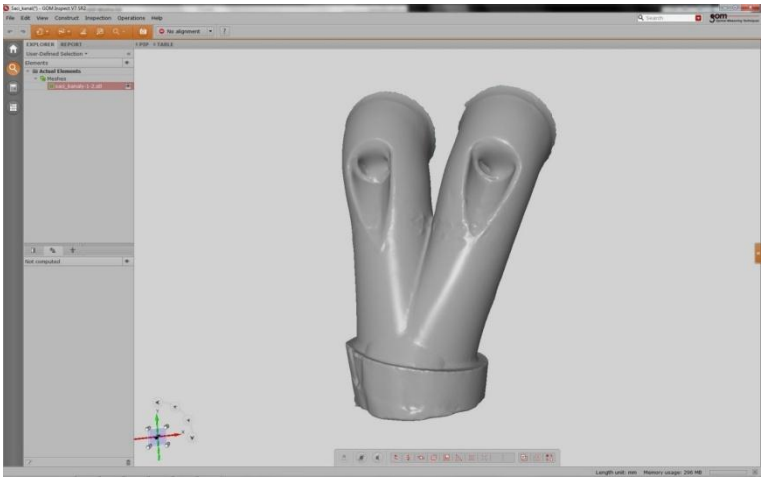

Fig.53 Scanned model of inlet port casting

7.1.3 INLET PORT DATA EXPORT

In Lotus the inlet ports consist of pipe elements that are ended by a port element and a valve element (Fig. 54). For the simulation model improvement, the above mentioned loss junctions elements can be used. These are placed to a point where the common inlet port is divided into two separate ports that open into the cylinder. Port flow coefficients and length of the port can be defined at the port elements menu. The cam profile, valve lift and timing can be defined at the valve elements menu. Data acquisition for these last named elements was mentioned in the previous chapter.

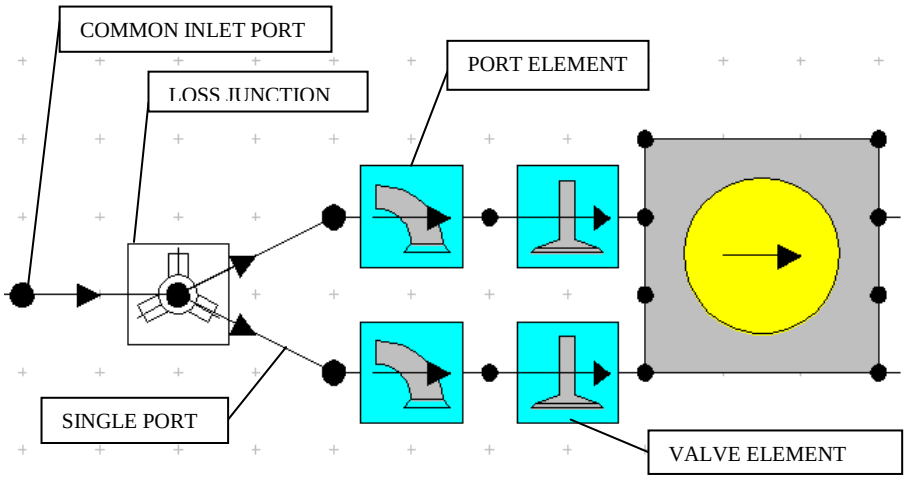

Fig. 54 Inlet part of the cylinder head model

I measured the length of a common inlet port from the CAD model and its cross section area as well. Other dimensions that I needed to obtain were lengths of the divided ports and the angle between them and also a few cross section areas of these ports. All these dimensions I measured from the CAD model again and I exported them to Lotus.

7.2 STOCK ENGINE PERFORMANCE/TORQUE CHARACTERISTIC

I aimed to set every parameter of the simulation model as close to reality as possible to be able to compare the outputs from the simulation model with the dynamometer testing outputs. Unfortunately, there appeared several problems with the dynamometer and due to our laboratory reconstruction there was no other ready-to-operate dynamometer available therefore I had to manage without the measured performance/torque course.

At the purchase of the engine the salesman gave us approximate values of the torque and engine performance. It was around 60 Nm and 45kW. These values were the only ones I could compare my results with. In (Graph. 7) there is a performance/torque characteristic of a simulation model of the Husaberg engine. As you can see, the peak of torque is around 7,500 min^{-1} and its value is 57 Nm. You can also see an apparent torque loss between 3,000 and 5,000 min^{-1}. This is a result of a resonance intake system which is tuned for a larger spectrum of engine speeds. Engine performance has the peak 8,000 $min^{-1}$with 46 kW. This computed data will be a basis used for the following engine tuning.

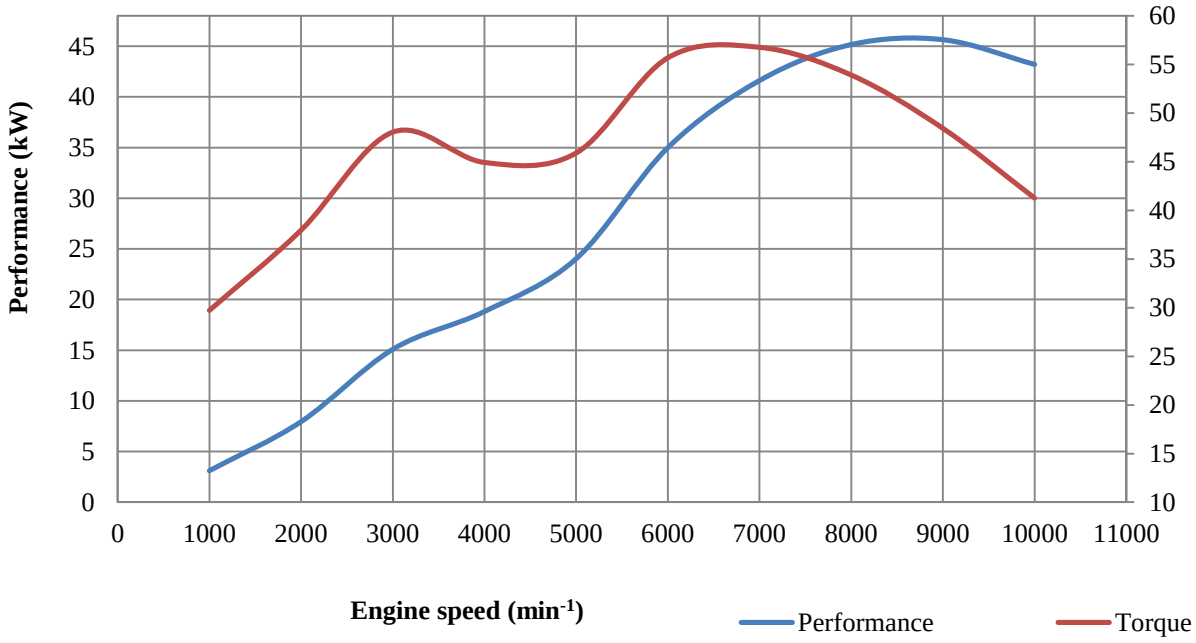

Graph. 7 Simulation model Performance/Torque course

8 OPTIMIZATION OF FORMULA STUDENT INTAKE SYSTEM

One of the major parts of this thesis is the study of the intake system changes and their influence on the engine torque and performance. The main aim of these changes was to optimize the intake system so that it meets our requirements in terms of the engine performance and torque courses. Based on the optimization of each element, I built up the final simulation model that will be shown in the following chapters.

8.1 INTAKE RUNNER LENGTH OPTIMIZATION

The first step in the successful intake runner tuning is the assessment of an engine speed for which the runners will be tuned. After the consultation with our "drivetrain team" and because of good performance values and torque course of a serial engine at around 8,000 and 9,000 min^{-1}, I decided to optimize the length of the intake runners for 8,000 min^{-1}. I decided to use the value of theoretical length of the ram wave runner which I calculated before formula (2), then I made several other simulations close to this value. I evaluated the results of the simulations and the length 220mm appeared to be the best. The total length of the intake manifold was then 320 mm. In (Graph. 8) you can see the comparison of the optimized and stock intake runner lengths and their influence on the performance and torque

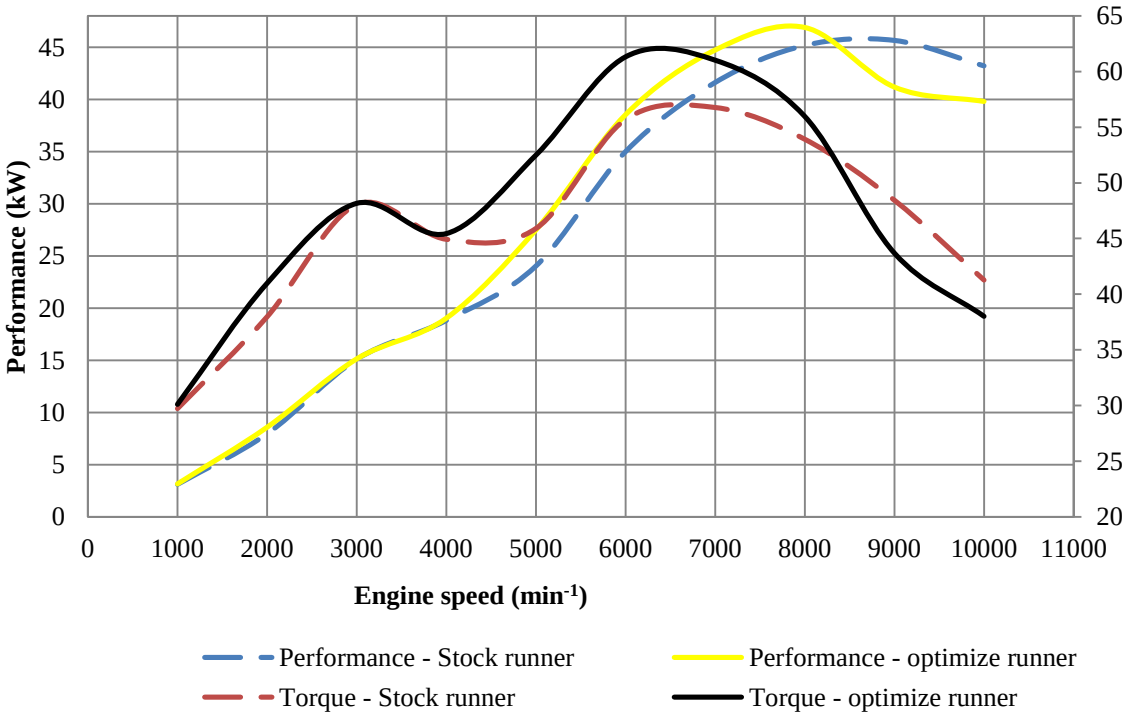

Graph.8 Comparison of stock and optimize intake runner length

characteristics.

Results of the optimization are evident from (Graph. 8). There is a major performance increase (around 3-4 kW) in the spectrum from 4,000 to 8,000 min^{-1} (47 kW) as I had expected. The course of the engine performance also meets our requirements better than the stock. As you can see, the peak of the performance is at 8,000 min^{-1} and due to the optimized intake runner we have more power at lower engine speeds than with the stock runner. Of

course, there is a massive decrease in the performance after 8,000 min^{-1}, but it does not matter because we will not run the engine above this level. I also achieved a good improvement in the torque. There is a considerable increase (around 5 Nm) in the spectrum from 4,000 to 8,500 min^{-1}. The course is much more positive than in the stock because, as you can see, in the spectrum from 3,000 to 5,000 min^{-1} the stock engine has an adverse drop, while with the optimized runner I partially managed to remove this drop and thus improve the torque course. As you can see, the peak of the torque (61 Nm) is between the 6,000 and 7,000 min^{-1} before the torque starts to drop.

Optimizing the runner length has also some minor influence on the course of cylinder and valve throat pressure, which fact strongly influences the engine charging efficiency. As you can see in (Graph. 9), at the valve opening the cylinder pressure almost equals to the valve throat pressure. This is convenient because the charge does not flow back to the intake, and when the valve throat pressure is higher than the cylinder pressure, it brings even better results. At the inlet valve closing there is a major pressure difference: the cylinder pressure is higher than the valve throat pressure which means that the charge flows back to the intake; but this effect is insignificant because of a very small valve lift which is typical for the valve closing area. Naturally, at the maximum valve lift the difference between the pressures is the

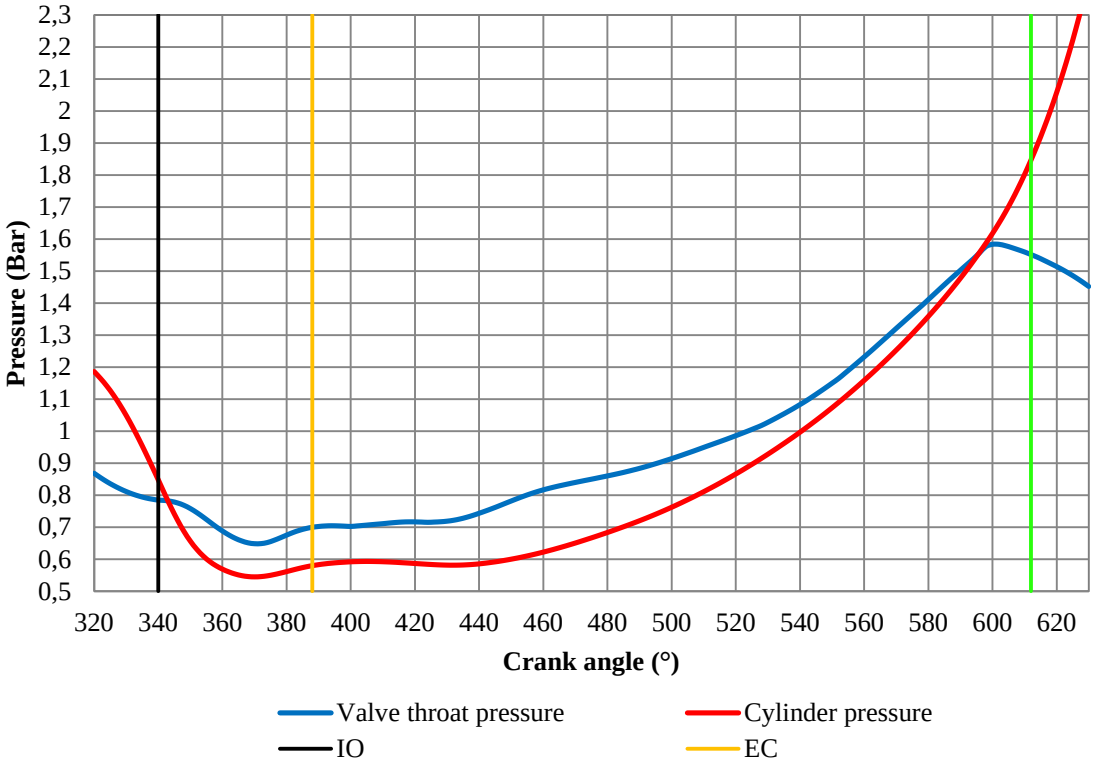

Graph.9 Valve throat and cylinder pressure course at 8000 rpm

biggest - this is an area of the maximum flow through the port.

8.2 INTAKE RUNNER LENGTH INFLUENCE ON ENGINE POWER

Now we will have a look at the influence of the intake runner length on the torque and engine performance. As we can expect, with lengthening of the intake runner the engine

torque will be higher at lower engine speeds. I made several simulations with different runner lengths to compare changes in the torque and performance course (Graph. 10).

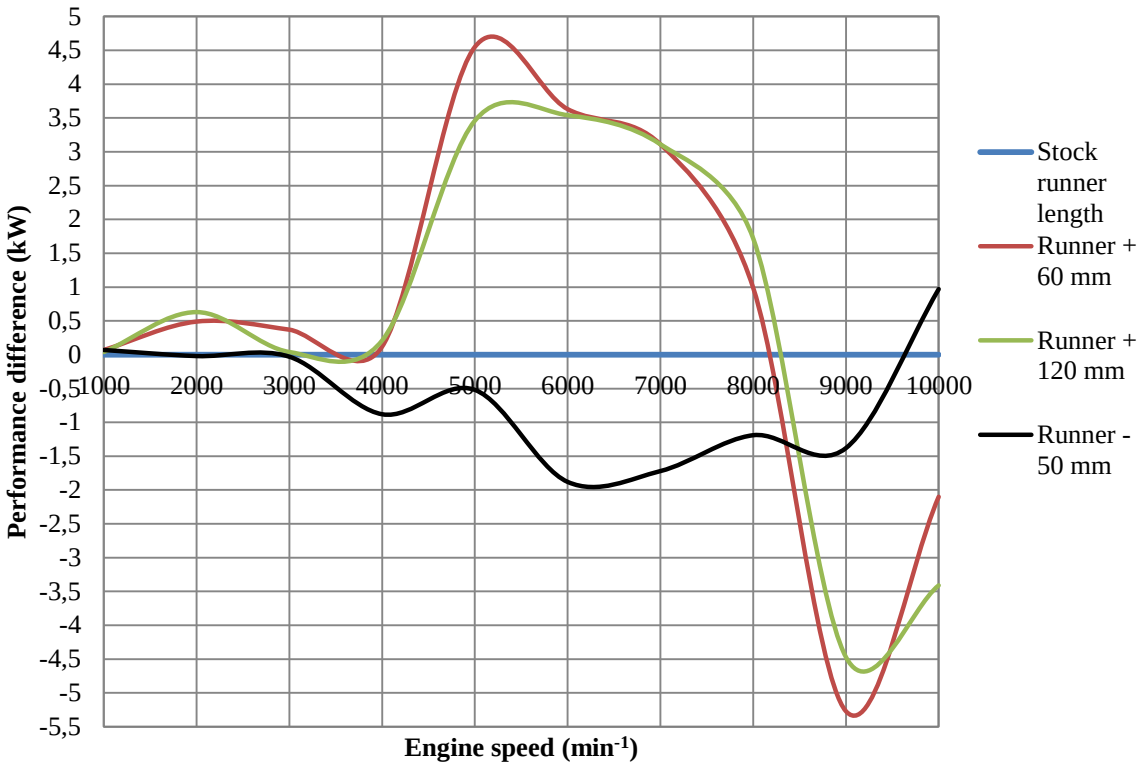

Graph. 10 Influence of runner length comparison

As it turned out, the aforementioned optimized length (green) was the best option; it provides the performance improvement in comparison with the stock runner at almost all engine speeds up to 8,000 min^{-1}. The shorter version of the runner (red) would not necessarily be a bad choice either; but it provides a high power improvement at 5,000 min^{-1} which is not our working engine speed, and on the other hand there is less power around 8,000 min^{-1} where we need a major performance improvement. The last runner (black) in the graph is 50mm shorter than the stock runner. It provides a power increase only in the spectrum from 9,500 min^{-1} which is predictable. It might also be interesting to see how large the improvement could the runner provide at engine speeds above 10,000 min^{-1}, where I have not carried out any testing.

These differences in the engine performance and the torque course are induced by the pressure pulsations in the intake manifold. This fact proves once again that the ram wave overcharging only works in a narrow spectrum of engine speeds. Therefore the intake manifold tuning mostly consists in a compromise between the maximum of power at maximum engine speeds and an acceptable torque course. Important thing here is to recognize what we want to obtain and what is our aim.

8.3 RESTRICTOR INFLUENCE ON ENGINE PERFORMANCE

As it has been mentioned before, the intake system for the Formula Student car includes a restrictor which is placed between the throttle body and the engine. The restrictor is

aimed to reduce the mass flow at higher engine speeds. Chapter 1 deals with the detailed description of the restrictor.

In our case the restrictor consists of a reduced circular section, that reduces the intake air mass flow to the engine. This reduced section sets a maximum air flow which can flow through the restrictor because of the critical flow velocity (speed of sound) which occurs at high air flows. This effect reduces the maximum engine speed and thus also the maximum engine performance, the result of which is a reduction of the maximum speed of the car. Our team decided to buy a throttle body with the restrictor from the AT Power manufacturer. This restrictor is designed like a De Laval nozzle, composed of a convergent part known as a nozzle and a divergent part known as a diffuser. The diminishing section is typical for the convergent part. For a divergent part an opposite effect is typical, the section expands along the diffuser length. There are other possibilities of restrictor designs, more suitable for situations where the intake air mass flow is at the restrictor limit for a major spectrum of engine speeds. Turbocharged engines can serve as a good example.

Graph. 11 Restrictor influence on engine performance and torque

8.4 AIRBOX INFLUENCE ON ENGINE PERFORMANCE

A stronger influence of the airbox on the basic engine parameters occured after I had added the restrictor into the simulation model. Suddenly the engine did not have enough intake air due to a small section of the restrictor and – as was explained and shown in the previous chapter in (Graph. 11) – both the engine performance and torque dropped.

There are several main purposes of the airbox; it functions as the engine air reservoir and it also damps and reflects pressure waves from the runners. The air, flowing from the restrictor to the airbox, should be influenced by a pressure wave from the intake runners as little as possible, thereby it should enable a full utilization of the restrictor. When the air flowing from the restrictor is influenced by pressure waves from the intake runners, a turbulent flow in the restrictor may occur; this is caused by an earlier reaching the critical velocity inside the restrictor and thereby its earlier overloading as well. A properly-working airbox should increase the engine volumetric efficiency and thereby compensate the performance losses caused by the intake restriction, until the critical velocity in the restrictor is reached.

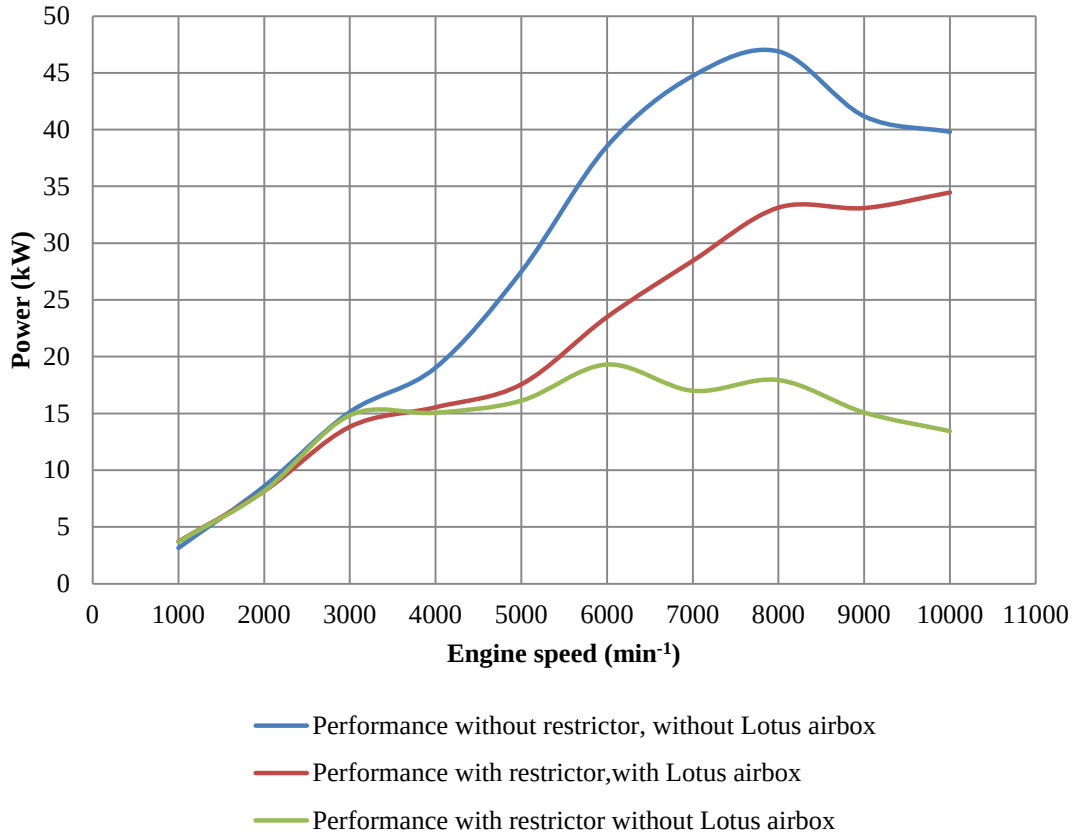

Graph. 12 Airbox influence on engine performance

In the first simulations with an optimized simulation model I used a standard Lotus airbox model. But it soon turned out that the standard model is quite inadequate for my purpose. This standard airbox compensates the engine power by approximately 15 kW, but – as you can see in (Graph. 12) – the intake air flowing through the restrictor still reaches the critical velocity very early (around 3,000 min^{-1}), which means that the airbox is not working properly. I tried to change the airbox volume and it brought some improvement in the engine performance course, but the throttle response got worse with the increasing volume of the airbox, which feature is not desirable in a racing engine. Because the Lotus standard airbox model only offers volume changes, I have decided to create my own airbox model (Fig. 55, Fig. 56).

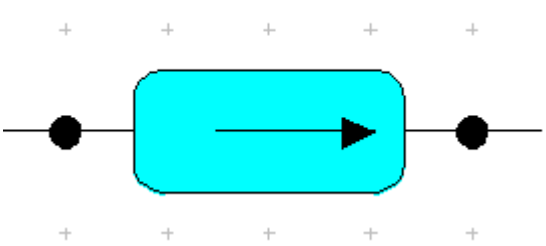

Fig.55 Standard lotus airbox

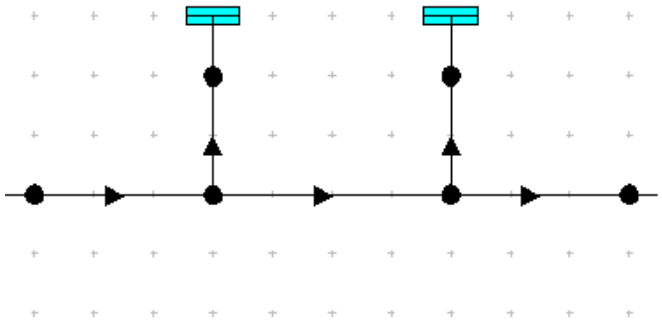

Fig.56 My airbox model

8.4.1 OWN CONCEPT OF AIRBOX.

wanted to make an airbox that would be a good compromise between the volume and the volumetric efficiency, therefore I decided to use a concept similar to that one used in the Formula 3,000 engines (Fig. 57). A divergent part of the restrictor, placed inside the airbox, is the basis of the concept. Pressure waves from the intake runner expand through the airbox and due to a major area difference between the restrictor outlet and the airbox wall, the pressure wave expands to the airbox wall along the inserted part of the restrictor. That means that the restrictor is influenced by pressure waves very little, thereby there is minimum turbulent flow, minimum velocity changes and that results in better air flow through the restrictor.

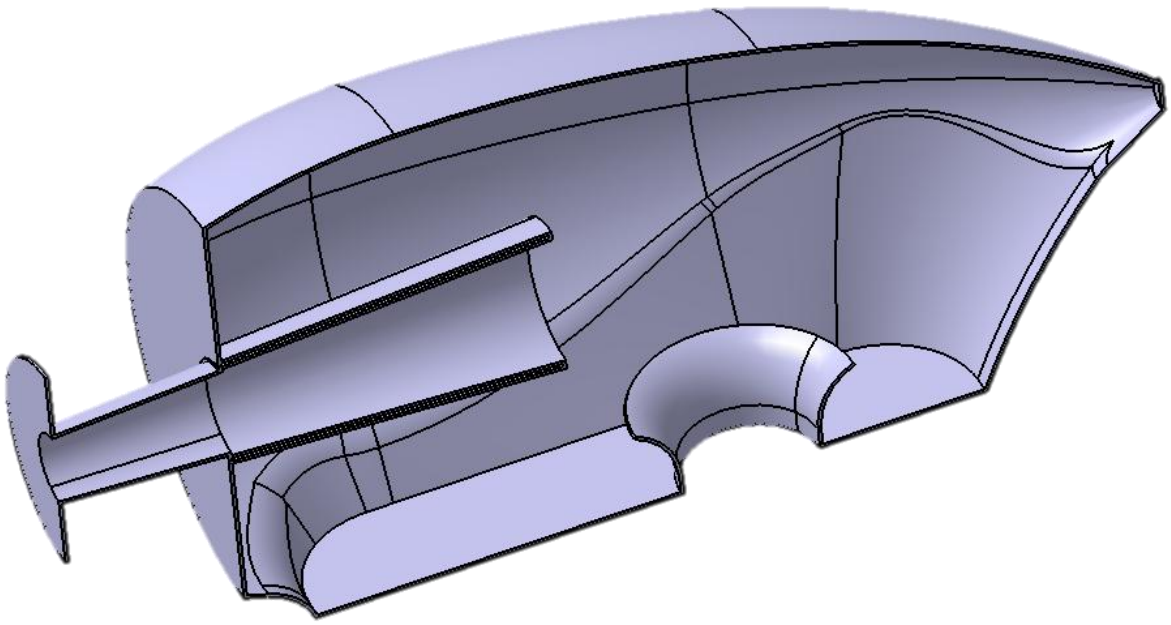

Fig.57 CAD model of my airbox concept

Using a standard Lotus airbox it was impossible to simulate the aforementioned effect, that is why I had to create my own simulation model (Fig 56). I started with a Lotus model for the intake silencer because it works with similar conditions; there is also a pipe which is inserted inside another pipe, which was the most serious problem in the standard Lotus

airbox. The Lotus help center describes the principle with which the intake silencer operates... There is also a structure of pipes which the silencer is composed of. I used this pipe layout and my own values that are related to the CAD model of the airbox. I also had to make a little change here because the intake silencer model does not count with a conical inserted pipe. Afterwards I carried out several simulations with different airbox volumes and different lengths of the inserted pipe. It turned out that the best solution is the airbox volume around 3.5 l, the inserted pipe length 100mm and its outlet diameter 42 mm.

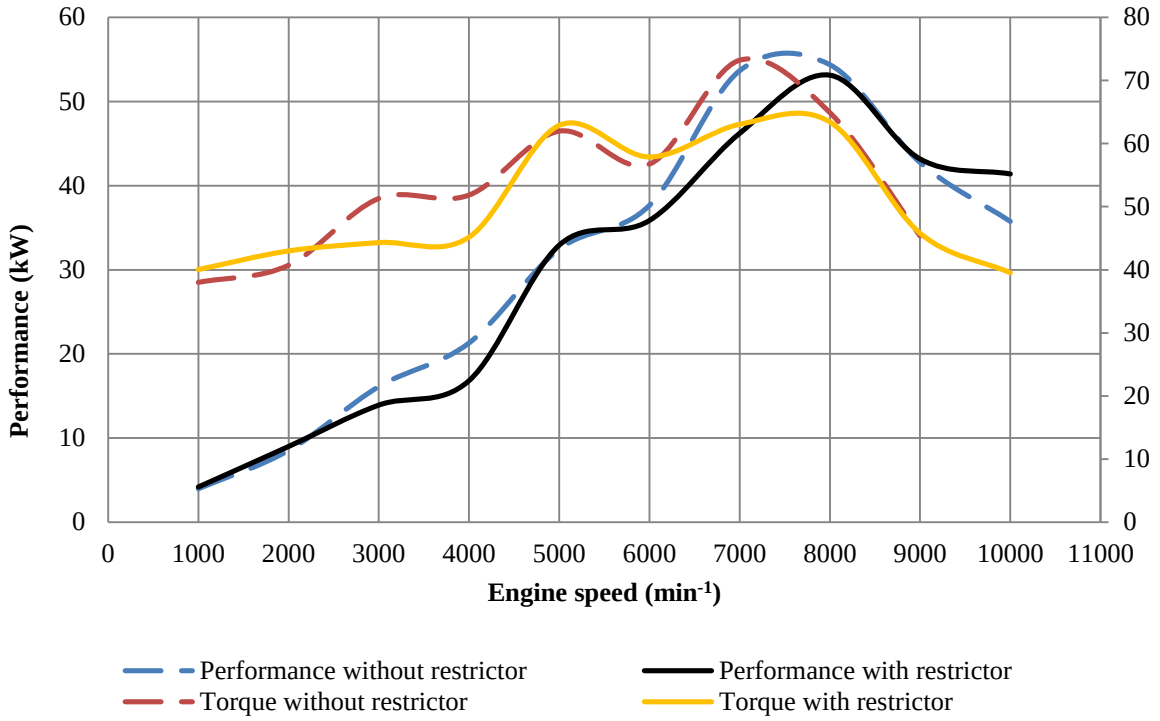

Graph.13 Influence of airbox to engine power and torque compensation

In (Graph. 13) you can see, how my airbox concept compensates the power and performance losses. There is a small performance and torque loss between 3,000 and 4,000 min^{-1} due to a momentary insufficiency of the pressure in the airbox. This loss could be reduced by the increase in the airbox volume, but it would mean that a response of the throttle will be worse. I decided to keep the airbox volume (3.5l) because values of the aforementioned losses are 3 kW and 5 Nm which is a very small difference at non-working engine speeds. Both curves (performance and torque) are quite similar to the curves of the model without a restrictor up to 6,000 min^{-1}. At these engine speeds the velocity in the restrictor starts mounting to the critical speed and the engine performance and torque begin to be limited. A total maximum performance loss is around 2 kW and a total maximum torque loss is around 10 Nm at the same engine speeds as in the model without a restrictor.

8.5 OPTIMIZATION RESULTS

I started the optimization from the intake runners and I continued through the restrictor to the airbox optimization. As I have already mentioned, I prepared several simulation

variants that were tuned afterwards. A variant with the intake runner length 220 mm and a constant diameter 41mm which is opened into the 3.5l airbox seemed to be the best option. Inside the airbox there is a conical pipe which is 100 mm long and its outlet diameter is 42 mm. This pipe freely verges into the restrictor with the smallest diameter of 19 mm and its distance from the wall of the airbox is 100 mm.. At the cylinder head there is one common inlet port which is divided into two separate ports that are opened into the cylinder. The length of the common port is 44 mm and the lengths of the separate ports are 40 mm and 45 mm. The valve timing was kept the same as in the stock engine.

Maximum engine performance was increased by 7.5 kW comparing with the stock engine (maximum performance of the tuned engine is 53kW and maximum performance of the stock engine is 45.5 kW, both a 8,000 min^{-1}) and maximum torque was increased by 10 Nm compared with the stock (maximum torque of the tuned engine is 63.5 Nm and maximum torque of the stock engine is 54 Nm at 6500 min^{-1}). The performance increase occurs at the spectrum between 6,500 to 8,000 min^{-1} due to the optimized intake runners. The torque increase occurs at speeds above 5,000 and up to 8,000 min^{-1} the course of the torque remains almost constant. The torque improvement at higher engine speeds occurs due to an optimized runner length whereas at lower engine speeds the improvement may occur due to the airbox volume. Both performance and torque courses are shown in (Graph. 14).

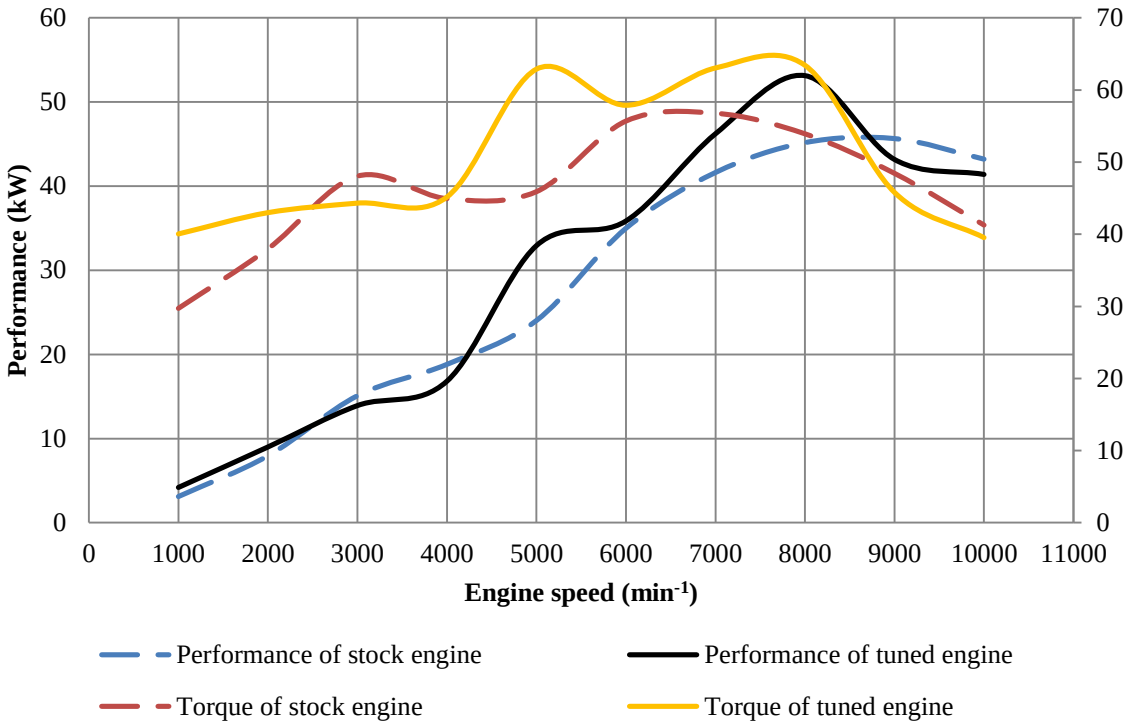

Graph.14 Comparison of performance/torque characteristics of stock and tuned engine

I assume that the optimization has been successful and that I have met all the primary goals. The best way to verify the conclusions will certainly be the engine testing on the

dynamometer. Due to complications with our laboratory dynamometer I will not be able to test the tuned engine until June.

9 INTAKE MANIFOLD FLOW

9.1 FLOW BASIC QUANTITIES

The flow is created by randomly moving particles that are simultaneously moving in the flow direction. The hydraulic gradient is the basic condition of the flow.

Intake air that flows through the engine could be described in the terms of the thermodynamics as an inert gas mixture which can be regarded ideal gas if the atmospheric boundary conditions are convenient. Ideal gas is composed of a set of randomly-moving, non-interacting point particles that have a zero volume. It also has constant physical properties.

Intake air can be parametrically described by the state quantities like the temperature, density, velocity and the pressure that are described at formula (19)

$$T = f(x, y, z, t),$$
$$\rho = f(x, y, z, t),$$
$$v = f(x, y, z, t), \tag{19}$$
$$p = f(x, y, z, t),$$

The flow can be subdivided into a steady-state flow and an unsteady flow. The steady-state flow refers to the condition where the fluid properties do not change over time at a certain point in the system. Otherwise the flow is called unsteady. An unsteady flow is very difficult to calculate , therefore it is practically solved as a steady-state flow. This approach is called a quasi-stationary solution.

Every flow particle moves along its own streamline. Streamlines are a family of curves that are instantaneously tangent to the velocity vector of the flow. These show the direction in which the fluid element will travel at any point in time (Fig. 58).

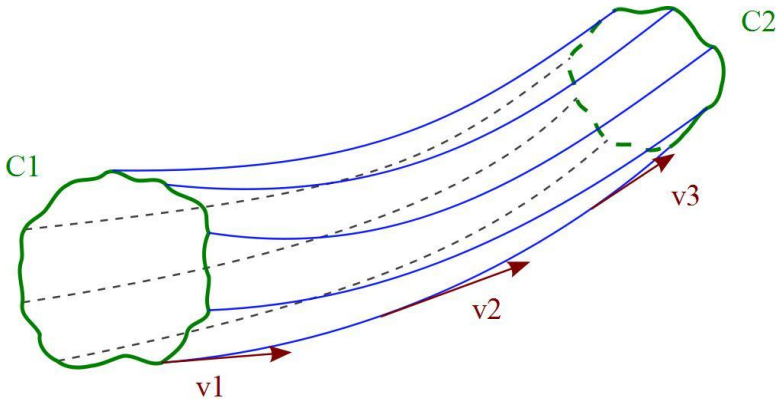

Fig. 58 Flow streamlines [23]

9.2 LAMINAR FLOW

The laminar flow occurs when the fluid flows in parallel layers, with no disruption between the layers. At low velocities the fluid tends to flow without mixing and adjacent layers slide past one another. In the laminar flow the motion of the particles of the fluid is very orderly with all particles moving in straight lines parallel to the pipe walls. The laminar flow is usual for fluids with higher viscosity and lower flow velocities. As you can see in (Fig. 60), on the pipe wall there is zero flow velocity which rises with the increasing distance from the pipe wall. The flow velocity is at its maximum in the middle of the flow velocity profile. Then the mean velocity is a half of the maximum flow velocity (Fig. 59).

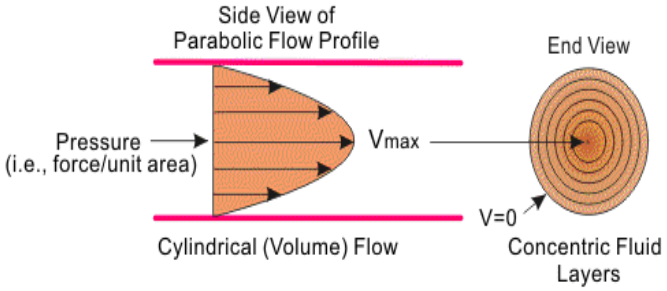

Fig. 60 Laminar flow [23]

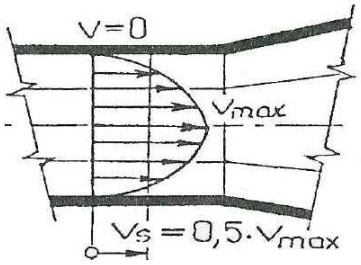

Fig. 59 Laminar flow mean velocity [22]

9.3 TURBULENT FLOW

The turbulent flow is a flow regime, characterized by chaotic and stochastic property changes. This includes a low momentum diffusion, a high momentum convection and a rapid variation of pressure and velocity in space and time, which generates whirls. The turbulent flow generates a significant pressure reduction in the flow direction contrary to the laminar flow. In (Fig. 61) you can see the velocity profile of the turbulent flow.

T is the core of turbulent flow, *M* is the turbulent boundary layer, *P* is the transition

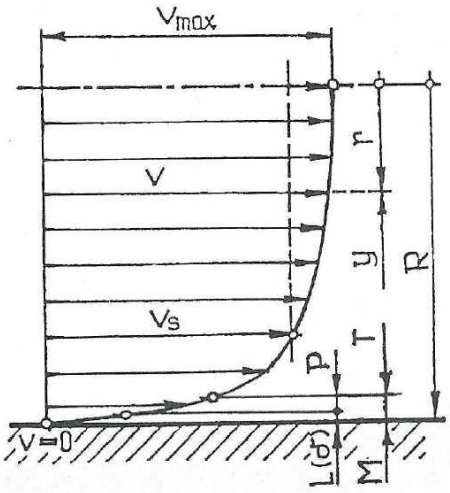

Fig.61 Turbulent flow velocity profile [22]

layer, *L* is a laminar sub-layer.

The velocity gradient close to the pipe wall is higher than anywhere else in the velocity profile. The turbulent flow generates fluctuation velocity components which are cumulated close to the pipe wall and the flow character is near to the laminar flow

The turbulent flow is changing to a laminar one close to the pipe walls, which effect generates the laminar sub-layer. The transition layer lies between this laminar sub-layer and the turbulent flow. These two layers form the boundary layer.

9.4 BOUNDARY LAYER

A boundary layer is the layer of the fluid in the immediate vicinity of a bounding surface, where the effects of viscosity of the fluid are considered in detail. A particle adhering to the wall has a zero velocity, the friction force equals to the dynamic force and therefore a part of the kinetic energy is changed into heat. In (Fig. 62) you can see the laminar and turbulent boundary layers.

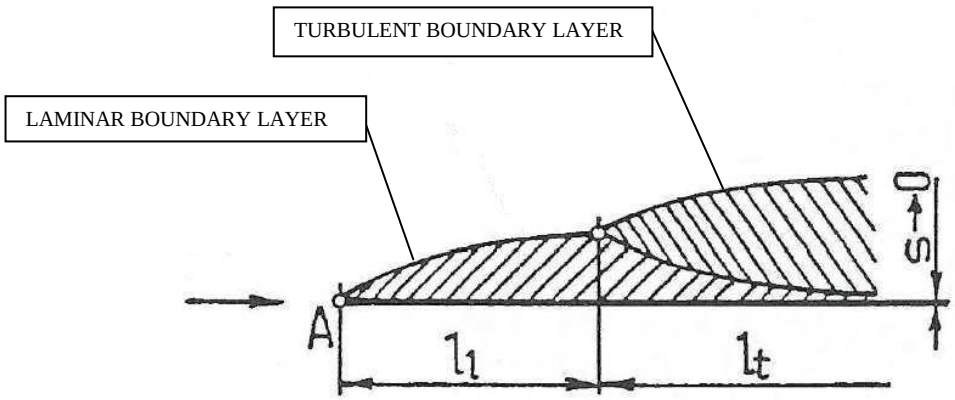

Fig. 63 Turbulent and laminar boundary layer [22]

When the flow runs around an obstacle (point A), then a part of the flow is ripped off at the entering edge and forms a laminar layer on length (l_l). After this length the partial flow is converted to a turbulent layer on length (l_t). But a part of the laminar layer stays under the turbulent layer and thereby a laminar sub-layer is formed.

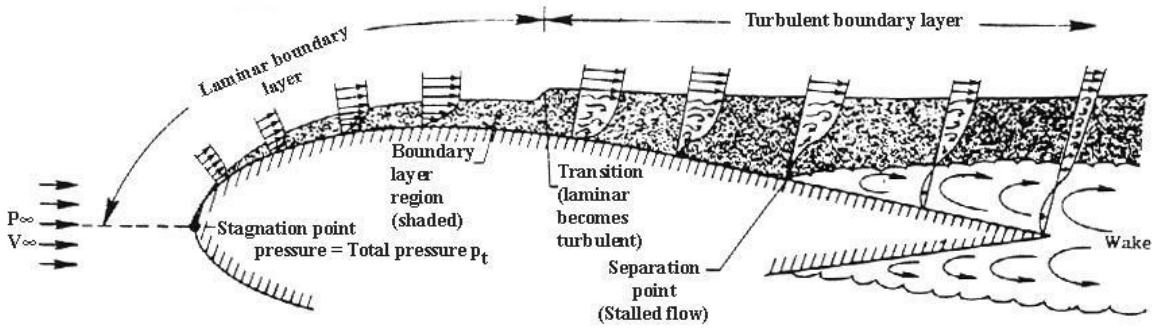

Fig. 62 Wake formation [24]

The kinetic energy is converted to the pressure force at the object being run around. The flow starts to rip off at the separation point and the wake starts to be formed. Particles start to be

ripped off when the pressure force is sufficient to stop those particles which are going to separate.

9.5 CONTINUITY RELATION

$$\frac{\partial(\rho S v)}{\partial s} + \frac{\partial(\rho S)}{\partial t} = 0\,, \tag{20}$$

where: $\frac{\partial(\rho S v)}{\partial s}$ – convective mass change,

$\frac{\partial(\rho S)}{\partial t}$ – local mass change,

$$\rho . S_T . v = Q_m = konst\,. \tag{21}$$

The formula (20) is a continuity relation for the 1D flow. It represents the conservation of the mass law. In our case the second part of the equation equals zero which means that the equation can be simplified to formula (21). The mass flow is constant for every section of the pipe which you can see in formula (21).

9.6 EULER'S FORMULA FOR HYDRODYNAMICS

The formula for hydrodynamics represents an application of the second Newton's law in hydrodynamics. The formula (22) represents this law for a compressible flow, when the external forces have vanished.

$$\frac{\partial \vec{c}}{\partial t} + \left(c\vec{V}\right)\vec{c} + \frac{1}{\rho}\vec{V}\rho = 0\,, \tag{22}$$

The first equation term represents a local acceleration. The second equation term represents a convective acceleration, which is formed when the fluid flows through the manifold with a variable section.

9.7 BERNOULLI'S FORMULA

The Bernoulli's formula represents the conservation of the energy law in fluids. It is a sum of the kinetic energy, the pressure energy and the potential energy that equals zero (formula (23)).

$$\frac{c^2}{2} + \frac{p}{\rho} + g . z = 0\,, \tag{23}$$

The formula (24) is applicable to the flow through variable section manifolds, because it includes length and local losses.

$$\frac{c_1^2}{2} + \frac{p_1}{\rho} + g . h_1 = \frac{c_2^2}{2} + \frac{p_2}{\rho} + g . h_2 + E_z\,, \tag{24}$$

10 COMPARISON OF ANALYTICAL AND CFD SOLUTION

To verify my CFD simulation, I decided to make a basic testing model of the tube and to compare the results from my CFD analysis with an analytical result which I calculated on the basis of generally known formulas.

10.1 VERIFICATION MODEL AND BOUNDARY CONDITIONS

I have chosen a pipe which is similar to the optimized intake runner. The pipe has a constant circular section, the diameter 40 mm and the length 1,000 mm. Temperature of the air flowing through the pipe is 20°C and it is of constant density. The pressure drop is 5,000 Pa. I left out the heat transfer between the air and the tube which influences the air density. I have also left out the material and wall thickness of the tube and I chose a turbulent type of the flow.

10.2 ANALYTIC SOLUTION

As I have mentioned before, I used generally known formulas for this analytic solution and I compared the results with my CFD model.

10.2.1 ANALYTIC BOUNDARY CONDITIONS

Tab 12 Pipe basic dimensions

DIAMETER	40 mm
LENGTH	1,000 mm
VOLUME	$1.256.10^{-3}$ m^3
SECTION AREA	$1.256.\ 10^{-2}$ m^2

Tab 13 Analytic boundary conditions

DENSITY	1.2041 $kg.m^{-3}$
AIR TEMPERATURE	293.15 K
VISCOSITY	$1.817.\ 10^{-5}$ Pa.s
ATMOSPHERICAL PRESSURE	101,325 Pa
INLET PRESSURE (RELATIVE)	0
OUTLET PRESSURE (RELATIVE)	-5,000 Pa

10.2.2 ANALYTIC CALCULATION

First I calculated the velocity of the flow from the Bernoulli's formula (formula (23)). I removed a potential energy component, due to a zero difference in the altitude. I specified other quantities. The inlet velocity is $v_1=0$, the inlet pressure p_1, the outlet pressure is p_2, the outlet velocity is v_2.

The pressure difference from the Bernoulli's formula gave us the dynamic pressure between the inlet and the outlet and on its basis I expressed the flow velocity (formula (25))

$$v = v_2 = \sqrt{\frac{2(p_1 - p_2)}{\rho}} = \sqrt{\frac{2p_d}{\rho}}, \tag{25}$$

After the substitution I calculated (formula (26)).

$$v = \sqrt{\frac{10{,}000}{1.2041}} = 91.13\ m.\mathrm{s}^{-1}\ . \tag{26}$$

Reynolds number calculation, which defines a type of the flow (turbulent or laminar), was the following step. First I had to calculate the mean velocity which is one of the Reynolds number equation terms. I expressed the mean velocity from the mathematical equation of the turbulent velocity profile (formula (27)).

$$v_s = v_{max}(\frac{y}{R})^n\ , \tag{27}$$

where: y – is a distance from the pipe wall,

n – is a function of Reynolds number Re,

R – pipe radius,.

Mean speed of turbulent flow is approximately 85% of maximum flow velocity (26).

$$v_s = (0.82 - 0.87)v_{max}\ , \tag{28}$$

I chose a value 85% for the mean speed calculation. After the substitution I obtained the mean velocity of the turbulent flow which I substituted to Reynolds number equation -formula (29).

$$v_s = 0.85v_{max} = 0.85\ .\ 91.13 = 77.46\ m.\mathrm{s}^{-1}, \tag{29}$$

$$Re = \frac{v_s.l}{\nu} = \frac{77.46\ .\ 1}{1.817\ .\ 10^{-5}} = 4.26\ .\ 10^6. \tag{30}$$

From the result of Reynolds number equation it is obvious that the flow is a turbulent one. The mean velocity and the maximum velocity ratio results from the mass flow equation. After the equation editing I obtained formula (31). After that I expressed the mean velocity and the maximum velocity ratio m from formula (31).

$$Q = \frac{2\pi R^2 v_{max}}{(n+2)(n+1)} = \pi R^2 v_s, \tag{31}$$

$$m = \frac{v_s}{v_{max}} = \frac{2}{(n+2).(n+1)}, \tag{32}$$

Index n=0.125 and velocity ratio m=0.837 are experimentally found values for the Reynold number range $8.10^4 < Re > 5.10^6$. I calculated a more accurate value of the mean flow velocity, then I also calculated the mass and volumetric flow through the pipe.

Mean flow velocity:

$$v_s = m.v_{max} = 0.837\,.\,91.13 = 76.27\ m.\mathrm{s}^{-1}, \tag{33}$$

Volumetric flow:

$$Q = S.v_s = \pi.R^2.v_s = \pi\,.\,0.02^2\,.76.27 = 0.095\ m^3.\mathrm{s}^{-1} \tag{34}$$

Mass flow:

$$Q_m = Q.\rho = 0{,}0958\,.\,1{,}2041 = 0.12\ kg\,.\mathrm{s}^{-1}, \tag{35}$$

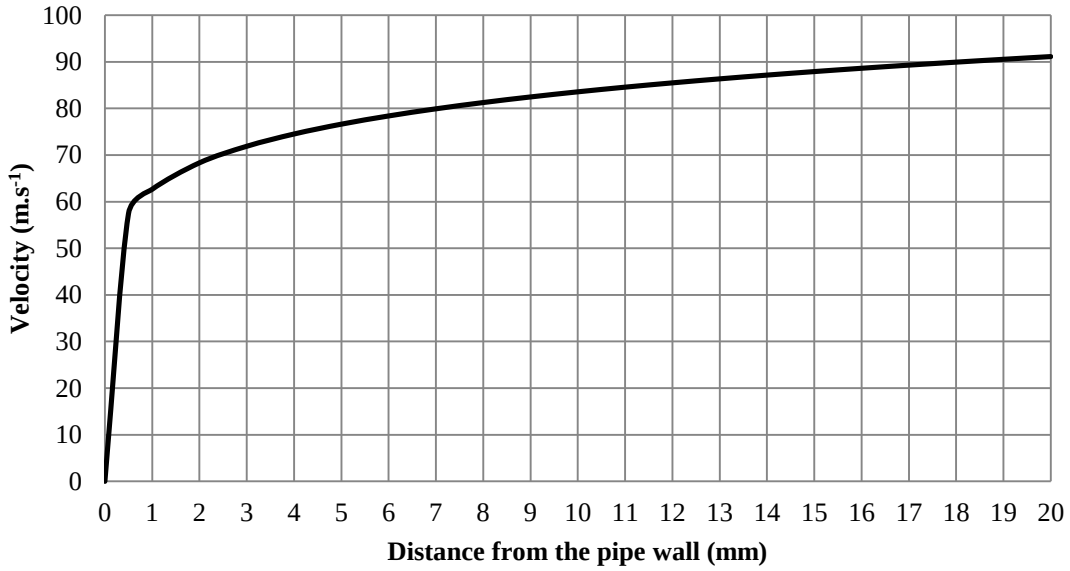

Graph. 15 Dependance of the velocity on the pipe wall distance

In (Graph. 15) you can see the dependence of the flow velocity on the distance from the pipe wall.

10.3 CFD SOLUTION

I have used the simulation software for the CFD simulations. The software is divided into several parts. Two main parts consist of the preprocessor and the postprocessor. Geometry export, material of the flow medium, boundary conditions and mesh are set in the preprocessor part. The postprocessor enables to work with the results of the simulation.

10.3.1 BOUNDARY CONDITIONS

It is important to set the boundary conditions before each simulation. I designed the model as an air model therefore I left out the wall thickness and the surface roughness. First of all I imported the model geometry to the CFD software, then I set the material properties (Tab 14) and the boundary conditions (Tab 15). I placed the inlet at the end of the pipe and at the opposite end I placed the outlet. After that I set the hydraulic gradient that is given by the boundary conditions. Finally I set the flow parameters (Tab. 16).

Tab 14 Material properties

DENSITY	1.2041 $kg.m^{-3}$
VISCOSITY	$1.817.10^{-5}$ Pa.s
GAS CONSTANT	287.05 $m^2.s^2.K^{-1}$
ATMOSPHERIC PRESSURE	101,325 Pa
TEMPERATURE	293.15 K

Tab 15 Boundary conditions

INLET PRESSURE (GAGE)	0 Pa
OUTLET PRESSURE	-5,000 Pa

Tab 16 Flow parameters

FLOW COMPRESSIBILITY	INCOMPRESSIBLE
FLOW MODEL	TURBULENT (K-EPSILON)
SOLUTION MODE	STEADY STATE
NUMBER OF ITERATION	1,000

10.3.2 MODEL MESHING

I meshed the model at the CFD software which has its own meshing tool. I set the number of elements at 50, 000 and at both ends I compressed the mesh because of a better calculation course. After that I set the 3 layers of prisms which enable to simulate the boundary layer. In (Fig. 64) you can see the meshed model.

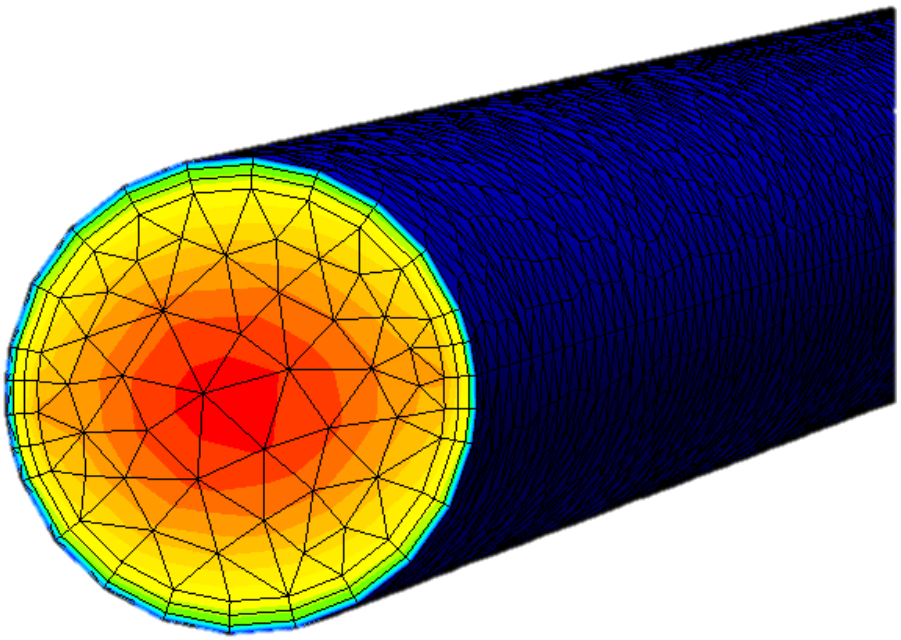

Fig. 64 Meshed model

10.3.3 CFD RESULTS

The simulation software finished the solution after 500 iterations because I had set the monitor point, monitoring the conditions convergence; when all these conditions are fulfilled, software finishes the solution. In (Tab. 17) there are results of this simulation.

Tab 17 Simulation results

MEAN FLOW VELOCITY	73.96 $m.s^{-1}$
MAXIMUM FLOW VELOCITY	91.23 $m.s^{-1}$
VOLUMETRIC FLOW	0.093 $m^3.s^{-1}$
MASS FLOW	0.11 $kg.s^{-1}$

After the simulation I put the results to the Microsoft Excel and I made a graph of the velocity dependence on the distance from the pipe wall. (Graph. 16)

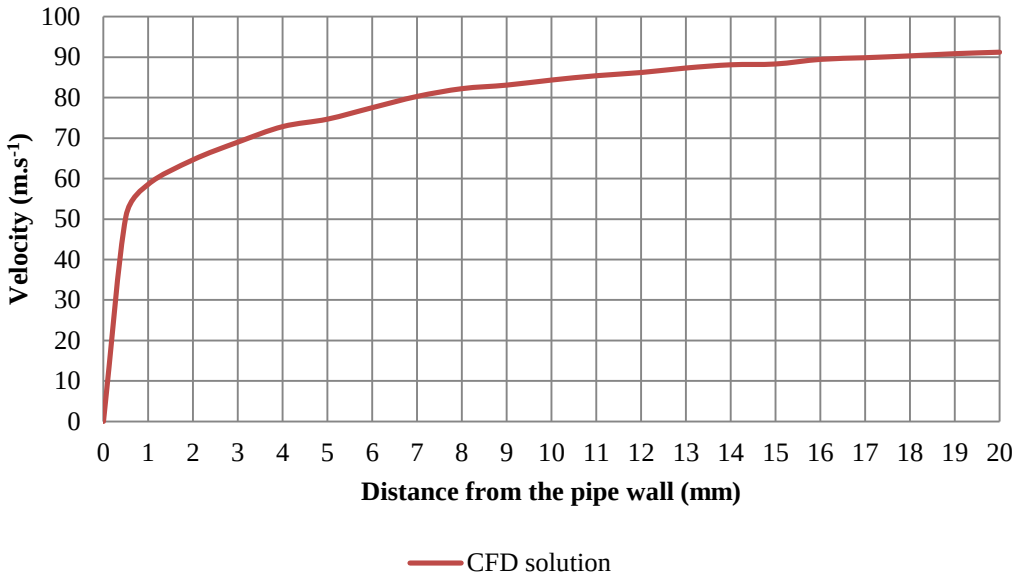

Graph. 16 Dependence of speed on the distance from pipe wall of CFD solution

10.4 COMPARISON OF ANALYTIC AND CFD SOLUTION

As you can see in (Tab. 18) and (Graph. 17), the analytic solution is very similar to the CFD solution. This basic model proves the accuracy of the CFD analysis. The type of elements and a mesh size have major influence on the results accuracy. Generally, the mesh could be more compressed at narrow and more complicated places.

Tab 18 Comparison of analytic and CFD solution

COMPUTED QUANTITIES	ANALYTIC SOLUTION	CFD SOLUTION
MEAN FLOW VELOCITY	76.27 $m.s^{-1}$	73.96 $m.s^{-1}$
MAXIMUM FLOW VELOCTY	91.13 $m.s^{-1}$	91.23 $m.s^{-1}$
VOLUMETRIC FLOW	0.095 $m^3.s^{-1}$	0.0925$m^3.s^{-1}$
MASS FLOW	0.12 $kg.s^{-1}$	0.11 $kg.s^{-1}$

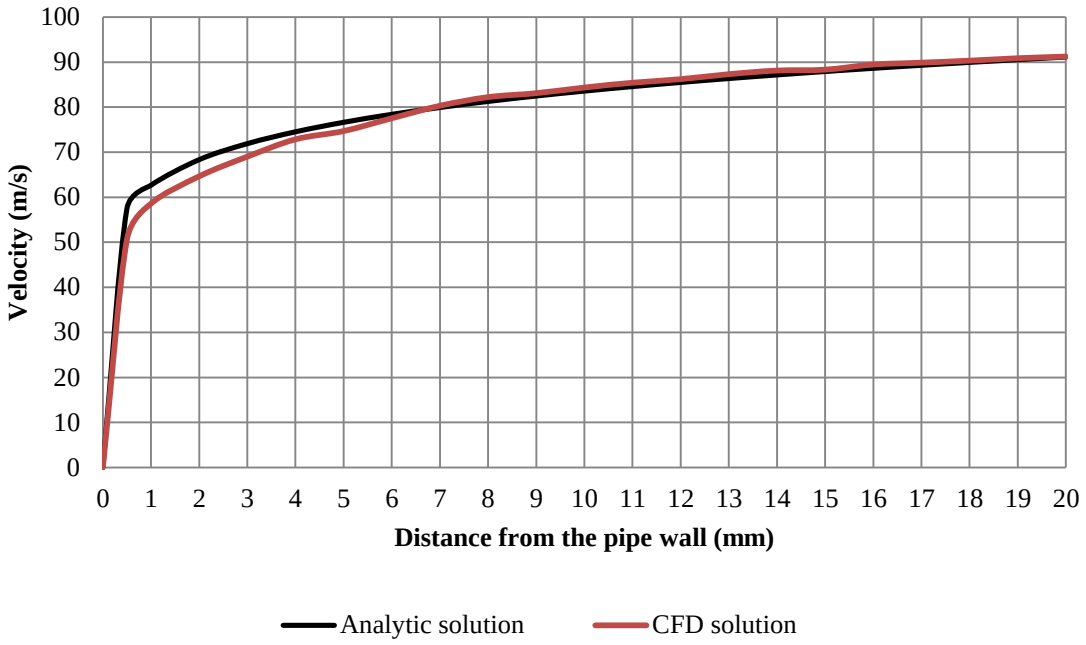

Graph. 17 Comparison analytical and CFD solution dependence of speed on the length from pipe wall

11 CFD SIMULATION OF AIRBOX

As a part of the design of the whole intake system, I also had to project the airbox. I had projected three variants, and because I was the first one who solved the shape and properties of the airbox for a single cylinder SI engine, I did not have any basis to compare them with. Therefore I decided to simulate the airflow through the airbox to find out which of the designed variants will be the most suitable for our engine. Because our 'Engine Team' was slightly short of time, I decided to do steady state simulation only. This type of simulation helps to find the mass flow rate of each of the designed airboxes, and as a result I can decide which airbox is able to provide the best engine charging. The purpose of these simulations is to choose the best variant which goes into production.

11.1 CREATION OF 3D MODELS

To create a 3D model, I used the data of the optimized intake, obtained from the Lotus Engine Simulation (chapter 8). Important data for the model creation included: the volume of the airbox, the length and diameters of the restrictor part inserted inside the airbox, and the length of the bellmouth which was also inserted inside the airbox. I designed the models by CATIA V5 R19 software. I have selected this software because the models are quite complicated as far as the shape is concerned and therefore they have to be designed in

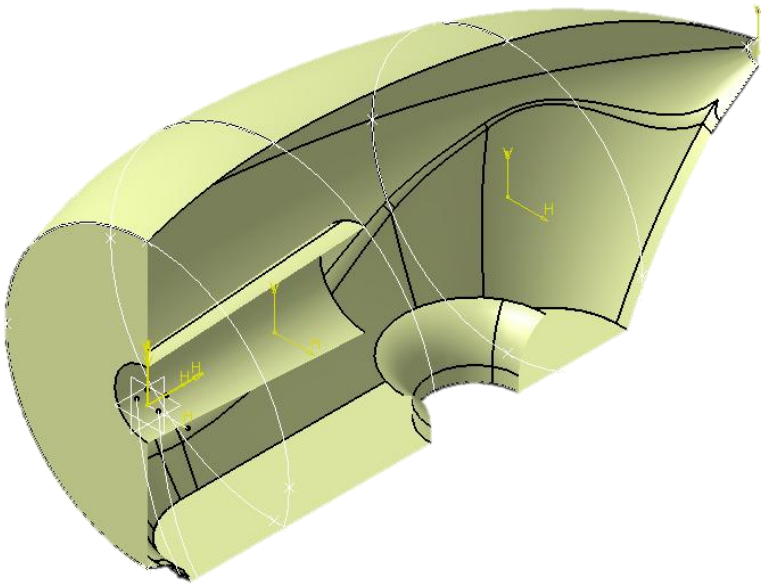

Fig. 65 section of surface model of airbox(variant 1)

surfaces.

To build the surface model I used functions like the multisection surface, which draws the surface from section to section along the designed spine or guides. I also used the trim, revolute and extrude functions for the model creation. I had to design an air model of the airbox due to the CFD simulations. This model is composed of the air plenum, which has to simulate surrounding air, the whole airbox model and the steadying tube. The length of the steadying tube should be 20 times longer than the diameter of the tube so that the air flow

could be stabilized and we are able to get undistorted results. In our case the length of the steadying tube is 800mm and its diameter is 40mm

11.1.1 VARIANT 1

When creating the first variant of the airbox, I started with the aforementioned Formula 3,000 airbox which has quite similar requirements to the Formula Student airbox. But I found only few pictures of the Formula 3,000 airbox; apart from that there are other two big differences between these airboxes: Formula 3,000 engines are 4 cylinder SI with 2 liter displacement and in contrast to the Formula Student rules, the Formula 3,000 concedes a throttle body for each cylinder which is placed inside the intake runner.

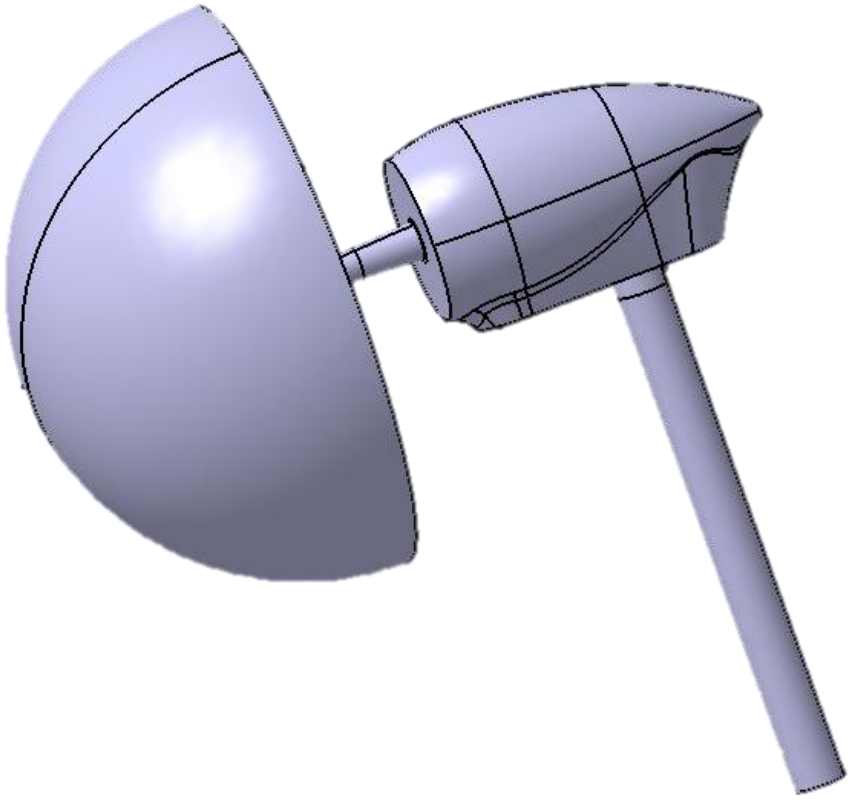

Fig. 66 Air model of variant 1

In (Fig. 66) you can see the air model of the airbox (variant1). On the left-hand side you can see the air plenum which I created first like a surface by the revolute function. On the right-hand side at the bottom you can see the steadying tube which I also designed in surfaces by the revolute function. In the centre you can see the airbox body which I created by using the multisection surface function and also trim and join functions. When preparing the complete model of the airbox in surfaces, I started with the volume conversion. I had to switch CATIA to the part design (volume program unit), then I created the volume model of intake air by the close surface and split functions. The section of the final volume model is shown in (Fig. 67).

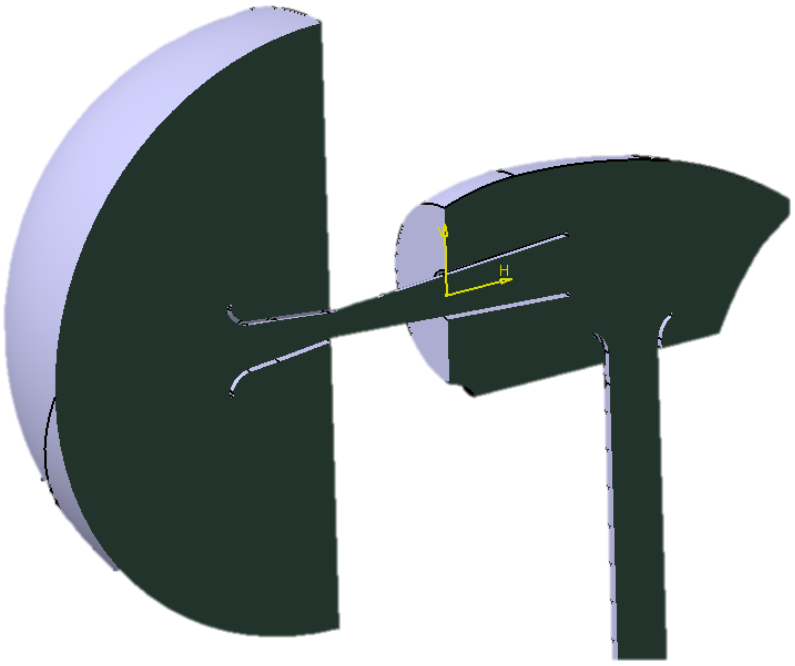

Fig. 67 Section of variant1 air model

11.1.2 VARIANT 2

Variant 2 is quite similar to the variant 1; the only difference between them is in the intake runner location. The intake runner is moved by 60mm towards the front of the airbox wall, under the restrictor outlet (Fig. 68). The section of the air model is shown in (Fig. 69).

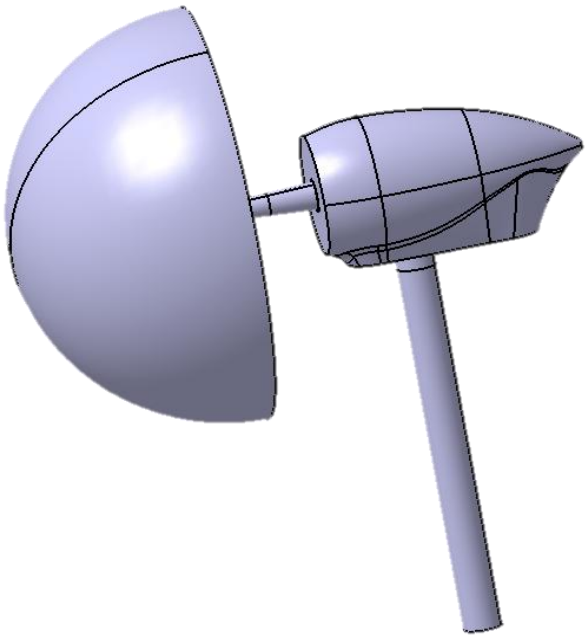

Fig. 68 Air model of variant2

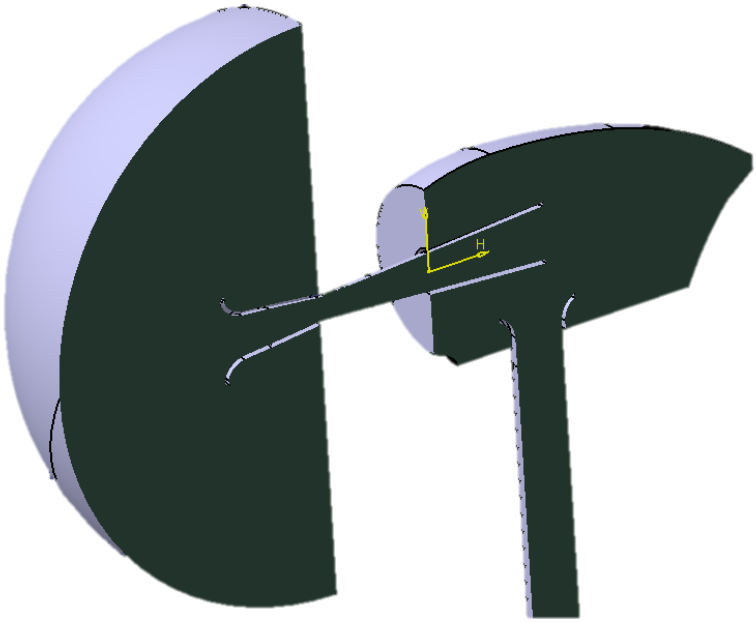

Fig. 69 Section of variant2 air model

11.1.3 VARIANT 3

The third variant is radically different from the previous ones. I started with the sphere shape because as far as hydraulic losses are concerned, the sphere is shaped in an ideal way. I also eliminated the single bellmouth which is now included in the airbox shape. There is also a place for the injector at the upper side of the airbox.

I started with the airbox body. First I used the revolute function for the airbox base, than I joined the sketch of the upper base to the bottom base with tangential curves. After that I used the multisection surface function to design the shape. After I had obtained the basic airbox shape, I started to design the space extension for the restrictor outlet (Fig. 70) which I shaped by the multisection surface function.

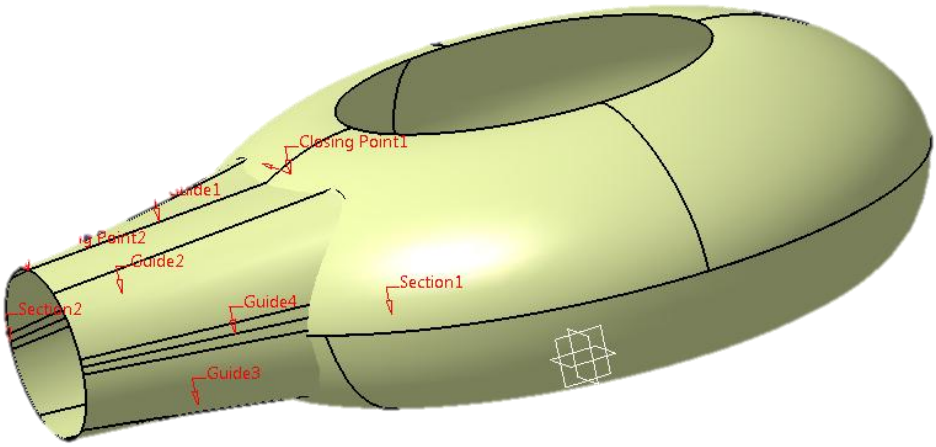

Fig. 70 Work with surfaces at airbox variant 3

Next step consisted of the designing the air plenum and the steadying pipe which had been described in variant 1.

You can also see the air model and the section of the air model in (Fig. 71,72).

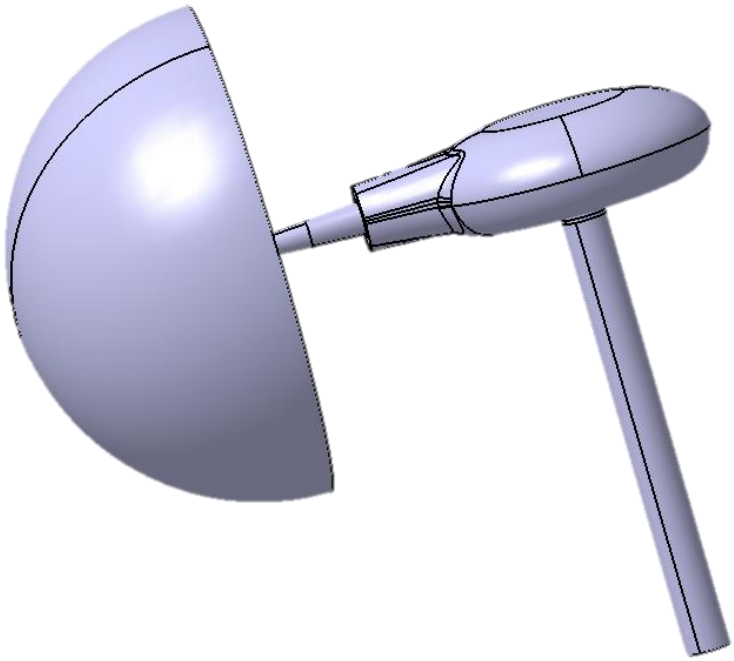

Fig. 72 Air model of variant 3

You can also see the above mentioned elimination of the single bellmouth which is replaced by the airbox shaping in (Fig. 72).

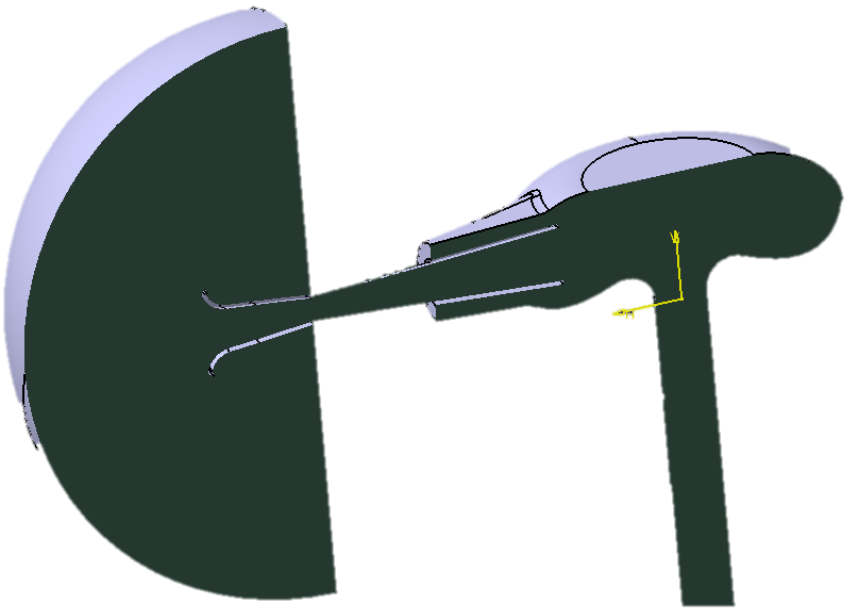

Fig. 71 Section of variant 3 air model

11.2 BOUNDARY CONDITIONS

It was necessary to set the same boundary conditions for all of the models because of the results comparability. The set boundary conditions are listed in (Tab. 19,20,21).

First I had to set the material properties (Tab. 18). I calculated with a model of air, therefore I chose one of the preset air materials. This air model has a changeable density because I use the compressible flow, which means that the air density changes in dependence on the temperature.

Tab 19 Material properties

DENSITY	EQUATION OF STATE
VISCOSITY	$1.817 . 10^{-5}$ Pa.s
GAS CONSTANT	287.05 $m^2.s^2.K^{-1}$
ATMOSPHERIC PRESSURE	101,325 Pa
TEMPERATURE	293.15 K

Setting the boundary conditions was the following step.(Tab. 20). I applied the pressure load first on the air plenum and then at the end of the steadying pipe, in which way the hydraulic gradient was created.

Tab 20 Boundary conditions

INLET PRESSURE (GAGE)	0 Pa
OUTLET PRESSURE	-5,000 Pa

The last step was setting the flow parameters (Tab. 21)

Tab 21 Flow parameters

FLOW COMPRESSIBILITY	COMPRESSIBLE
FLOW MODEL	TURBULENT
SOLUTION MODE	STEADY STATE
NUMBER OF ITERATION	3,000
FLOW MODEL	K-EPSILON

11.3 MODEL MESHING

I used the CFD meshing tool for the meshing of the models. I pre-set the basic number of elements for each model, then I set special regions, which have their own mesh density, at critical airbox areas. The last step was prism creation.

11.3.1 VARIANT 1

I set the basic mesh density at 100, 000 elements, then I started to mesh more critical places. For more accurate meshing I used the regions that are shown in (Fig. 72).

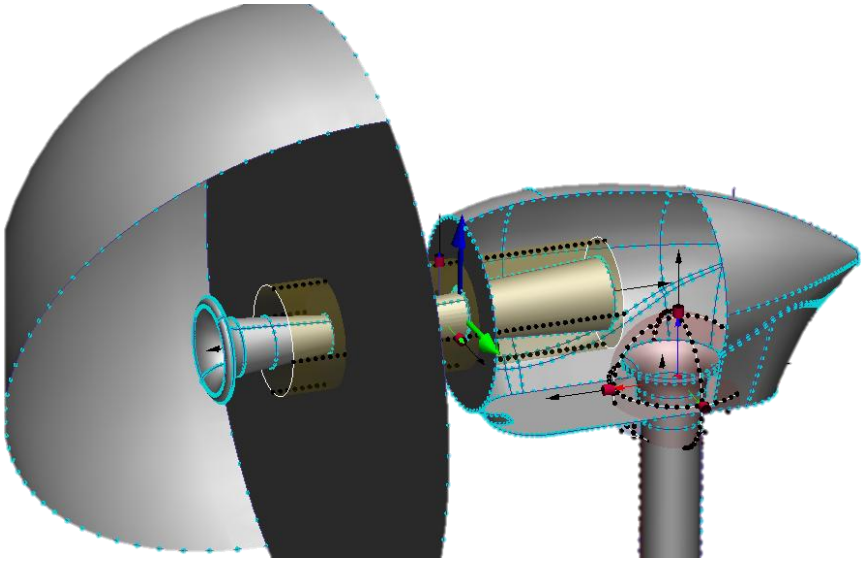

Fig. 73 Meshing regions variant 1

I placed the regions on the restrictor and the bellmouth with the intake runner because these are the most critical places for the flow. Finer mesh means that the solution will be more data intensive and more accurate as well. In (Fig. 74,75) you can see the top view of the

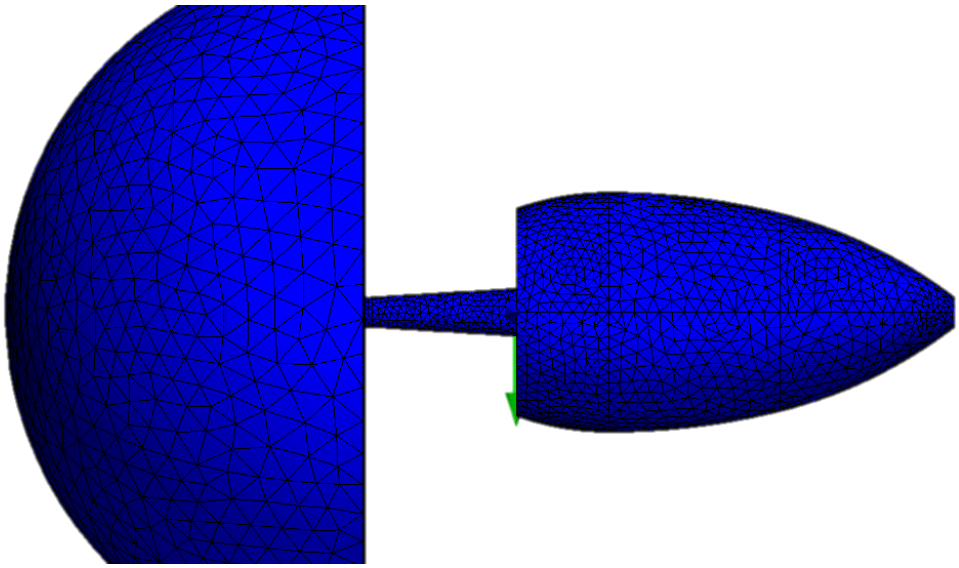

Fig. 74 Mesh of variant 1(top view)

meshed airbox.

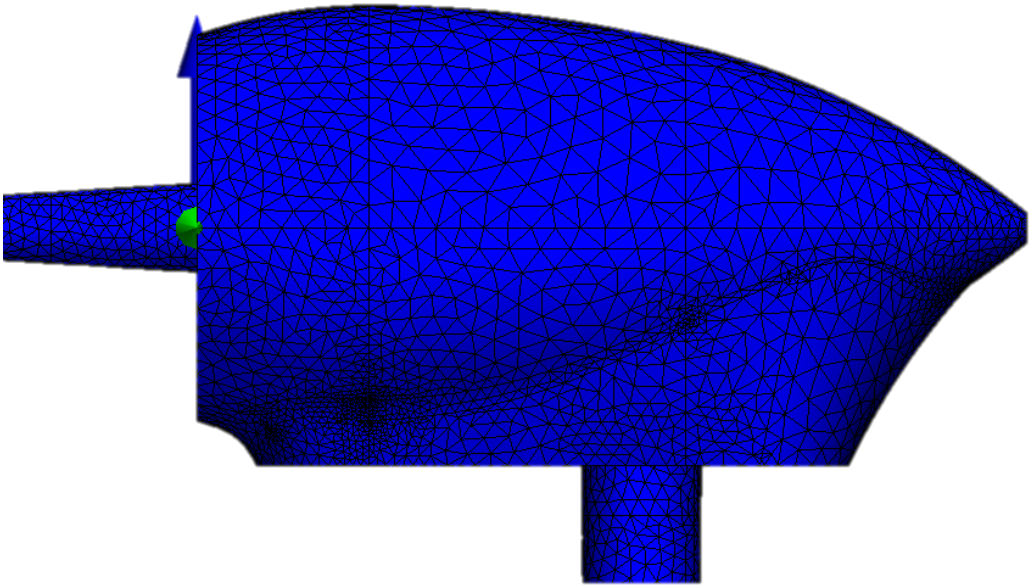

Fig. 75 Mesh of variant1 (side view)

The final mesh of variant 1 had 350,000 elements and solution time was around 2 hours.

11.3.2 VARIANT2

As has been mentioned before, variant 1 and variant 2 are very similar to each other, therefore I kept the same meshing procedure as in variant 1. In (Fig. 76) you can see the used

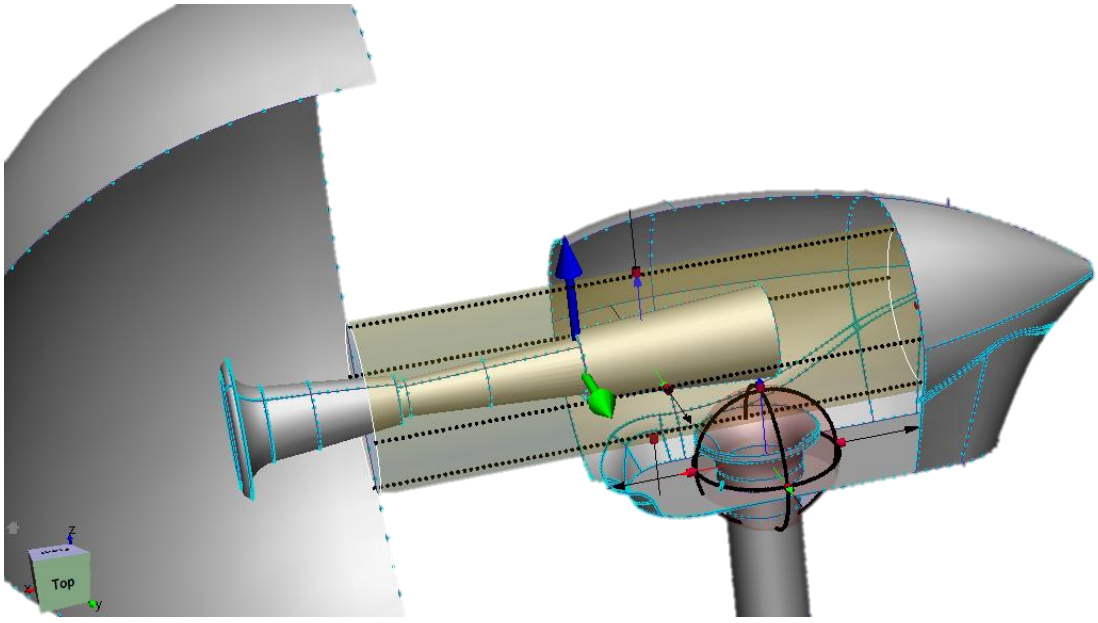

Fig. 76 Meshed regions of variant 2

meshing regions.

The final mesh of variant 2 had around 350, 000 elements and solution time was similar to variant 1 (around 2 hours). In (Fig. 77) there is the mesh of variant 2.

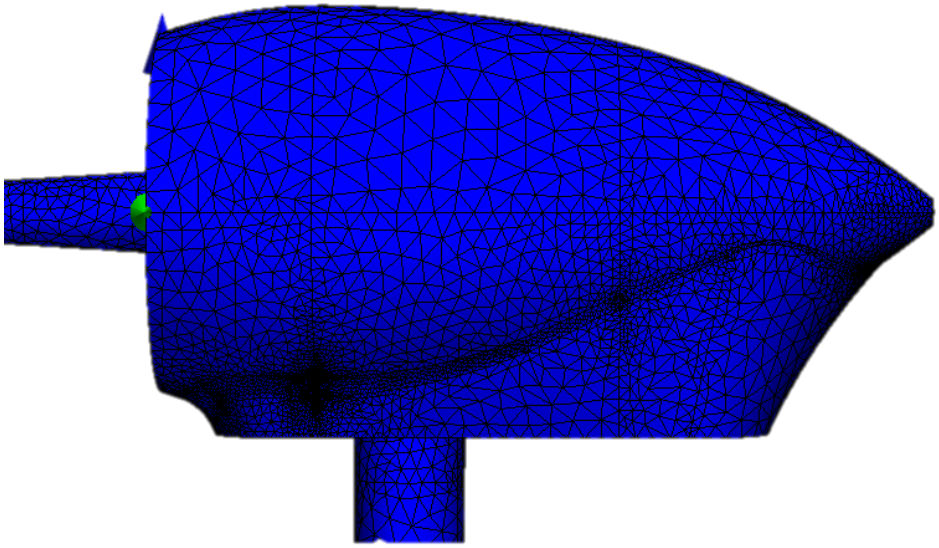

Fig. 77 Mesh of variant 2 (side view)

11.3.3 VARIANT 3

For variant 3 I set the basic mesh density at 150, 000 elements because this variant was more shape complicated than previous two variants; then I placed the regions to the restrictor and also to the bottom of the airbox (Fig. 78).

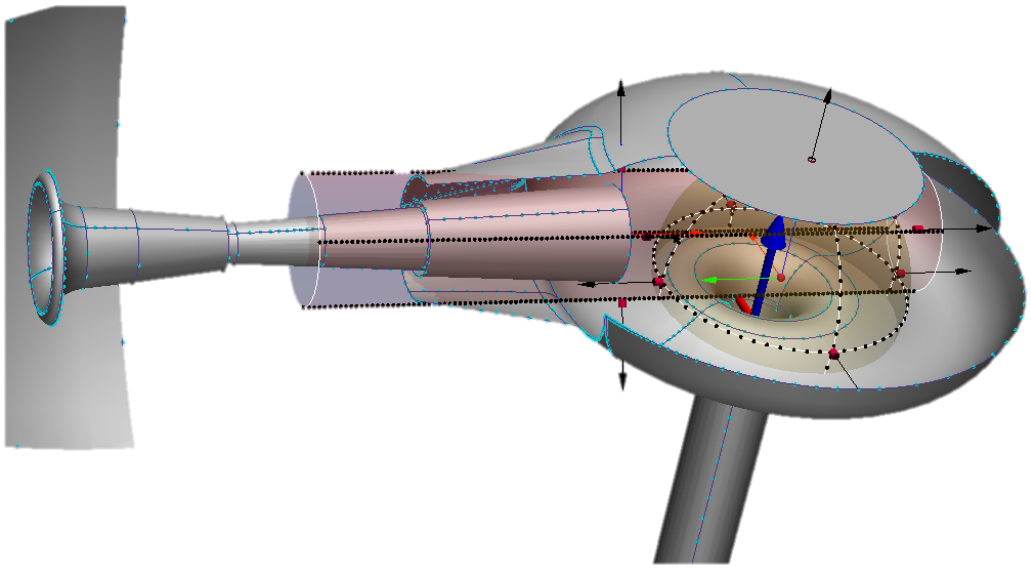

Fig. 78 Meshed region of variant 3

The final mesh (Fig. 79,80) of variant 3 had around 400,000 elements and solution time was around 3 hours.

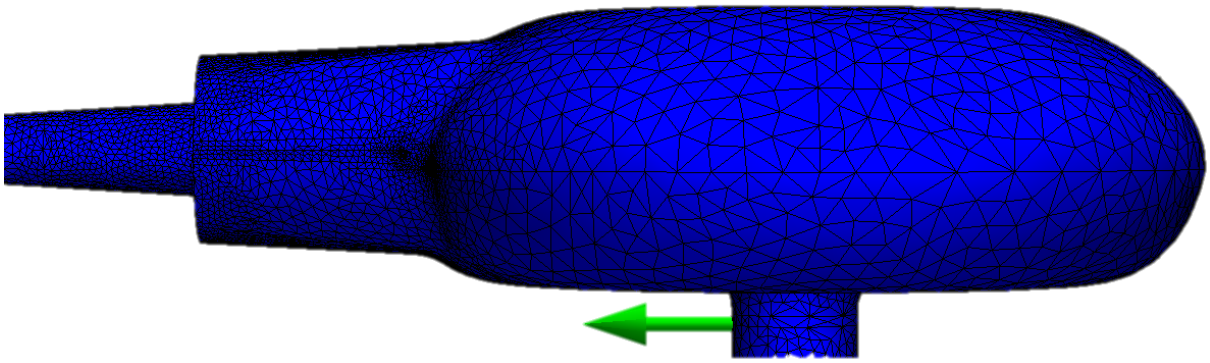

Fig. 79 Mesh of variant 3(side view)

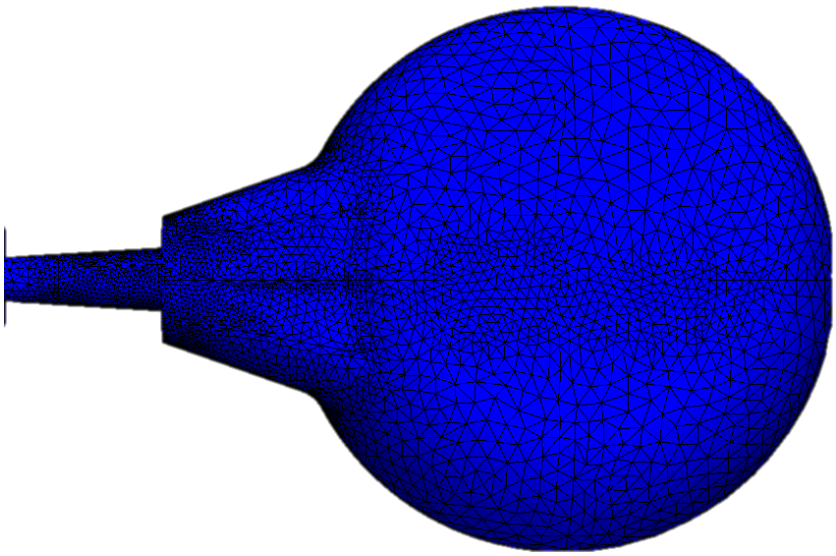

Fig. 80 Mesh of variant 3 (top view)

11.4 RESULTS

I set the number of iteration at 2,000 for each simulation and after the calculation I switched the program to the postprocessor to verify the results.

I made 2 sections through each of the models. First section divided the model into two halves and it crossed the air plenum and the steadying pipe. This section was important because it showed the flow direction and I was able to predict eventual hydraulic losses on the walls. The second section was perpendicular to the first section and it was placed at the end of the steadying pipe to secure the results accuracy. As the flow is steady at the end of the pipe, accuracy of the results is high.

As I have explained before, I wanted to compare the mass flow rate through each of the variants and then to choose the best one, i.e the variant with the maximum mass flow rate. I started with variant 1(Fig. 82).

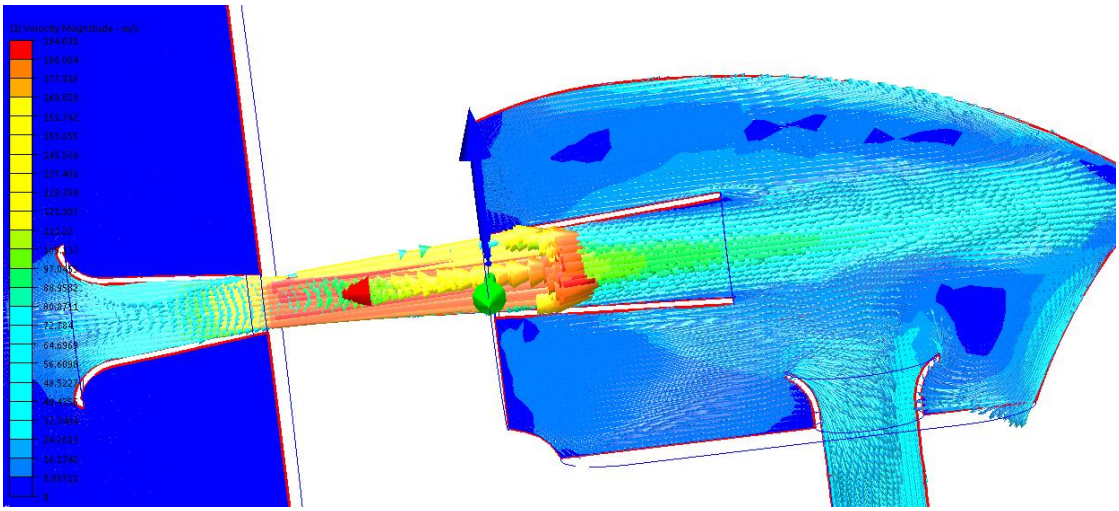

Fig. 81 Flow direction expresed by vectors (variant1) Velocity magnitude MIN =0 , MAX =194 m. s^{-1}

As you can see, the intake air uses the whole volume of the airbox, which is very promising in terms of the influence on the restrictor. This is also a highly promising base for the transient air flow mode in which the engine operates. When the engine is in the intake period, we need the air to flow to the intake runner as short the way as possible; and also the influence of the aforementioned pressure waves from the intake runner on the restrictor has to be as little as possible. That is the reason why the restrictor outlet has been inserted here. Because when the pressure wave extends across the airbox volume, it should flow towards the airbox front wall rather than to the restrictor, as this part of the airbox has a bigger volume than the restrictor outlet part. In (Fig. 81) you can see the flow traces flowing through the airbox.

The results of the variant 2 were not as promising as the results of the previous variant. As I have mentioned before, I moved the bellmouth closer to the front wall of the airbox, which

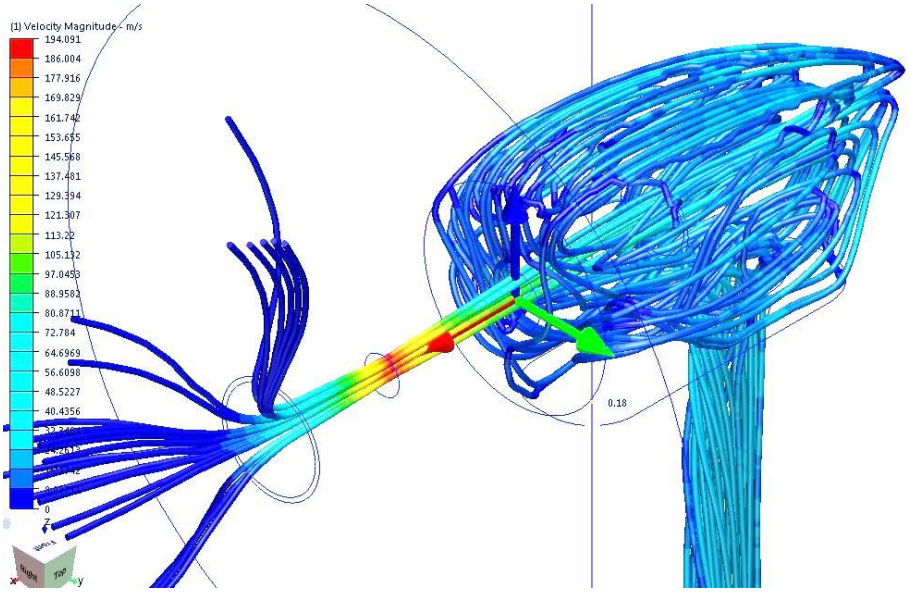

Fig. 82 Flow traces (variant1) Velocity magnitude MIN =0 , MAX =194 m. s^{-1}

also brought the bellmouth and the intake runner under the restrictor outlet. This could be an advantage in terms of pressure waves effect on the restrictor, but on the other hand the utilization of the airbox volume is worse than in variant 1. In (Fig. 84) you can see velocities

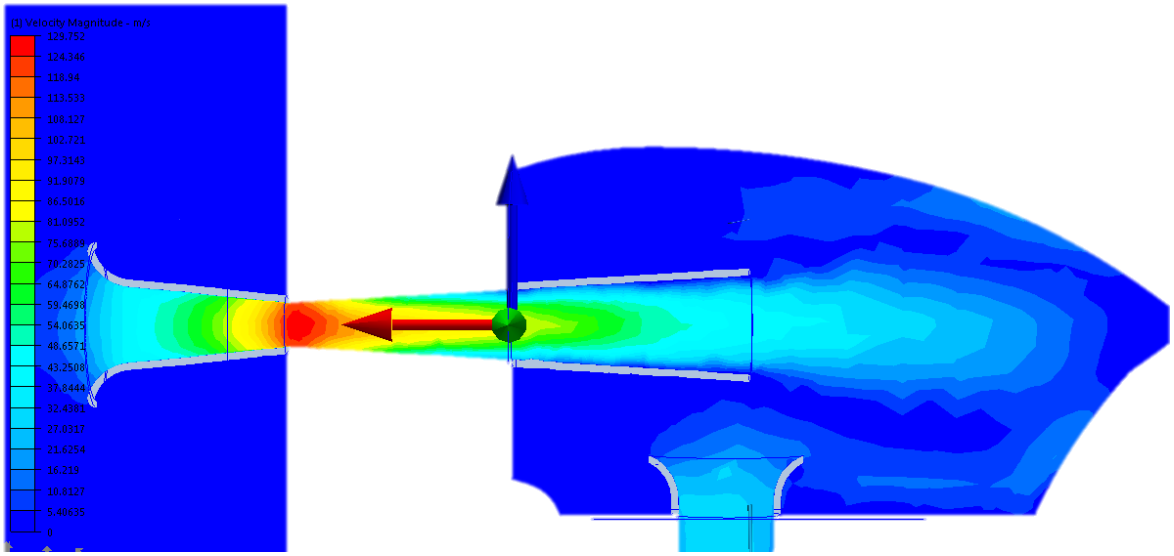

Fig. 83 Velocity course (variant 2) Velocity magnitude MIN =0 , MAX =129 m. s^{-1}

in the airbox (variant 2).

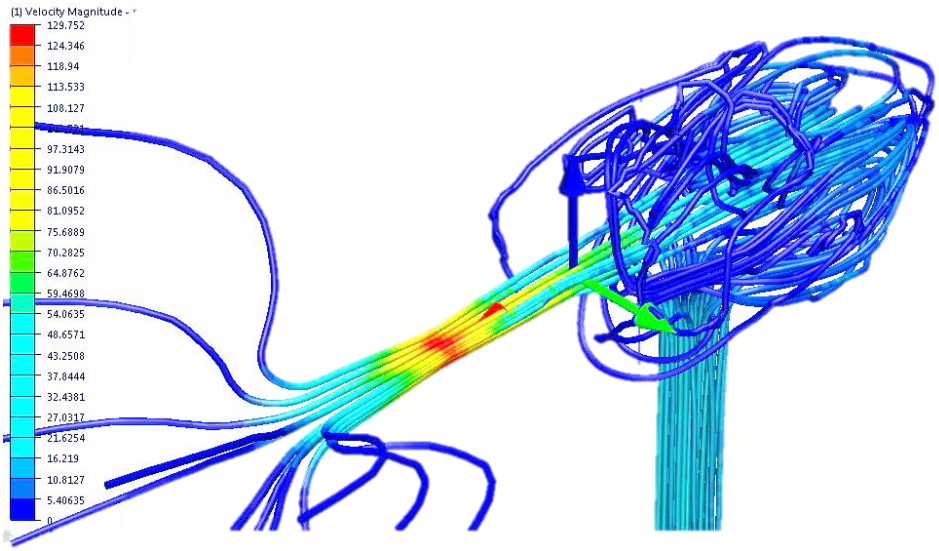

Fig. 84 Flow traces (variant 2) Velocity magnitude MIN =0 , MAX =129 m. s^{-1}

In (Fig. 83) there are flow traces which flow through the airbox variant 2 You can also compare the above mentioned use of the airbox volume with (Fig.79). I used the same number of traces as in the variant1 and at the first sight the utilization of the volume is lower.

The results of the variant 3 were very promising as well. The utilization of the airbox volume was very high and the hydraulic losses were also low due to the semi spherical shape. In (Fig. 85) there are velocity vectors in variant 3.

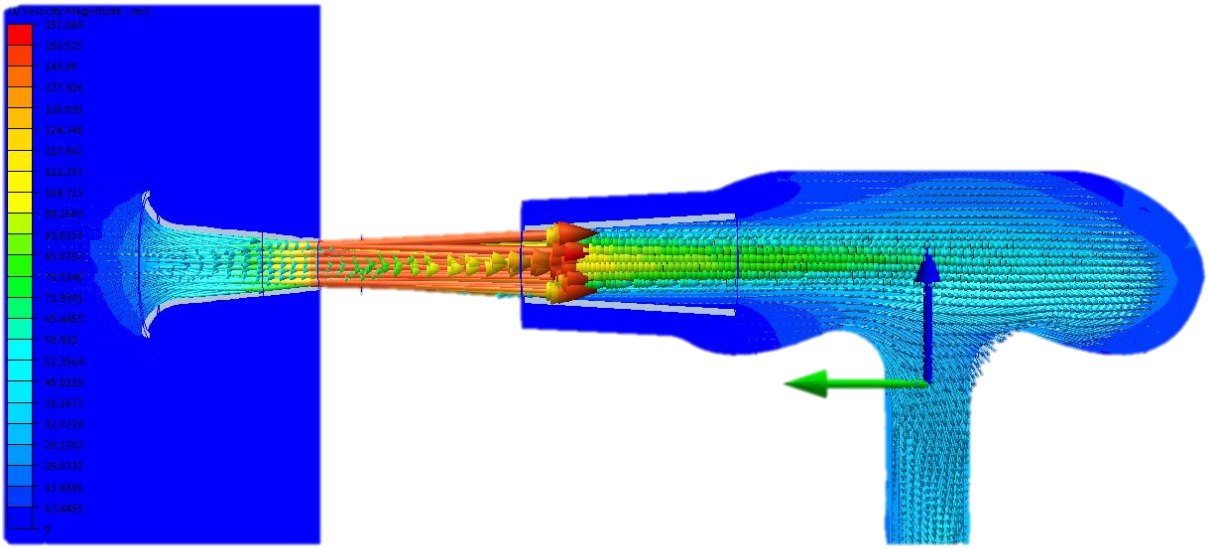

Fig. 85Flow direction expresed by vectors (variant3) Velocity magnitude MIN =0 , MAX =157 m. s^{-1}

You can also see the precise volume splitting (Fig. 86), in the presented simulation there is a swirl which is a result of the circular shape of the airbox. This swirl could be an advantage in

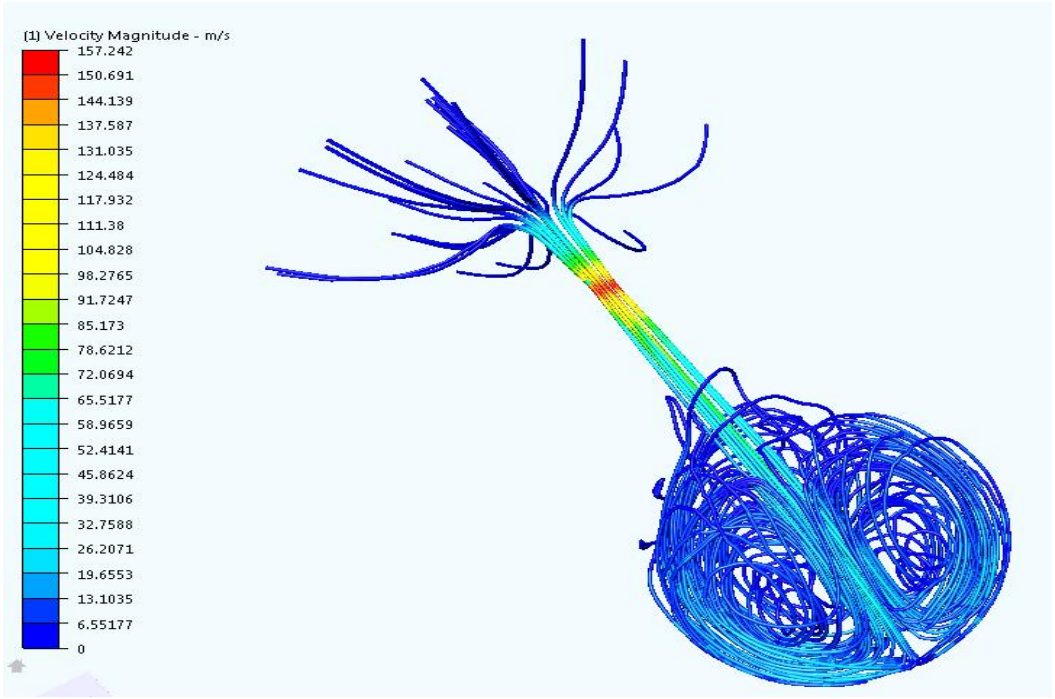

Fig. 86 Flow traces (variant 3) Velocity magnitude MIN =0 , MAX =157 m. s^{-1}

terms of the air fuel mixing and the engine charging.

11.4.1 RESULTS COMPARISON

In (Fig. 82,83,85) there are flow traces through all the variants. A flow trace is a trace of an intangible particle which is drifted by the air flow. In (Fig 82) the airbox variant 1 is split to the two flow parts which both create the thumble and perfectly utilize the airbox volume. This effect could lead to the charging efficiency improvement. In (Fig. 83) you can see that the flow through the airbox is chaotic and this could lead to higher hydrodynamic losses, restrictor influence and charging efficiency lowering. In (Fig. 85) the airbox is divided into two flow parts that make the swirl and make a very good use of the airbox volume. This effect could lead to the charging efficiency improvement.

From all the simulations I obtained the mass flow rate values which were measured at plane, placed at the end of the steadying pipe, and afterwards I compared these results (Tab. 22).

Tab 22 Results comparison

VARIANT	MASS FLOW RATE ($g.s^{-1}$)
1.	50.1
2.	36.9
3.	41.2

Having considered the simulation results, I decided to choose the airbox (variant1) due to its mass flow rate and also its assembling dimensions.

12 FINAL DESIGN OF INTAKE SYSTEM

I have designed the final variant of the intake system on the basis of the Lotus and CFD simulations. Lengths and diameters of the intake runner are results of the Lotus simulations and the airbox resulted from the CFD simulation.

When I had the final variant of the intake system, I started to solve the airbox manufacturing. To select the material was the first step. I had the three options that are shown in (Tab. 23).

Tab 23 Material comparison

MATERIAL	DENSITY (kg/m^3)
ALUMINUM	2,800
GLASS FIBRE LAMINATE	1,800
CFRP (CARBON FIBRE COMPOSITE)	1,500

Material surface should be as smooth as possible to minimize hydraulic losses of the air flow. Another requirement is the weight of the material which depends on the material density. The intake system should be as lightweight as possible because it is a self-supporting construction; another reason is the total car weight. Last of the main material requirements is the material strength. The intake system has to be strong enough to endure nonstop pressure loading during the engine running and it must not implode or destruct itself.

I decided to choose the CFRP (carbon fibre composite) material because it is very lightweight and strong. It is rather expensive but the total price of our airbox material is not high thanks to total dimensions of the airbox.

Next step was to create of moulds for manufacturing (Fig. 87).

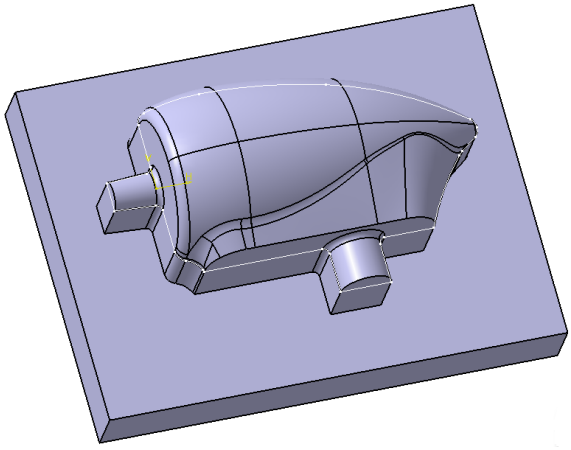

Fig. 87 Airbox mould (left part of airbox)

I wanted to present a photography of the real manufactured airbox but, because of the delay in the material delivery, the whole intake system could not been manufactured yet. Therefore in (Fig. 88,89) there are models of the final intake system inCATIA.

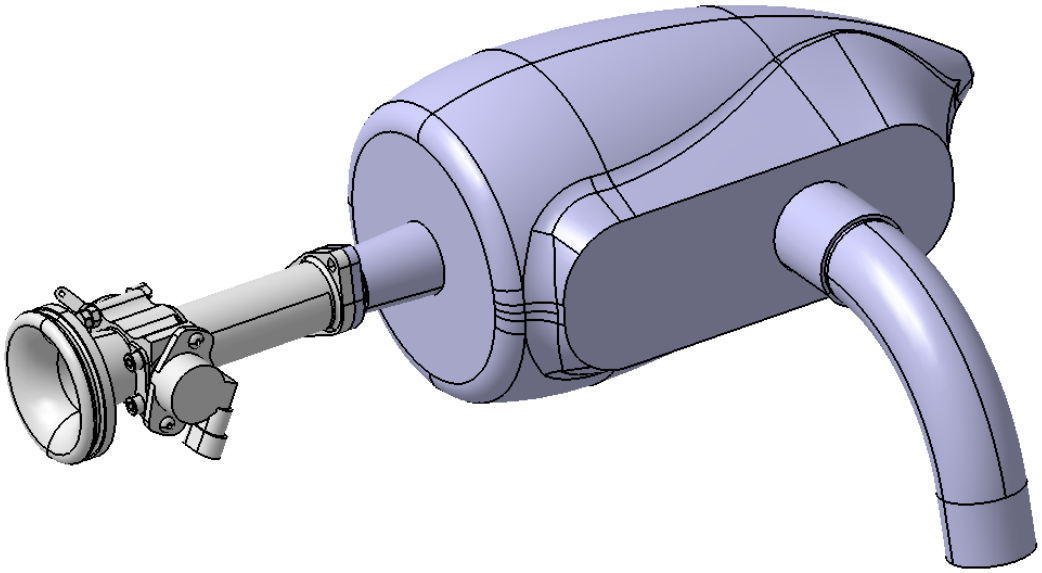

Fig. 89 Intake system model

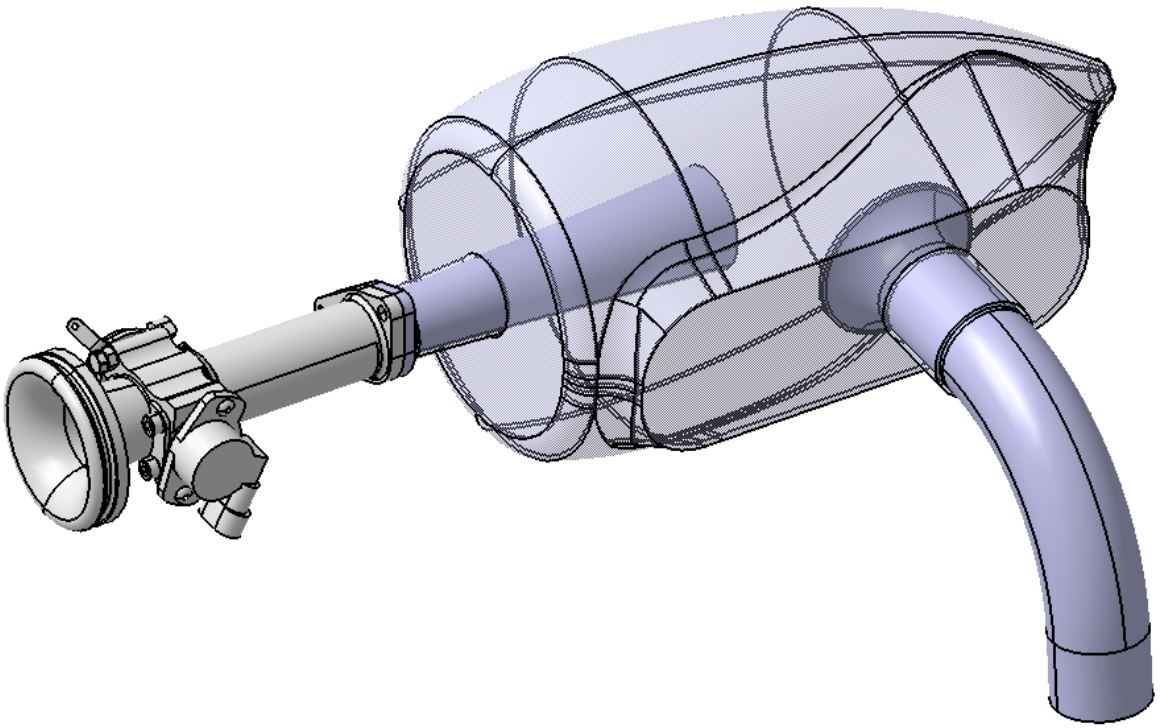

Fig. 88 Model of intake system

You can see our completed Formula Student car in (Fig. 90).

Fig. 90 Model of our Formula Student car.

CONCLUSION

The aim of this diploma thesis was to create the design and optimization of the single cylinder SI engine intake manifold for a Formula Student car. The creation of the stock engine simulation model was the first step. My aspiration was to create this simulation model as close to reality as was possible, therefore I measured the cam profile, I cast, I scanned and reshaped the inlet ports and measured the port flow coefficients on the flow bench. I had intended to measure the performance and torque course of the stock engine; however, our school laboratories were under reconstruction and it was not possible to measure these parameters. Therefore I had to start with the performance/torque outputs that I simulated on the stock engine model in the Lotus Engine simulation.

The stock engine simulation model was a good basis for the intake manifold concept. In the following step I designed main manifold dimensions and studied their influence on the engine performance and the torque course. I found out that the results of basic formulas for calculation of the resonance manifold lengths, which ignore some factors that have an effect on the dynamics of the air flow, are very similar to the results of the simulation.

The intake system of the Formula Student car includes a restrictor, which has to be placed between the throttle body and the engine according to the Formula Student rules. The restrictor has the main influence on the engine performance. This fact significantly complicated the simulation because I had to work with a model of the airbox which was quite complex because I applied a technology of the inserted restrictor, used by Formula 3,000 engines. After the optimization of the inserted parts lengths, the airbox eliminated the influence of the restrictor up to 9,000 min^{-1}.

I tried to adapt the maximum engine performance to the racing conditions, which means the maximum performance in a thin spectrum of engine speeds with reasonable torque. The dimensions optimization resulted in the performance increase in the spectrum from 7,000 to 8,500 min^{-1} and the torque increase in spectrum from 4,000 to 7,000 min^{-1}. The maximum performance was achieved at 8,000 min^{-1}, the maximum torque at 7,000 min^{-1} with values approaching to maximum torque from 5,000 min^{-1}. These results, obtained from the Lotus Engine Simulation, are absolutely sufficient because the working engine speeds for our formula car vary from 6,000 to 8,000 min^{-1}.

After the optimization of the main manifold dimensions I created three variants of the airbox 3D models in CATIA. After that I created an air model of each airbox for the CFD analysis.

During the CFD analysis I monitored the flow direction and utilization of the airbox volume, which factors are very important for the engine charging efficiency. I also monitored the velocity amplitude in the narrowest area of the restrictor for each airbox. These values predicate how much is the restrictor influenced by the intake pressure waves. All three variants were loaded by the same hydraulic gradient (5,000 Pa). The velocity amplitude at the narrowest area of the restrictor was 194.2 $m.s^{-1}$ in the best variant, which was by far the most in comparison with the other variants. But the most important result of these CFD simulations consisted in the mass flow rate which flows through the airbox. I decided to measure these values at the end of the steadying pipe because there is a streamline flow which provides the best results. The final mass flow rate includes the hydraulic losses in the whole airbox and its

value predicates the engine charging. I compared all the three variants with each other and the best variant achieved the mass flow rate of 50.1 $g.s^{-1}$.

After finishing the CFD analysis I designed the final variant of the intake system in CATIA, I inserted it to the final car assembly and checked, if it is not in collision with any other part or the car frame.

The airbox manufacturing was the final step, which I started to realize with the Aircraft Institute at Brno University of Technology, because they have great amount of experience with the composite material forming. First I chose the airbox material which is the carbon fibre fabric with the fibre density 200 g/m^2. In cooperation with the Aircraft Institute we set the manufacturing process and then I started to create the 3D models of the moulds. According to the plan, the airbox will be manufactured after this diploma thesis release.

I and the whole 'Engine Team' have an intention for the future to measure the performance /torque outputs of the engine with the optimized intake system on the new dynamometer, to tune the engine ECU (electronic control unit) and to prepare the whole engine and its accessories for the first Formula Student competition.

In the course of a step-by-step process, all aims of this diploma thesis have been achieved.

SOURCES

[1] FORMULASTUDENT.COM, *Formula SAE rules* [online] 2011,.Available from: <www.formulastudent.com>

[2] ARPEM.COM [online]. 2004 – 2011, Available from: <www.arpem.com>

[3] HUSABERG.COM, *Owners manual* [online] 2010, Available from: <www.husaberg.com/fileadmin/user_upload/Owners_Manual_FE_09_EN.pdf >

[4] MOTORKARI.CZ, *Články / Husabergy 2010* [online] 2011, Available from: <www.motorkari.cz >

[5] GW-RACING-PARTS.DE, [online] 2011, Available from: < www.gw-racing-parts.de >

[6] M3ADDICT.COM, *M3 engine* [online] 2011, Available from: < www.m3addict.com/whats-good/tag/m3-engine >

[7] ITGAIRFILTERS.COM, [online] 2011, Available from: < www.itgairfilters.com >

[8] F1TECHNICAL.COM, *Formula One 1.6l turbo engine formula as of 2013* [online] 2011, Available from: < www.f1technical.net/forum/viewtopic.php?f=4&t=9259&start=120 >

[9] PRODUCTS.DINAN-MOTORSPORT.COM, *Parts* [online] 2011, Available from: < www.products.dinan-motorsport.com/post/72689743 >

[10] FORUMS.AUTOSPORT.COM, *F1 cylindrical throttle body* [online] 2011, Available from: < www.forums.autosport.com/lofiversion/index.php/t111306.html >

[11] FORUMS.EVOLUTION.NET, [online] 2011, Availible form: < www.forums.evolution.net >

[12] MACKERLE, Julius. *Motory závodních automobilů*. Praha : SNTL, 1980. 118 s

[13] BLAIR, Gordon P. *Empiricism and Simulation in the Design of the High Performance Four-Stroke Engine.* The Queen´s University of Belfast : Society of Automotive Engineers, Inc. 89 s

[14] RET-MONITOR.COM, The hollow feeling [online] 2011, Available from: < http://www.ret-monitor.com/articles/528/that-hollow-feeling >

[15] RACING.TUGRAZ.AT, [online]. 2002 – 2011, Available from: < www.racing.tugraz.at >

[16] DURTRACING.NL, [online]. 2001 – 2011, Available from: < www.dutracing.nl >

[17] JOANNEUM-RACING.AT, [online]. 2002 – 2011, Available from: < www.joanneum-racing.at >

[18] HEISLER, H. *Advanced engine technology*. 1. Edition. Warrendale : SAE International, 1995. p. 794. ISBN 1-56091-734-2.

[19] MOTORCYCLE-USA.COM, [online]. 2001 – 2011, Available from: < www.motorcycle-usa.com >

[20] ATZONLINE.COM, *The First Continuously Variable Intake System in the New Eight-Cylinder Engine from BMW*, [online]. 2011, Available from: < www.atzonline.com >

[21] ŘEHÁK, I. *Návrh sacího traktu pro vůz Formule SAE*. Brno: Vysoké učení technické v Brně, Fakulta strojního inženýrství, 2008. 75 s.

[22] BAUMRUK, Pavel. *Problematika náplně válce spalovacích motorů.* Vydavatelství ČVUT, 1996. 62 s

[23] CVPSYLOGY.COM, [online]. 2001 – 2011, Available from: < www.cvphysiology.com/Hemodynamics/H006.htm >

[24] CENTENNIALOFFLIGHT.GOV, [online]. 1998 – 2011, Available from: < www.centennialofflight.gov/essay/Theories_of_Flight/Skin_Friction/TH11G3.htm >

LIST OF USED ABBREVIATIONS AND SYMBOLS

κ	[-]	Poisson constant
P	[kW]	Engine performance
M_t	[Nm]	Engine torque
r	[J.kg^{-1}.K^{-1}]	Gas constant
T_s	[K]	Mean air temperature
a_s	[m.s^{-1}]	Speed of sound
l_{rez}	[mm]	Resonance runner length
n	[min^{-1}]	Engine speed
Q_B	[J]	Heat released from fuel
H_u	[J.kg^{-1}]	Calorific value of fuel
m_b	[kg]	Amount of burned fuel
p	[Pa]	Pressure, gage pressure
Q_m	[kg.s^{-1}]	Mass flow rate
Q_T	[m^3.s^{-1}]	Theoretical volume flow rate
Q_S	[m^3.s^{-1}]	Real volume flow
R_e	[-]	Reynolds number
S	[m^2]	Flow area
v	[m.s^{-1}]	Flow velocity
v_s	[m.s^{-1}]	Mean flow velocity
C_f	[-]	Port flow coeficient

ENCLOSURE LIST

ENCLOSURE 1 (AIRBOX ASSEMBLING DIMENSIONS)

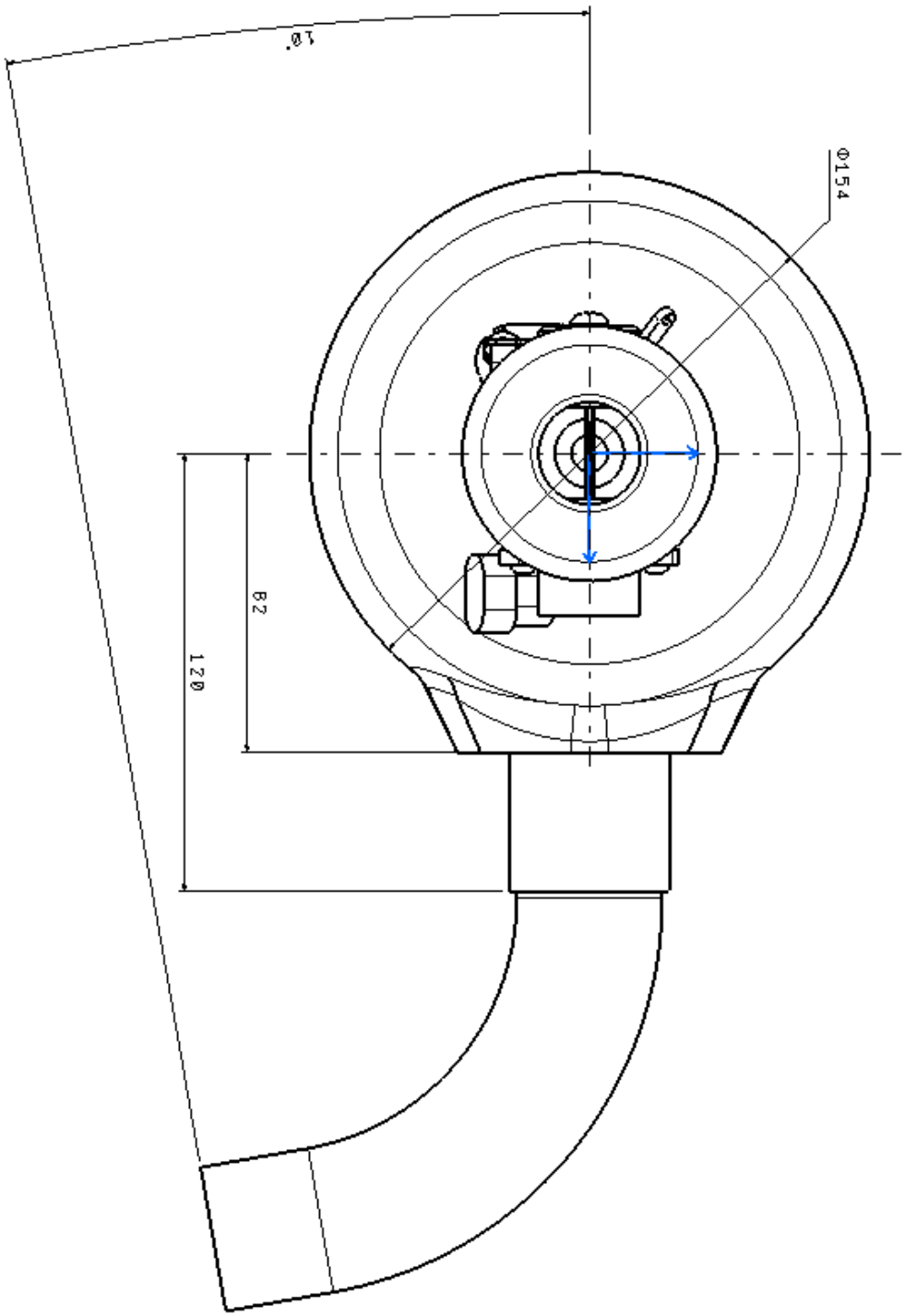

ENCLOSURE 2 (AIRBOX ASSEMBLING DIMENSIONS)